COMMON SIGNALING ELEMENTS IN RESPONSE PATHWAYS ACTIVATED BY THE ENDOTHELIAL SURVIVAL FACTORS VEGF AND INSULIN

Amanda Cyphers Wang

Thesis submitted to the faculty of the Virginia Polytechnic Institute and State University
in partial fulfillment of the requirements for the degree of

Master of Science
In
Biomedical and Veterinary Sciences

William R. Huckle
Willard H. Eyestone
Brenda S.J. Winkel

December 2, 2008
Blacksburg, Virginia

Keywords: Vascular Endothelial Growth Factor, Insulin, Receptor Tyrosine Kinases, Cellular Signal Transduction

COMMON SIGNALING ELEMENTS IN RESPONSE PATHWAYS ACTIVATED BY THE ENDOTHELIAL SURVIVAL FACTORS VEGF AND INSULIN

Amanda C. Wang

(ABSTRACT)

Damage to the vasculature is a common occurrence in diabetes mellitus. At the cellular level, dysfunction of vascular endothelial cells is often associated with diabetic conditions. Multiple agents maintain the endothelium, including vascular endothelial growth factor (VEGF), an endothelial cell mitogen/survival factor, and insulin, which has anti-apoptotic effects on endothelial cells in addition to regulating glucose homeostasis. Insulin and VEGF, upon activating their respective tyrosine kinase receptors, can engage the PI3-kinase/Akt, MAPK, and PLC-γ/PKC pathways. Thus, crosstalk between VEGF and insulin signaling may occur at numerous points. Our objectives were twofold: 1) to characterize the combined effects of insulin and VEGF on downstream elements, and 2) to determine the ability of signaling intermediates principally associated with either insulin or VEGF signaling to interact directly. After treatment with VEGF, insulin, or both, cells expressing both VEGF receptor-2 (KDR) and the insulin receptor were immunoprecipitated for total Akt and PLC-γ. Isolates from cells stimulated with both ligands demonstrated activation of PLC-γ and Akt that was less than additive over fifteen minutes. Conversely, cells pretreated with advanced glycation end products showed increased Akt phosphorylation. The effect of insulin on VEGF bioactivity was also measured by PLC-γ-mediated hydrolysis of phosphatidylinositol. These studies suggested suppressed VEGF activity in the presence of insulin. To examine direct signaling interactions, recombinant reagents capable of selective binding (via SH2 domains) to phosphorylated receptors were generated. Overall results showed relatively unaffected VEGF activity in the presence of insulin; however, this relationship is likely altered within the diabetic state.

ACKNOWLEDGMENTS

I am very grateful to Dr. William Huckle for the opportunity to be a member of his lab and a contributor to this project. Dr. Huckle's guidance and expertise have been invaluable during the past several years. His thoughtful instruction and ongoing encouragement have greatly contributed to my academic accomplishments. I hope future professional relationships will be as positive and productive as the one I enjoy with Dr. Huckle.

I would also like to thank the additional members of my graduate committee—Dr. Brenda Winkel and Dr. Willard Eyestone. Their constructive criticism and sound advice have challenged and guided me during this process.

I am thankful for the lifelong friendships formed with past and present lab members-- Rebecca Pickin, Matthew Rittler, and Burouj Ajlouni. Their willingness to share of their time and expertise has far surpassed all expectations.

I would also like to acknowledge my family. The thoughts and prayers of my loving parents, Mr. and Mrs. Lynn D. Cyphers, and grandparents, Mr. and Mrs. Carroll G. Lineberry, have upheld me in all circumstances. Their lives are a testament to their belief in hard work, perseverance, and the inherent value of an education.

I would especially like to thank my husband and best friend, Josh. His unconditional love and patience are the greatest blessings in my life. No truer words have ever been written than those of Mary Ann Evans-- *What greater thing is there for two human souls than to feel that they are joined together to strengthen each other in all labor, to minister to each other in all sorrow, to share with each other in all gladness, to be one with each other in the silent unspoken memories?*

Above all, I would like to acknowledge salvation through my Lord and Savior, Jesus Christ. *For from Him and through Him and to Him are all things. To him be the glory forever! Amen.* (Romans 11:36; NIV).

TABLE OF CONTENTS

LIST OF FIGURES

INTRODUCTION

Damage to the vasculature is a common occurrence in diabetes mellitus. At the cellular level, dysfunction of vascular endothelial cells is often associated with diabetic conditions, notably hyperglycemia and dysinsulinemia (Morisco et al, 2006). Insulin resistance and endothelial dysfunction are often precursors (Rask-Madsen and King, 2007) to these and other clinical conditions, such as cardiovascular diseases, the metabolic syndrome, hypertension, retinopathy (Spranger and Pfeiffer, 2001), and a host of other physiological abnormalities (Tennyson, 2002 and Zimmet et al., 2001). Patients with type 2 diabetes have a highly increased risk of developing cardiovascular diseases (Yamagishi et al., 2006), which lead to approximately 70% of total morbidity and mortality in diabetics (Laakso, 1999). In 2005, Hadi et al. reported that endothelial cell function measured by Doppler echocardiography, phase-contrast magnetic resonance imaging, and invasive quantitative coronary angiography was a reliable indicator of obstructive coronary artery disease. This same group also examined peripheral vascular circulation by ultrasound, upper arm occlusion, and strain-gauge venous impedance plethysmography (Hadi et al., 2005).

Multiple agents act to maintain homeostasis in the endothelium, including vascular endothelial growth factor (VEGF), an essential endothelial cell mitogen and survival factor. VEGF regulates angiogenesis in several stages: early vessel development (embryogenesis), normal growth, tissue repair, and tumor development (Ferrara et al., 2001 and Kendall et al., 1999). VEGF signal transduction is primarily mediated by two high-affinity cell surface receptors, VEGFR-1 (*fms*-like tyrosine kinase, *Flt*-1) and VEGFR-2 (kinase insert domain receptor, KDR/Flk-1) (Dvorak, 2002). These receptors are structurally similar, but lead to different physiological effects (Ferrara et al., 2003). Flt-1 is critical in stabilizing the VEGF response during embryogenesis, activating macrophages (linked to tumor growth and metastasis) (Shibuya, 2006), and responding to placental growth factor (PlGF) (Ahmed et al., 2000). In contrast, VEGF signaling through KDR instigates endothelial cell proliferation, migration, and angiogenesis (Dvorak, 2002). KDR signaling often occurs through the phospholipase C- γ/ Protein Kinase C (PLC-γ/PKC) and phosphoinositide 3-kinase/Akt (PI3-Kinase/Akt) pathways (Shibuya, 2003). One extensive response to VEGF signaling is

the production of NO by endothelial nitric oxide synthase, or eNOS (Blanes et al., 2007). Nitric oxide release from endothelial cells leads to vasodilation and is also important for the maintenance and protection of vessels (Ahmad et al, 2006).

Insulin also functions in the maintenance of vascular tissues (Jiang et al., 2003), in addition to its significance in glucose metabolism and macromolecule storage (Cohen, 1999). Vascular-specific responses to insulin include the induction and upregulation of VEGF expression, activation of eNOS, and retinal neovascularization (Jiang et al., 2003). Other general responses to insulin signaling include protein synthesis and storage (Guyton, 2006), mitogenic functions (Ornskov et al., 2006), and anti-apoptotic behavior through Akt signaling (Hermann et al., 2000). Insulin binding to the insulin receptor (IR) prompts the recruitment and phosphorylation of insulin receptor substrate-1 or 2 (IRS-1/2) (Bjornholm and Zierath, 2005) docking proteins that mediate association of the IR with downstream effectors (van der Geer et al., 1999). Both insulin and VEGF, upon activating their respective tyrosine kinase receptors, are capable of engaging the PI3-kinase/Akt, MAPK, and PLC-γ/PKC pathways. Thus, crosstalk between the VEGF and insulin signaling pathway may occur at numerous points.

Given the shared features between the insulin and VEGF signaling pathways and their opportunities for interaction, we decided to probe for specific downstream targets common to both pathways, particularly phosphorylated Akt. Akt, a mediator of both VEGF and insulin signaling, is a rational endpoint for several reasons: 1) Akt phosphorylation is directly associated with its activation and signal transduction through an Akt mediated pathway (Lawlor and Alessi, 2001), 2) Akt phosphorylation is easily and rapidly detected after stimulation with VEGF (Wu et al., 2000) or insulin (Alessi et al., 1993), and 3) Akt is directly associated with physiological and pathological processes mediated by both VEGF and insulin. These include cell proliferation, angiogenesis, eNOS activation, and tissue homeostasis (Lawlor and Alessi, 2001 and Sen et al., 2003).

We hypothesize that VEGF and insulin activate shared signaling proteins in a cooperative fashion that is altered under conditions associated with diabetes. In order to test this hypothesis, we developed two major project aims that directed our study of insulin and VEGF signaling. Aim1 was to characterize the effect of VEGF and

insulin signaling on common downstream elements, in order to determine whether these effects were additive or inhibitory. To do this, we developed cell lines overexpressing KDR and the IR, stimulated these cells with VEGF, insulin, or both, and screened specific phosphorylated signaling intermediates. Other experiments used to further understand collective signaling effects included pre-treatment of cells with a model advanced glycation end product (AGE-BSA) to further mimic the diabetic state.

For Aim 2, we considered the possibility of cross-talk between the VEGF and insulin pathways. Signaling intermediates principally associated with one pathway or the other were isolated based on their interaction with recombinant domains that specifically bind tyrosine-phosphorylated proteins. GST fusion proteins were created for the selection of target proteins using conserved binding domains as previously shown by our lab (Huckle and Earp, unpublished; Rittler dissertation). We examined protein activation after timed exposure to insulin and/or VEGF through interactions with GST fusion proteins or after specific immunoprecipitation and analyzed via immunoblotting. VEGF-stimulated hydrolysis of inositol-containing phospholipids was also used as a means of studying the VEGF pathway and how it is affected by varying concentrations of insulin. This phospholipid assay was used to gauge the effect of insulin on the VEGF response through the lipid substrates of PLC-γ.

Though current data shows sites of possible overlap between insulin and VEGF signal transduction, the nature of these interactions has not been well defined. One precursor to insulin resistance and Type II diabetes is hyperinsulinemia, which may have a constructive or destructive affect on VEGF signaling in endothelial cells. Considering this and the correlation between diabetes and vascular abnormalities, we anticipated positive cooperativity between pathways as evidence of both ligands stimulating the same processes. Further understanding of how VEGF and insulin signaling are linked could reveal previously unidentified disease mechanisms and possibly introduce novel therapeutic targets for treating diabetes associated endothelial dysfunction.

LITERATURE REVIEW

I. The Diabetes Epidemic

Diabetes mellitus and cardiovascular disease (CVD) are two leading causes of death in the United States (Insel, 2006). Diabetes alone represents one of the greatest healthcare challenges of this century. Type II diabetes, or non-insulin dependent diabetes mellitus (NIDDM), accounts for over 90% of total cases, while Type I diabetes, or insulin-dependent diabetes mellitus (IDDM), and other forms, such as gestational diabetes, comprise the remaining percentage (CDC, 2005). Global estimates report that more than 150 million people have diabetes, with that figure projected to surpass 220 million by 2010 (Zimmet et al., 2001). In the United States alone, it is estimated that there are over 20 million people with diabetes (CDC, 2005).

Diabetes mellitus (literally meaning "to run through" and "honey") is characterized by chronic fasting hyperglycemia due to insufficient insulin production, action, or a combination of both (Pratt and Cornely, 2004). Type I diabetes, also known as juvenile-onset diabetes, occurs when beta cells of the endocrine pancreas are destroyed and cease to produce insulin. This type of diabetes is not preventable and can only be managed with insulin treatment (CDC, 2005). Causes of type I diabetes are most likely autoimmune, genetic, and/or environmental. In contrast, type II diabetes, often referred to as adult-onset diabetes, is primarily characterized by insulin resistance, hyperinsulinemia, hyperglycemia, all of which are exacerbated by a decline in beta cell function (Kruger et al., 2006). Type II diabetes may be caused by any or all of the following factors: advanced age, race, family history, diet, weight, and physical inactivity (CDC, 2005).

Most diabetics concurrently experience diabetes-associated complications, such as endothelial dysfunction, hypertension, dyslipidemia, systemic inflammation, kidney disease, and macro- and microvascular abnormalities, including blindness induced by diabetic retinopathy (Spranger and Pfeiffer, 2001; Tennyson, 2002). Incidence of CVD is particularly high in type II diabetics (Laakso, 1999), with cardiovascular complications responsible for over half of diabetes-associated mortalities (Yamagishi et al., 2006). At present, there is no cure for either diabetes or CVD. However, a thorough

understanding of the molecular mechanisms and risk factors related to both may identify new therapies and curb the incidence rate of these two disorders.

The challenge of managing diabetes hinges on understanding insulin and how it regulates glucose and fat metabolism in the body. The primary function of insulin is to recruit glucose transporters to the cell surface, which leads to an influx of glucose into the cell (Saltiel and Kahn, 2001). This process involves several intermediate proteins, giving rise to many possible points of interaction with other signaling pathways. One potential area of crosstalk is in the endothelium between the signaling pathways of vascular endothelial growth factor (VEGF) and insulin.

VEGF and insulin are both necessary for endothelial cell regulation and survival through interactions with their respective tyrosine kinases receptors (Shibuya, 2006; Groop, 2005). Both ligands are also capable of activating the phosphoinositide 3-kinase/protein kinase B (PI3-kinase/Akt), mitogen activated protein kinase (MAP kinase), and phospholipase C-γ/protein kinase C (PLC-γ/PKC) pathways [Figure 1]. This suggests that there are several possible points of interaction between the VEGF and insulin pathways, which may explain why endothelial dysfunction is associated with type II diabetes and CVD (Rask-Madsen, 2007; Saltiel and Kahn, 2001; Shibuya, 2006). Therefore, it is likely that abnormalities in the signaling interactions between insulin and VEGF in the endothelium may affect the progression of diabetes and endothelial dysfunction leading to cardiovascular complications (Yamagishi et al., 2006).

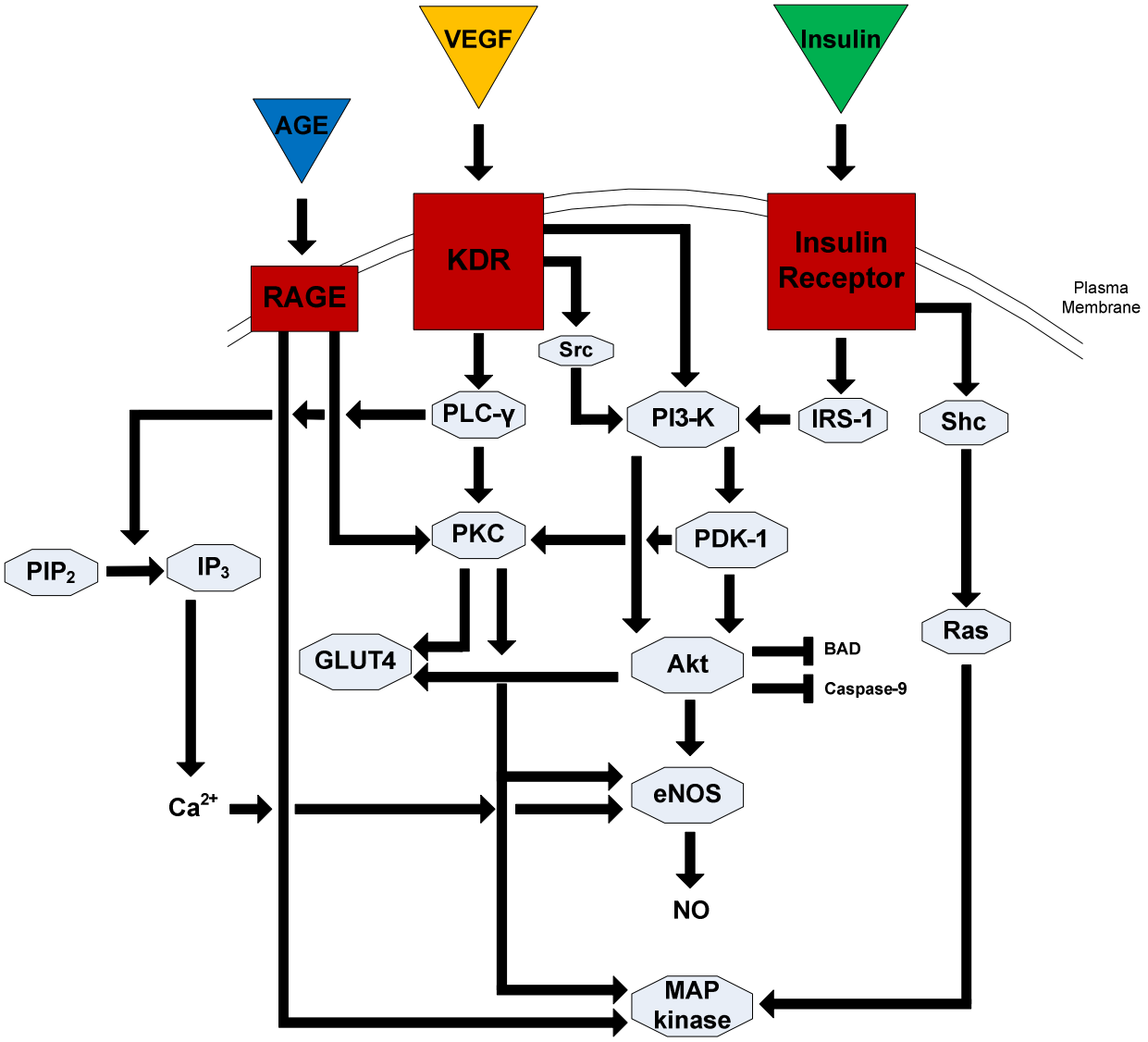

Figure 1. Signaling diagram highlighting VEGF and insulin signaling, as well as points of possible crosstalk between the pathways. VEGF binds and activates its primary receptor tyrosine kinase: the kinase insert domain containing receptor (KDR). Likewise, insulin binding to the insulin receptor leads to activation of several important signaling cascades. Cell surface receptors are labeled in red boxes and downstream effectors are in grey. Arrows indicate modes of activation and lines indicate inhibition. This schematic also includes advanced glycation end product (AGE) signaling through its receptor (RAGE). Note that this diagram does not include all possible proteins present within these signaling cascades, nor does it indicate every possible mode of interaction.

II. Review of Energy Metabolism

Glucose

Glucose, the most abundant organic compound on earth, is the primary source of energy for mammalian cells and is necessary for the production of amino acids and lipids (Pratt, 2004). It is an optically active, cyclic, 6-carbon monosaccharide with the chemical formula: $C_6H_{12}O_6$. Glucose facilitates the process of oxidative phosphorylation, or the oxidation of hydrogen from glucose, which leads to the generation of adenosine triphosphate (ATP) (Guyton, 2006). ATP is a necessary component for most energy-requiring biological reactions. One molecule of glucose can ultimately lead to the production of 38 molecules of ATP (Guyton, 2006).

There are several ways that the body can obtain and maintain healthy glucose levels. One way to acquire glucose is through starches from food. Another mechanism for producing glucose is glycogenolysis, or the breakdown of stored glycogen back into glucose. This process occurs in the liver and is triggered when blood glucose levels decline (Roach, 2002). Glycogen phosphorylase breaks specific glycosidic linkages, which result in the reformation of a glucose molecule and a truncated glycogen molecule. Another way of obtaining glucose is through the process of gluconeogenesis, or glucose synthesis (Guyton, 2006). This process also occurs in the liver and forms up to a quarter of the glucose needed for homeostasis between meals. Both amino acids and glycerol (a central component of triglycerides) can be converted to glucose when necessary (Guyton, 2006).

When glucose is not immediately required for metabolic functions, it is stored as either glycogen or fat. Glycogen is a large, branched polymer of glucose molecules that resides primarily in the liver and in skeletal muscle cells (Roach, 2002). The process of converting several glucose molecules into glycogen is called glycogenesis (Roach, 2002) and is catalyzed by glycogen synthase (Guyton, 2006). About 90% of glucose is stored in this way, with the remainder converted to fat in the liver and stored in adipose tissue (Rosen and Spiegelman, 2006). Fatty acids from adipocytes are a primary source of energy for the body when glucose levels are low. Fat synthesis allows for long term storage of ingested glucose and sequesters at least two times more energy (per gram) than glycogen (Guyton, 2006).

Endocrine Control of Glucose Metabolism

The human pancreas is a secretory organ essential for blood glucose regulation. Pancreatic functions are both exocrine (digestive) and endocrine in nature (Collombat et al., 2006). Acinar cells release digestive enzymes into the intestine, and the islets of Langerhans secrete hormones into the bloodstream (Guyton, 2006).

The islets of Langerhans, or "islands" of endocrine cells surrounded by pancreatic acini, are composed of 3 primary cell types: alpha, beta, and delta. Glucagon released from alpha cells stimulates the hepatic production of glucose into the bloodstream when blood glucose fall below homeostatic levels (Campbell, 2002). Beta cells account for over half of all cells present in the islets of Langerhans. The main function of beta cells is to monitor circulating glucose levels and release the hormones insulin and amylin accordingly (Guyton, 2006). Amylin inhibits insulin secretion and is involved with monitoring the gastrointestinal system. In contrast, insulin is secreted in response to increased glucose levels and is necessary for carbohydrate and fat metabolism (Kruger et al., 2006). Glucose enters beta cells through glucose transporters and assists in the production of ATP. This action triggers calcium ion gated channels that stimulate the release of insulin (Guyton, 2006). Since insulin is only produced and released by beta cells, beta cell replacement therapy is a valuable area of current diabetes research (Collombat et al., 2006).

Normal plasma glucose levels should steadily remain between 4 and 7 mM (Kruger et al., 2006). When circulating glucose concentrations escape this range chronically, serious health complications or death may ensue. Hypoglycemia may lead to seizures or coma. Even slightly elevated glucose levels are associated with microvascular dysfunction, hyperinsulinemia, hypertension, and protein glycosylation resulting in the formation of advanced glycation end products (Laakso, 1999).

Extreme hyperglycemia is characterized by diabetes, blindness, neuropathy, retinopathy, CVD, and/or endothelial dysfunction (Hadi et al., 2005; Watson and Pessin, 2006). Hyperglycemia has been directly linked to increased oxidative stress due to glucose-stimulated oxidant production (King and Loeken, 2004). In turn, oxidative stress may contribute to beta cell dysfunction or injury, characteristic of type II diabetes (King and Loeken, 2004). Several large scale studies of type II diabetics have shown

that intensive treatment of hyperglycemia leads to a decrease in cardiovascular events. This was found to be more effective than treating other risk factors (such as hypertension) that affect a smaller percentage of overall diabetics (Laakso, 1999).

Glycation End Products

Hyperglycemia is also associated with the appearance of advanced glycation end products (AGEs) (Peppa and Vlassara, 2005). Nonenzymatic glycation of proteins, followed by other reactions including rearrangement, dehydration, and condensation (Wautier and Schmidt, 2004), generate irreversibly cross-linked end products. The resulting derivatives are collectively referred to as AGEs (Bierhaus et al., 1998). The process is also known as the Maillard reaction (Yamagishi et al., 2005). AGEs are specifically linked to diabetes-related micro- and macroangiopathies, such as nephropathy, retinopathy, nephropathy, and atherosclerosis (Peppa and Vlassara, 2005; Wada and Yagihashi, 2005).

The accumulation of AGEs and their collection on vessel walls is a common occurrence with normal aging and cellular damage, but AGE formation is especially rapid under diabetic conditions (Chakravarthy et al., 1998). AGEs may also be ingested or inhaled from external sources, such as processed foods and tobacco smoke (Bierhaus et al., 1998; Peppa and Vlassara, 2005). One study concluded that diabetics had an impaired ability to clear food AGEs from their system (Koschinsky et al., 1997).

AGEs are believed to act in part through a transmembrane receptor, RAGE (Yamagishi et al., 2005). It is a member of the immunoglobulin superfamily of receptors and expressed in many cells, including endothelial cells (Yonekura et al., 2003). AGEs binding with RAGE initiate a variety of signaling events, often leading to an imbalance of protein activation within other signaling pathways and undesirable outcomes. However, the AGE-RAGE interaction may actually provide a unique therapeutic measure. A splice variant of RAGE that expresses a soluble form of the receptor (still capable of binding AGE) has been shown to sequester AGEs and protect against vascular damage and hyperglycemia (Yonekura et al., 2003).

On a cellular level, the AGE-RAGE interaction may initiate signaling through MAP kinase and PI3-kinase, among others (Wautier and Schmidt, 2004). AGE

formation also increases PKC activation, which leads to hypertension through increased sensitivity to vasoconstrictors (Gugliucci, 2000). PKC mediated vascular dysfunction is also characterized by increased vascular permeability particularly associated with diabetic retinopathy, nitric oxide (NO) dysfunction, and increased VEGF expression (Sheetz and King, 2002; Yamagishi et al., 2005).

Endothelial nitric oxide synthase (eNOS) activity and NO output are both reduced by AGE bioactivity (Chakravarthy et al., 1998). AGEs amplify the effects of oxidative stress and endothelial dysfunction by sequestering NO, leading to abnormal vasorelaxation (Xu et al., 2003). AGEs may also alter the structure of proteins and lipids or create excessive cross-links within vessels, causing them to malfunction or generate an abnormal response (Peppa and Vlassara, 2005; Bansilal et al., 2007). These and other changes in the extracellular matrix may compromise cellular responsiveness to growth factors and other external stimuli (Spranger and Pfeiffer, 2001). Other signs of AGE-induced endothelial dysfunction include the significant increases in cell number, VEGF synthesis, and the kinase insert domain containing receptor (KDR) in endothelial cells exposed to AGEs (Yamagishi et al., 1997). Since AGEs have been linked to so many abnormal conditions, it is likely that they cause cellular damage long before formal disease onset (Cai et al., 2007). Appreciating the scope of AGE bioactivity represents another step towards understanding hyperglycemia and endothelial dysfunction, and more importantly, how they interact within the diabetic state.

III. Insulin Signal Transduction

Insulin signaling may follow many different courses depending on the cell type and conditions. This section will focus on elements principally associated with insulin signaling [Figure 2] (IRS-1, Shc, and GLUT4) and the following section will focus on elements associated with VEGF signaling in the endothelium [Figure 5]. Proteins common to both the insulin and VEGF signaling pathways are further described in Section V.

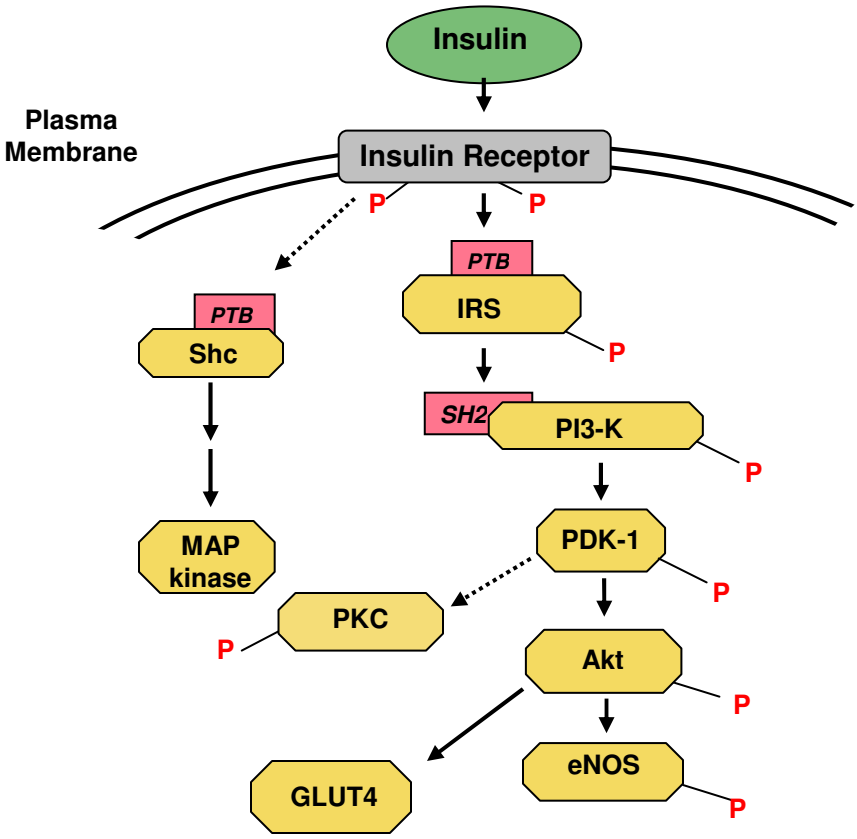

Figure 2. An overview of the insulin signaling pathway. Intracellular signaling proteins are labeled in yellow and binding domains are labeled in red. The dashed arrows indicate alternative routes of kinase activation. Insulin binding leads to phosphorylation (activation) of the insulin receptor, which in turn phosphorylates downstream effectors, particularly a family of docking proteins, insulin receptor substrates (IRS-1, for example) via its phosphotyrosine binding domain (PTB). Insulin stimulates glucose metabolism through translocation of the glucose transporter (GLUT4), gene expression through the MAP-kinase pathway, cell survival and glycogen synthesis through Akt, and vasodilator actions through eNOS production of NO.

Insulin

Insulin was discovered in 1921 by Frederick Banting and Charles Best at the University of Toronto. Their work involved treating diabetic dogs with pancreatic extracts that alleviated the dogs' symptoms (Bliss, 1982). This breakthrough was soon followed by clinical tests on humans and large scale preparations of insulin. By 1955, Frederick Sanger had deduced the primary sequence of insulin, and, in the 1960s, it became the first protein to be entirely synthesized by chemical means (De Meyts, 2004). Over the next decade, advancements in genetic engineering lead to the development of recombinant human insulin, synthesized by bacteria or yeast. By 1982, it was the first marketed recombinant DNA drug (Heller et al., 2007).

Insulin is a relatively small protein with a molecular weight of 5808 Daltons (Guyton, 2006). It is composed of 51 amino acids that make up 2 separate chains, the A-chain and B-chain, linked by two disulfide bridges (Kruger et al., 2006; De Meyts, 2004). The A-chain also contains an intrachain disulfide bridge (Guyton, 2006). As mentioned above, beta cells synthesize and store insulin that is later secreted into the hepatic portal vein and transported to the liver. The liver degrades approximately 60% of imported insulin and exports the remaining 40% into circulation (Jones, 2002).

Circulating insulin stimulates several processes including: glucose uptake by target cells, glucokinase activity, and triglyceride, protein and glycogen synthesis and storage (Kruger et al., 2006; Guyton, 2006). Insulin is also responsible for suppressing certain biological events such as glucagon secretion, glycogenolysis (through inactivation of glycogen phosphorylase), gluconeogenesis in the liver, and protein and/or fat degradation (Guyton, 2006).

Other non-metabolic functions of insulin have also been described, but are less well characterized. For example, insulin has shown mitogenic behavior in endothelial cells and early embryos (Ornskov et al., 2006). Insulin may also act as a growth factor through interactions with the type-1 insulin-like growth factor receptor (IGF-1R) (Accili et al., 1996). Experiments with insulin-deficient mice revealed that the pups exhibited growth retardation, abnormally large islets of Langerhans, diabetes, and neonatal lethality within 48 hours (Duvillie et al., 1997). This and other work has raised questions regarding the role of insulin in human intrauterine growth and development.

Insulin-like Growth Factor

Insulin-like growth factors (IGF-1 and IGF-2) and their receptor, IGF-1R, are homologous to insulin and the insulin receptor (IR) (Duvillie et al., 1997). Both insulin and IGF-1 are capable of binding to the other respective receptor (with lesser affinity) and to heterodimeric IR/IGF-1R receptors (Accili et al., 1996) that contain a pair of alpha/beta chains from the IGF-1R and a pair from the IR (Accili et al., 1996). Binding of either insulin or IGF-1 to the IGF-1R has been shown to cause downstream effects (e.g. phosphorylation of IRS-1), similar to those of insulin binding with the IR (Kaburagi et al., 1995). In mice with the IR gene knocked out, the IGF-1R was shown to mediate the activity of insulin (Accili et al., 1996). IGF-1 and IGF-2 are predicted to share some of the same functions with insulin, which may explain why similar phenotypes have been observed in animals missing either IGF-1 or insulin (Duvillie et al., 1997).

Additional experiments have documented the importance of IGFs in beta cell growth and development. One study focused on the specific functions of the IR verses IGF-1R in the growth and development of mice (Rother and Accili et al., 2000). Both receptors were deemed necessary for normal growth of neonates, as targeted knockouts of either the IR or IGF-1R were smaller than normal. Consistent with this, mice missing both receptors exhibited severe growth retardation.

The Insulin Receptor

The IR is a receptor tyrosine kinase [Figure 3] in the src family and has a high affinity for insulin binding (K_d= 0.1-1nM in non-diabetic subjects) (Ullrich et al., 1985). This multimeric glycoprotein is composed of 4 subunits: 2 alpha chains and 2 beta chains (Guyton, 2006). The IR precursor exists as a single polypeptide (coded for by one IR gene) that is cleaved and glycosylated during processing and dimerized by disulfide bonds (Ullrich et al., 1985). The alpha chains are composed of mostly hydrophilic amino acids and are located on the extracellular face. The beta chains span both extracellular and intracellular regions and contain transmembrane (hydrophobic) domains [Figure 3]. The beta chains also contain an ATP binding site, similar to that found in the src family of tyrosine kinases (Ullrich et al., 1985). The most functionally dynamic regions of the beta chains are the several serine and tyrosine

residues that may be phosphorylated as a part of IR activation by insulin (Ullrich et al., 1985).

Insulin binds in an antiparallel fashion to a specific domain on each of the alpha chains (De Meyts, 2004). This idea later expanded into the theory of receptor "crosslinking" and was confirmed by the observation of insulin binding to half of the IR dimer (De Meyts, 2004). These binding events induce a conformational change in the alpha subunit that stimulates the autophosphorylation of tyrosine residues on the beta chains (Gual et al., 2005; Kanzaki, 2006). Following activation, the insulin receptor catalyzes the phosphorylation of additional proteins, such as insulin receptor substrate-1 (IRS-1) and Shc (Gual et al., 2005).

Asparagine-proline-X-tyrosine (*NPXY*) motifs on the beta chains are important sites of molecular recognition on the insulin receptor (Kaburagi et al., 1995). The autophosphorylated tyrosine residue, Tyr^{960}, in one such *NPXY* motif is essential for the recognition and subsequent tyrosine phosphorylation of IRS-1 and Shc (Wolf et al., 1995). One study demonstrated that exchanging Tyr^{960} for a different amino acid led to a cessation of interaction between the IR and IRS-1 (Kaburagi et al., 1995). This further established tyrosine phosphorylation as the second event (after insulin binding) in the insulin signaling cascade. Experiments implementing specific changes within the *NPXY* motif showed that the asparagine was the amino acid of second most importance (Kaburagi et al., 1995). Alterations in the sequence flanking Tyr^{960} also have an impact on the binding affinity of other insulin receptor substrates containing phosphotyrosine binding (PTB) domains (van der Geer et al., 1999). Thus, single replacements in the amino acid sequence of the insulin receptor can alter substrate specificity and all associated downstream signaling events. The *NPXY* motif is also present in the binding sites of other receptor tyrosine kinases, such as epidermal growth factor (EGF) receptor and the IGF-1 receptor (Kaburagi et al., 1995).

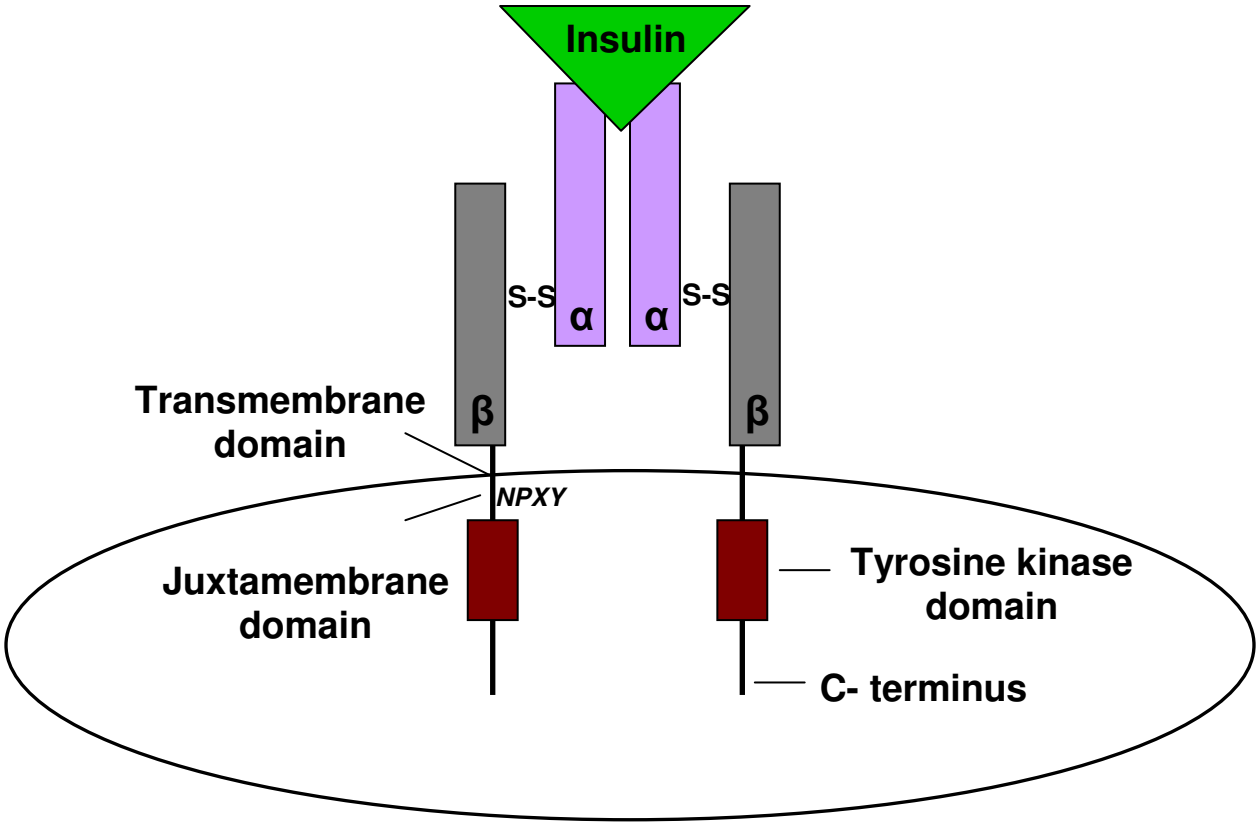

Figure 3. A schematic of the insulin receptor tyrosine kinase. Extracellular alpha subunits are linked by disulfide bonds to transmembrane beta subunits. Insulin binds to the alpha subunits, which leads to receptor autophosphorylation. The *NPXY* motif is critical for normal signal transduction and interaction with IRS-1.

Insulin Receptor Substrate-1

After insulin activates the IR, IRS-1 binds to the Tyr^{960} autophosphorylation site of the IR (Gual et al., 2005). IRS-1 is a hydrophilic, cytoplasmic, docking protein that binds to the IR tyrosine kinase through its N-terminal PTB domain. Its primary function is to mediate the association between the IR and downstream effector molecules (van der Geer et al., 1999). The IRS-1 PTB domain is also capable of interacting with activated IGF-1 receptor (Thirone et al., 2006). Another IRS-1 domain of importance is the pleckstin homology (PH) domain. While its specific purpose is unknown, its presence is necessary for a normal signal response, (Thirone et al., 2006).

IRS-1 also contains several serine and tyrosine phosphorylation sites that are essential for downstream signaling events (Thirone et al., 2006), such as those with PI3-K and Shc [Figure 4]. Most of these phosphotyrosine sites are within the Tyrosine-Methionine-X-Methionine (*YMXM*) or Tyrosine-X-X-Methionine motifs (*YXXM*) (Myers et al., 1993). IRS-1 contains over 20 tyrosine and 30 possible serine/threonine total phosphorylation sites (Gual et al., 2005; Sun et al., 1991). Phosphorylation at these sites is not only critical for IRS-1 metabolic and mitogenic activity, but also important for IRS-1 facilitated intracellular feedback mechanisms that materialize after external stimulation (Luo et al., 2007). For example, the Luo et al. (2007) study showed phosphorylation at $Serine^{629}$ created a positive feedback response after insulin signaling. Similarly, phosphorylation at $Serine^{636}$ led to inhibition of IRS-1 association with PI3-kinase,

IRS-1, as its name implies, is phosphorylated by the tyrosine kinase domain of the insulin receptor (Kaburagi et al., 1995). These phosphorylated tyrosines on IRS-1 create potential docking sites that bind various Src homology 2 (SH2) domain proteins (Watson and Pessin, 2006). For example, IRS-1 interacts with the SH2 domain in the p85 subunit of PI3-kinase, as well as other SH2 domains, including that in the adaptor protein, growth factor receptor-bound protein 2, or Grb2 (Chuang et al., 1994; Thirone et al., 2006). IRS-1 has been specifically linked to insulin-induced vasodilation. This is supported by studies by Montagnani et al. (2002) in which the authors created IRS-1 knockout mice that displayed hypertension and abnormal aortic relaxation.

There are six known insulin receptor substrate isoforms (Bjornholm and Zierath, 2005). Each variant has distinct functions and effects on downstream events. IRS-1 and IRS-2 are the most common isoforms described in the context of insulin signaling, with IRS-1 being more prevalent in fat and muscle cells (Thirone et al., 2006). IRS-1 also differs from IRS-2 in its interactions with Akt, PKC, components of the MAP kinase pathway, and the glucose transporter-4, GLUT4 (Thirone et al., 2006; Bjornholm and Zierath, 2005). Some isoforms have not been isolated in the human genome, such as IRS-3, an IRS variant only found in rodents (Thirone et al., 2006). Studying these isoforms is at the forefront of current research into insulin resistance, as IRS-1 and others have been implicated in the onset of insulin resistance and type II diabetes.

In addition to its metabolic roles, IRS-1 is necessary for optimal embryonic growth and development (Accili et al., 1996). Mice with the IRS-1 gene knocked out were growth retarded, in addition to showing signs of insulin and IGF-1 resistance (Araki et al., 1994). In another study, mice lacking the IRS-1 gene displayed hypertension, endothelial dysfunction, and insulin resistance (Abe et al., 1998). These observations suggested that the behavior of IRS-1 (and other IRS isoforms) in different signaling pathways may vary depending on the ultimate biological function of that pathway. For example, Tamemoto et al. (1994) determined that both IRS-1 dependent and IRS-1 independent pathways involving insulin and IGFs are important for normal insulin signaling transduction. Therefore, IRS-1 is capable of mediating the effects of insulin, including pre- and post-natal growth and glucose metabolism, through both the IR and IGF-R.

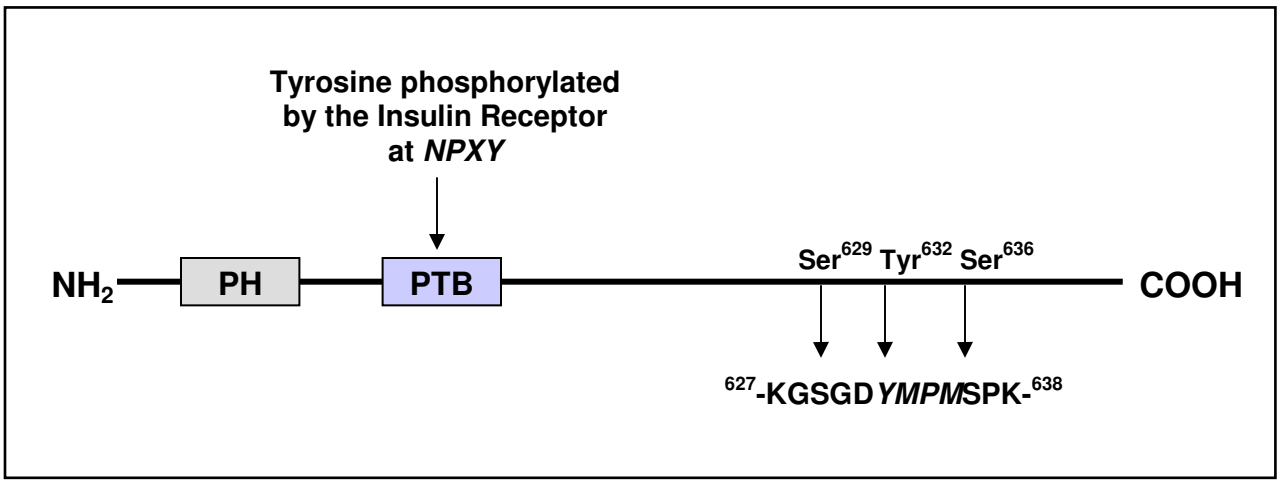

Figure 4. Schematic diagram of IRS-1. Amino acid sequence of an activation/regulatory site is included. Regions of importance include the N-terminal pleckstrin homology (PH) domain, the phosphotyrosine binding (PTB) domain, and several phosphorylation sites at the C-terminus. In particular, phosphotyrosine sites coordinate interactions between IRS-1 and substrates, such as PI3-kinase, Shc and other downstream effectors. Tyrosine^{632} phosphorylation is an important SH2 recognition site for the IRS-1 association with PI3-kinase. Regulatory sites, Serine^{629} and Serine^{636}, flanking Tyrosine^{632} have positive and negative effects respectively, on insulin signaling through IRS-1.

Src homology collagen (Shc)

Shc is a cytoplasmic substrate of receptor tyrosine kinases that has a PTB (homologous to the PTB domain in IRS-1) and SH2 domains (Wolf et al., 1995). Shc exists as one of three possible isoforms ranging in size between 46 and 66-kDa (Bevan, 2001). Similar to IRS-1, Shc recognizes phosphotyrosines that are components of conserved sequences, such as the *NPXY* motif (Wolf et al., 1995). In addition to the IR, Shc binds phosphotyrosines on Trk (nerve growth factor) receptors and the IGF-1R (van der Geer et al., 1999; Tamemoto et al., 1994). The IR preferentially activates IRS-1 after insulin binding; however, one study demonstrated that a single amino acid change in the IR (IR Ser^{955} was replaced with an isoleucine) altered the IR preference from IRS-1 to Shc (van der Geer et al., 1999). This verified two hypotheses: one, that conserved (e.g. PTB) domains often have multiple points of action in signaling cascades and, two, that slight changes in the binding location of signaling substrates can completely alter their binding affinities and biological responses (van der Geer et al., 1999).

Once Shc is phosphorylated, it binds and activates downstream SH2 domain containing proteins. Shc primarily interacts with SH2 domain of Grb2, which leads to the activation of the Ras/MAP kinase pathway and increased mitogenic activity (Saltiel and Kahn, 2001; Montagnani et al., 2002).

Glucose Transporter 4

GLUT4 is one of twelve known members of the GLUT family (Kanzaki, 2006). This intracellular transport protein is the most abundant glucose transporter in both muscle and adipose tissue (Thirone et al., 2006). GLUT4 is responsible for transporting glucose into these tissues after a meal (Watson and Pessin, 2006). The use of a transporter is necessary as glucose is too large and hydrophilic to freely diffuse through the plasma membrane at an adequate rate. GLUT4 is rapidly translocated to the cell plasma membrane after insulin binding and activation of Akt through PI3-kinase (Roach, 2002; Chang et al., 2004). After blood glucose levels have decreased, GLUT4 is internalized and recycled (Watson and Pessin, 2006). In the basal state, GLUT4 vesicles continuously cycle between intracellular compartments and the plasma membrane (Ishiki and Klip, 2005). Cytoskeletal elements are partially responsible for

GLUT4 trafficking through connecting signaling proteins or directing the passage of vesicles throughout the cell (Chang et al., 2004). Experimental evidence has confirmed these effects, as malfunctioning actin filaments and/or microtubules impair the translocation efficiency of GLUT4 (Kanzaki, 2006). The TC10 pathway regulates changes in cortical actin necessary for GLUT4 translocation (Chang et al., 2004). Therefore, integration of the TC10 and other signaling pathways, effector molecules, and physiological conditions may alter the GLUT4 response to insulin (Watson and Pessin, 2006). Many of these mechanisms remain incompletely understood, and glucose transporter trafficking studies continue to be an important part of diabetes research.

Insulin signal transduction through the IR is extremely complex and capable of initiating several physiological processes. Even within the small portion of the insulin signaling cascade presented in this review, there are several points of possible crosstalk and interaction between effector proteins. Insulin signaling through the IR exhibits both metabolic and mitogenic behavior, as well as feedback communication that either enhances or suppresses insulin activity.

IV. The VEGF Signaling Pathway

The regulation of normal angiogenesis and maintenance of the endothelium is also complex [Figure 5] and incorporates many of the same mechanisms (e.g. phosphotyrosine activation, specific binding domains, and multiple routes to the same outcome) seen in insulin signaling.

VEGF binding to KDR leads to receptor dimerization and autophosphorylation on select tyrosine residues (Kliche and Waltenberger, 2001). These phosphotyrosines provide targets for interaction with a number of SH2, SH3, and PTB domain containing proteins (Claesson- Welsh, 2003). These proteins include PLC-γ, PI3-kinase, and Src tyrosine kinases [Figure 5]. From VEGF stimulation of these, separate or mutual signaling pathways may be activated (Kliche and Waltenberger, 2001).

Homeostatic VEGF signaling is also important for normal embryonic development, wound healing, maintenance of the female reproductive tract, bone growth, and tissue regeneration (Robinson and Stringer, 2001; Leung et al., 1989).

Several conditions point to abnormal angiogenesis as the central process in disease development and progression, including: tumor diseases, retinopathies, chronic inflammatory diseases, rheumatoid arthritis, preeclampsia in women, psoriasis, macular degeneration, and other abnormal cardiovascular events (Kendall and Thomas, 1993; Shibuya, 2003).

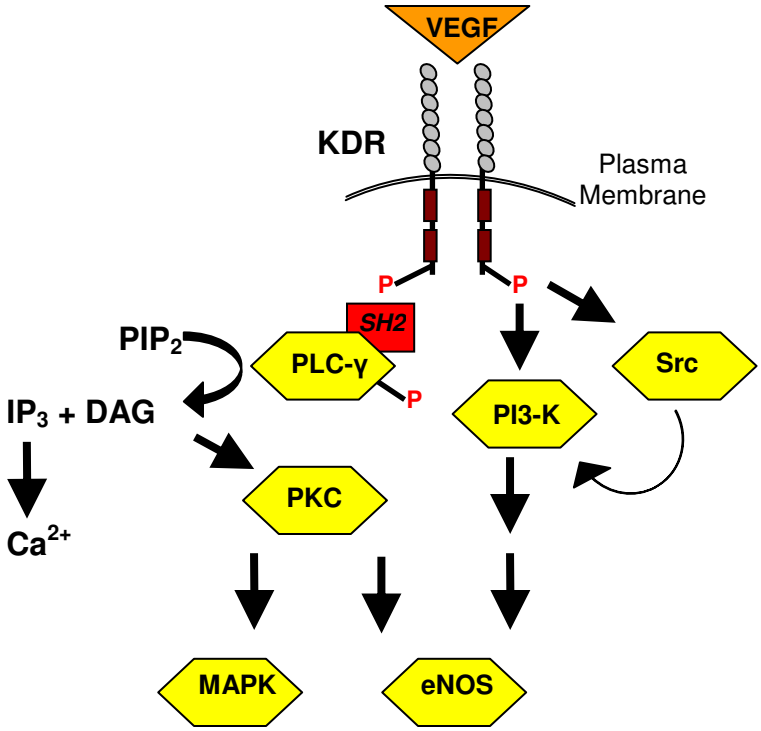

Figure 5. Portion of the VEGF signaling pathway reviewed in section IV. VEGF binding to KDR leads to receptor phosphorylation. Activated KDR is capable of interacting with several downstream effectors, notably phospholipase C-γ, phosphoinositide 3-kinase, and Src.

Vascular Endothelial Growth Factor

VEGF is a secreted mitogen that regulates endothelial cell growth, proliferation, and survival. It was originally described as vascular permeability factor because of its ability to induce hyperpermeability in blood vessels (Dvorak, 2002). VEGF also mediates endothelial cell migration, attachment, and scaffolding, including tissue invasion and repair, *i.e.*, the cellular phenomena that comprise angiogenesis (Ahmed et al., 2000). Experimental evidence has confirmed the necessity of VEGF during vasculogenesis in the developing embryo (Kliche and Waltenberger, 2001). This was demonstrated in rodents, as the deletion of a single VEGF allele led to embryonic mortality (Tsatsaris et al., 2003). VEGF also functions as a cytokine, or a soluble chemical messenger, with either autocrine or paracrine activities (McKeeman et al., 2004). Although primarily shown to affect endothelial cells, *in vitro* studies have validated that VEGF is capable of interacting with epithelial cells, pancreatic duct cells, and Schwann cells (Ferrara, 2001). As a result, VEGF activity in these cells instigates cell-specific functions that are often distinct from those associated with VEGF signaling in the endothelium (Robinson and Stringer, 2001).

The VEGF family of disulfide linked homodimeric glycoproteins belongs to the platelet derived growth factor (PDGF) superfamily and is composed of five VEGF members: VEGF-A, -B, -C, -D, and –E (also known as *orf*-virus derived VEGF), and placental growth factor (PlGF) (Dvorak, 2002; Ferrara et al., 2003). VEGF isoforms of these family members are splice variants with distinct properties. For instance, six different isoforms have been characterized for human VEGF-A alone, including: $VEGF_{121}$, $VEGF_{145}$, $VEGF_{165}$, $VEGF_{183}$, $VEGF_{189}$, and $VEGF_{206}$ (Ferrara et al., 2003). Some of these, such as $VEGF_{165}$, are more predominant and observed as having greater biological potency than others (Ferrara, 2001). The pathological significance of the different VEGF-A isoforms is indicated by the findings that $VEGF_{121}$ and/or $VEGF_{165}$ overexpression leads to intracerebral bleeding in the presence of brain tumors, while $VEGF_{189}$ does not (Cheng et al., 1997).

VEGF expression varies over time and physiological conditions (Kendall and Thomas, 1993). For example, VEGF-A is upregulated early in embryonic development, during hypoxia, and in tumors. Specifically, VEGF-A levels have been associated with

tumor size, malignant potential, metastasis, and survival (Dvorak, 2002). As is the case in this review, researchers are typically describing VEGF-A when they refer to VEGF, since it mediates most of the signaling related to endothelial growth and survival (Ferrara et al., 2003). VEGF-B expression is high during cardiac embryogenesis and in the adult heart and spinal cord (Matsumoto and Claesson-Welsh, 2001). VEGF-C is associated with lymphangiogenesis, and VEGF-D, like VEGF-A, appears to illicit a primarily mitogenic response (Kliche and Waltenberger, 2001). Humans or animals infected with parapoxvirus, *orf*, are characterized by excessive endothelial proliferation and vessel dilation presumably mediated by VEGF-E (Kliche and Waltenberger, 2001; Shibuya, 2003). This study also recommended VEGF-E as a potential contender for use in pro-angiogenic therapies (Shibuya, 2003). VEGF isoforms interact with VEGF related receptors (described below) with varying affinities and lead to a wide array of physiological responses.

The value of VEGF as a therapeutic target or agent in treating vascular pathologies remains to be fully understood. However, since VEGF is central to many vascular processes, it comes as no surprise that it is a major area of study. Current clinical trials are testing the use of neutralization and/or inhibition of VEGF as a means of countering increased VEGF activity associated with tumor formation and growth (Wu et al., 2000; Ferrara et al., 2003). In fact, specific VEGF-A inhibitors are already being used to treat colorectal cancers in the US (Hurwitz et al., 2004). Local VEGF concentrations are also high in the aqueous and vitreous humors of patients with diabetic retinopathy (Ferrara, 2001). The intraocular neovascularization that occurs during retinopathy and age-related macular degeneration have underlined the importance of VEGF inhibitors as therapies for these diseases (Ferrara, 2001). Utilizing VEGF as a biomarker for certain disease conditions may also prove to be a viable alternative for early diagnosis and treatments (Dvorak, 2002).

Vascular Endothelial Growth Factor Receptors

VEGF-A isoforms primarily interact with two homologous transmembrane tyrosine kinase receptors: Flt-1 (*fms*-like tyrosine kinase, VEGFR-1) and KDR (kinase insert domain containing receptor, VEGFR-2 [Figure 6], the human homologue of

murine fetal liver kinase, Flk-1). These receptors are composed of immunoglobulin (Ig)-like extracellular domains, a transmembrane domain, a tyrosine kinase domain with a kinase-insert region, and a carboxy-terminal tail region (Ferrara et al., 2003). The second and third Ig-like domains are most critical for VEGF binding, while the other domains are important for receptor dimerization and ligand retention (Robinson and Stringer, 2001). The intracellular domains of Flt-1 and KDR are very similar and contain several homologous phosphorylation sites for binding with specific substrates or adapter proteins that contain SH2, SH3, or PTB domains (Matsumoto and Claesson-Welsh, 2001). Phosphorylation of downstream proteins is often required for the activation or suppression of subsequent responses.

VEGF receptor expression and activity is dependent upon cell type, developmental stage, and local cellular conditions (Ferrara et al., 2003). Flt-1 expression is highest in the developing embryo and quiescent endothelium of adult organs (Peters et al., 1993). Though primarily expressed in the endothelium, Flt-1 is found in renal mesangial cells, trophoblast and choriocarcinoma cells, and vascular smooth muscle cells. Likewise, KDR is also present in non-endothelial cells, such as fetal liver cells, retinal progenitor cells, and pancreatic duct cells (Matsumoto and Claesson-Welsh, 2001; Waltenberger et al., 1994). KDR expression escalates in the presence of proliferating vessels (notably in vasculogenesis during early gestation), hypoxic conditions, and after positive feedback signaling from high levels of VEGF (Ahmed et al., 2000). Negative regulation of VEGF signaling by phosphatases also plays a part in receptor kinase activity. It has been predicted that the VEGF receptors activate tyrosine phosphatases through a negative feedback mechanism, though this concept has not been fully explored (Wong et al., 2000).

Though structurally homologous, it is clear that Flt-1 and KDR interact with different isoforms of VEGF and affect distinct intracellular substrates, which lead to independent physiological responses (Waltenberger et al., 1994). Flt-1 binds with PlGF and VEGF-B (Ferrara et al., 2003), while KDR is activated by VEGF-C, and –D and exclusively binds with VEGF-E, which specifically induces endothelial cell proliferation (Shibuya, 2006). VEGF-A is capable of high affinity binding to Flt-1 (K_d = 10 pM) and lower affinity interactions with KDR (K_d = 75-125 pM); however, the bioactivity of VEGF-

A is much more pronounced through KDR activation, rather than Flt-1 (Claesson-Welsh, 2003).

Traditionally, Flt-1 has been implicated in the negative regulation of angiogenesis and monocyte migration (Robinson and Stringer, 2001; Kliche and Waltenberger, 2001). There is some controversy over the functions of Flt-1 and whether or not it acts as a "decoy receptor" to the primary signaling receptor, KDR (Ferrara, 2001). However, several studies have supported this theory by showing a link between Flt-1 overexpression and decreased endothelial cell proliferation by KDR (Matsumoto and Claesson-Welsh, 2003). With respect to pathological angiogenesis, studies have uncovered a link between Flt-1 signaling and rheumatoid arthritis and atherosclerotic associated inflammation (Sawano et al., 2001). Also, wild-type mice showed increased metastasis and growth of some tumors compared to Flt-1 null mice (Hiratsuka et al., 2001). These results confirm the importance, through incompletely understood mechanisms, of Flt-1 as a contributor to these conditions.

Though all of the functions of these two receptors have yet to be determined, it is commonly accepted that both receptors are vital for normal angiogenic growth and development. Mice knockouts missing Flt-1 die *in utero* from excessive endothelial cell proliferation and vascular disorganization (Wu et al., 1999), consistent with the notion that Flt-1 down-regulates VEGF activity in embryogenesis. Intrauterine death also occurs in KDR-null mice due to deficient vasculogenesis (Shalaby et al., 1995).

Since signaling through KDR is necessary for most VEGF induced biological responses, the remainder of this review will concentrate on the VEGF signaling cascade through KDR. KDR is originally synthesized as a 150-kDa polypeptide before posttranslational glycosylation into a mature protein of 230-kDa (Shibuya, 2003). The second and third Ig-like domains on the extracellular portion of KDR are the ligand binding regions, similar to the ligand binding domains of other platelet derived growth factor receptors (Shibuya, 2003). The C-terminal region of KDR contains six highly conserved tyrosine residues that are autophosphorylated following VEGF binding. These phosphotyrosines are targets for binding with SH2, SH3, and PTB containing protein kinases (Kliche and Waltenberger, 2001). Certain sites have been linked to

specific signaling events, such as phosphor-tyrosine^{1175}, which binds to the C-terminal SH2 domain of phospholipase C-γ (Shibuya, 2003).

KDR is principally associated with VEGF signal transduction leading to endothelial cell differentiation, proliferation, survival, and the release of NO (Wu et al., 1999; Kroll and Waltenberger, 1999). Because of this, KDR, in addition to Flt-1, presents a unique therapeutic target for conditions distinguished by excessive neovascularization. Since KDR expression is highly correlated with tumor size, it is already being considered a viable target for anti-cancer/anti-angiogenic therapies (Shibuya, 2006).

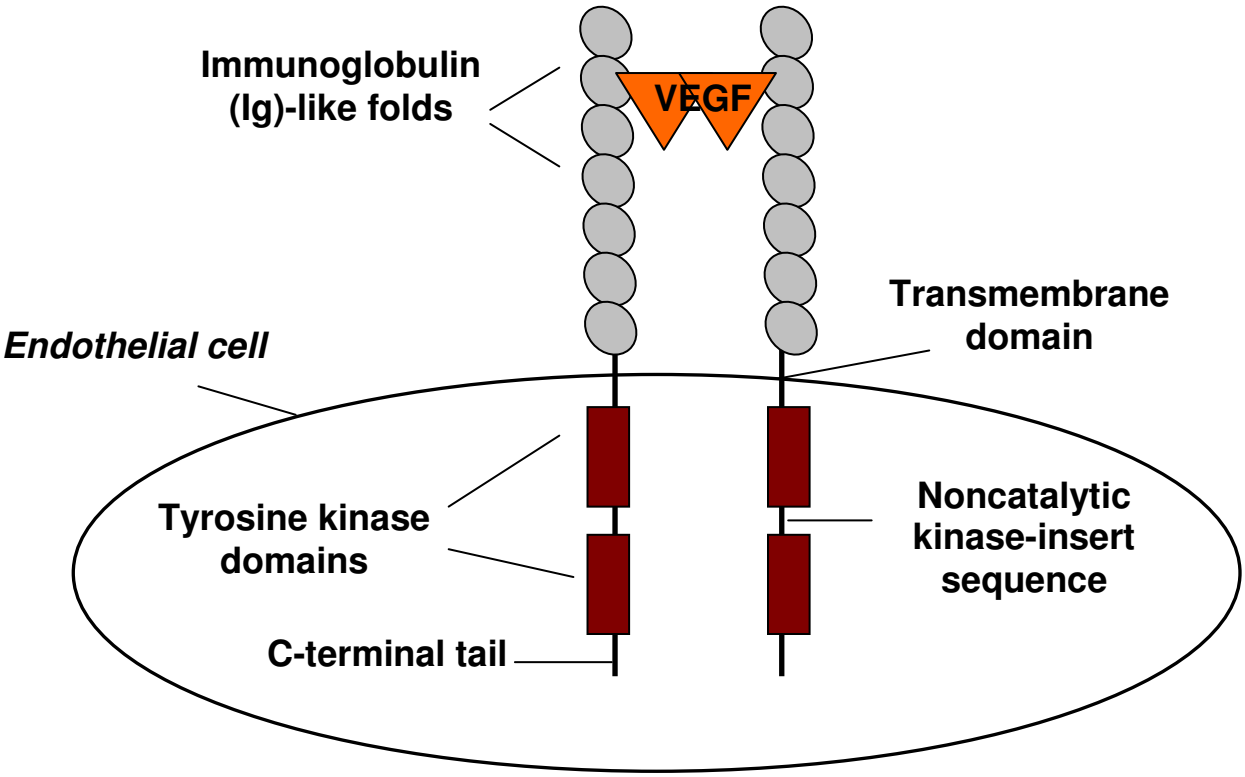

Figure 6. Domain structure of KDR (VEGFR-2). The KDR homodimer has an extracellular segment with seven Ig-like domains, a transmembrane domain, and intracellular kinase domains responsible for relaying signals from an extracellular binding event. Specifically, binding of the VEGF dimer leads to receptor dimerization and autophosphorylation of specific tyrosine residues.

Phospholipase C-γ

There are several known isoforms of phospholipase C, but VEGF stimulation leads to phosphorylation of PLC- γ1 or PLC- γ2 (Chattopadhyay et al., 1999). PLC-γ1 (145-kDa) contains two SH2 domains and a SH3 (Src homology 3) domain, and is phosphorylated following VEGF binding to KDR (Matsumoto and Claesson-Welsh, 2001). Phosphorylated KDR (tyrosine^{1175}) interacts directly with the C-terminal SH2 domain of PLC-γ to promote cell migration, proliferation, and other cellular effects (Wu et al., 2000; Takahashi et al., 2001). Mice with a phenylalanine substitution for their corresponding Tyr^{1175} residue experienced embryonic lethality from insufficient vasculogenesis (Shibuya, 2006). Aside from this direct interaction with KDR, PLC-γ may also be activated by Src (He et al., 1999).

PLC-γ activation leads to hydrolysis of phosphatidylinositol 4,5 bisphosphate (PIP_2) to inositol 1,4,5-triphosphate (IP_3), which releases internally stored calcium (Ca^{2+}), and diacylglycerol, which activates certain PKC isoforms [Figure 5 and Section V]. PKC activation engages the Raf-Mek-MAPK pathway that advances gene expression, cell proliferation, and angiogenesis (Shibuya, 2003). Ca^{2+}, in addition to other eNOS stimuli, mediates vascular permeability through NO release (Matsumoto and Claesson-Welsh, 2001; Dvorak, 2001). Ahmad et al. (2006) showed that phosphorylation of PLC-γ Tyr^{771} led to an increase in NO production.

In summary, VEGF activation of its primary signal transducing receptor tyrosine kinase, KDR, may lead to the stimulation of different intracellular signaling pathways. These pathways induce the necessary processes of endothelial survival, proliferation, and migration. A balance between available VEGFs and receptors is vital for normal development and disease prevention. Since several disease conditions are linked with VEGF and KDR expression, they may prove to be critical biomarkers or lead to the discovery of novel therapeutic agents.

V. Potential Sites of Insulin and VEGF Signaling Crosstalk

Though VEGF and insulin interact with discrete tyrosine kinases receptors and elicit some unique signaling responses, many effector molecules are used in both

pathways and lead to similar responses. More specifically, both pathways use elements of the PI3-kinase/Akt, eNOS, PLC-γ/PKC, and MAP kinase signaling cascades.

For example, both insulin and VEGF signaling may lead to eNOS activation and production of NO (Zeng et al., 1999; Li et al., 2002). Feliers et al., (2002) conducted a study using glomerular endothelial cells and found that VEGF signaling through the PI3-kinase/akt and PI3-kinase/extracellular signal-regulated protein kinase (ERK) pathways led to eNOS activation and NO production. This same group also noted a VEGF-stimulated association of IRS-1 with KDR, which they predicted was a strategy used by these cells to increase the eNOS response and other KDR mediated effects (Feliers et al., 2005). A study using kidney epithelial cells (Senthil et al., 2002) originally proposed the idea of IRS-1 interaction with VEGF activated KDR and an associated increase in IRS-1/PI3-kinase activation in endothelial cells. IRS-1 has also been reported to have a role in tumor angiogenesis, including the ability to increase VEGF expression through IGF-1/IGF-1R signaling (Neid et al., 2004)

Since crosstalk between the insulin and VEGF signaling pathways is a relatively unexplored concept, the possible physiological effects of pathway interactions have yet to be fully determined. However, initial observations have led to the following conclusions: insulin leads to increased VEGF expression through the PI3-kinase/Akt and MAP kinase pathways, insulin plays a role in regulating VEGF expression in response to hypoxia, and IRS-1 interaction with KDR triggers increases in protein synthesis (Jiang et al., 2003; Senthil et al., 2002). Current knowledge of insulin and VEGF crosstalk is extremely limited by cell type and treatment; however, results from these few studies have already challenged investigators to further explore the effects of VEGF and insulin interactions and how they lead to certain disease states.

The subsections below highlight some of the possible effector molecules shared by the insulin and VEGF signaling cascades.

Phosphatidylinositol 3-Kinase

PI3-K is one of the most biologically important signaling molecules in a cell. It is a versatile protein kinase composed of two subunits: the regulatory p85 subunit and the catalytic p110 subunit (Krasilnikov, 2000). The p85 subunit contains two SH2 domains

and a single SH3 domain (Sun et al., 1991). The SH2 domains have phosphotyrosine binding pockets that, similar to PTB domains, recognize and bind phosphorylation sites within specific amino acid motifs, including sites found in IRS-1 (van der Geer et al., 1999; Bjornholm and Zierath, 2005). The p110 subunit is activated after the p85 subunit of PI3-K binds to IRS-1 (Montagnani et al., 2002) leading to phosphorylation of phosphatidylinositols at ring position 3 and the formation of lipid products, including the second messenger phosphatidylinositol 3, 4, 5,-trisphosphate (PIP_3) (Bjornholm and Zierath, 2005).

Recent experiments have demonstrated that PI3-K is necessary for mediating several signaling pathways. In the insulin pathway, PI3-K has been implicated in the translocation of GLUT4 (via Akt or atypical PKCs) (Welsh et al., 2005; Kanzaki, 2006), nitric oxide (NO) stimulated vasodilation, and other insulin-mediated metabolic functions (Montagnani et al., 2002). PI3-K is also regulates several other processes, including: cell proliferation and differentiation, apoptosis, formation and degradation of proteins, lipids, and carbohydrates, and cytoskeletal movement (Krasilnikov, 2000).

Prosurvival effects are another outcome of PI3-kinase activation (Gerber et al., 1998). Antiapoptotic actions, a result of activating the PI3-kinase/Akt pathway, are executed by Akt phosphorylation and consequent suppression of the proapoptotic factors BAD (Bcl-2/Bcl-X antagonist) and Caspase-9 (Cardone et al., 1998). KDR association with Src may also stimulate PI3-kinase activity (Waltenberger, et al., 1994). Studies show activation of PI3-kinase as a signaling event independent of VEGF signaling through PLC-γ, which explains the different responses associated with each (Wu et al., 1999). Signaling through PI3-K also stimulates cell motility and increases NO production, as described below.

Phosphoinositide Dependent Kinase-1

Phosphoinositide-dependent kinases are a collection of serine-threonine kinases that are activated by the lipid products of PI3-K, which may be activated by insulin or VEGF (Krasilnikov, 2000). Similar to other members of the cAMP-dependent, cGMP-dependent and protein kinase C (AGC) protein kinase family, PDK-1 contains a C-terminal PH domain (Hanada et al., 2004). Activated PDK-1 can then phosphorylate

downstream protein kinases, such as PKC, PKC-related kinase, Akt, and others (Sonnenburg et al., 2001). Specifically, PDK-1 is implicated in insulin signaling through its ability to activate either Akt or the atypical forms of PKC in the course of GLUT4 translocation (Krasilnikov, 2000; Montagnani et al., 2002).

One study using endothelial cells found that overexpression of PDK-1 leads to an increase in NO production by eNOS. Appropriately, overexpression of a PDK-1 inactive mutant led to a significant reduction of NO levels (Montagnani et al., 2002). In contrast, ES cells with PDK-1 deletions showed an inhibition of Threonine^{308} phosphorylation and Akt activity (Williams et al., 2000).

Protein Kinase C

PKC is another common signaling intermediate involved in multiple processes, such as glucose regulation, gene expression, and cell proliferation and differentiation (Ishisaki et al., 2004; Farese et al., 2005). PKC is activated by PLC-γ (as described in section IV above), the lipid products of PI3-K (e.g. PIP_3), as well as PDK-1 phosphorylation (Watson and Pessin, 2006; Sonnenburg et al., 2001). There are at least 11 known isoforms in the PKC family, each with different modes of activation and distinct functions in various cell types (Ishisaki et al., 2004).

The two isoforms usually associated with the metabolic functions of insulin signaling are the 'atypical' (aPKCs) forms, PKC-**λ** and PKC-ζ. These two members of the PKC family contain a kinase domain that catalyzes the serine/threonine phosphorylation of Akt (Sonnenburg et al., 2001). For instance, phosphorylation of these isoforms has been detected in adipocytes stimulated with insulin (Sonnenburg et al., 2001). For optimal catalytic activity, PKC-ζ should be phosphorylated by PDK-1 on Threonine^{410} (Neid et al., 2004).

Recent studies have confirmed the importance of aPKCs in insulin stimulated glucose transport (Farese et al., 2005). However, it should be noted that aPKCs react in a tissue-specific manner, which also determines whether or not IRS1 activity is required (Farese et al., 2005). There has also been recent evidence that other PKC isoforms, including both novel and conventional PKCs, may substitute for those in short supply (either down-regulated or knocked out) (Farese et al., 2005). In addition,

abnormalities in the activity of PKC-**λ** and/or PKC-**ζ** have been implicated in insulin resistance (Kanzaki, 2006), obesity, atherosclerosis (Ishisaki et al., 2004), and type II diabetes (Farese et al., 2005).

A 2001 study by Takahashi et al. revealed that PLC-γ activation (immediately following VEGF stimulation and activation of KDR) favors the PKC-β form and stimulation of the Raf-MAP kinase pathway. Alternatively, activation of PLC-γ may also lead to PKC mediated upregulation of eNOS (Li et al., 2002).

Akt

Akt, or protein kinase B (PKB), is a serine/threonine kinase predominantly known for its anti-apoptotic effects. It also functions in cell proliferation and motility, NO production, glycogen synthesis, gluconeogenesis, glucose metabolism through GLUT4 translocation, and other cellular responses (Bjornholm and Zierath, 2005; Franke, 2008). One study of Akt in endothelial cells concluded that insulin was equally effective at downregulating apoptosis as VEGF (Hermann et al., 2000). These investigators also verified that the prosurvival effects of insulin-stimulated Akt were PI3-kinase dependent, as was phosphorylation/inhibition of caspase-9.

Akt is a member of the AGC protein kinase superfamily and has three isoforms, each encoded by an independent gene (Lawlor and Alessi, 2001). These isoforms have been individually linked to various functions and disorders, while remaining structurally similar (Franke, 2008). Each Akt isoform is composed of an N-terminal PH domain connected by a hinge region to a kinase domain (that contains Thr^{308}) and a C-terminal kinase catalytic region with hydrophobic tail (that contains Ser^{473}) (Lawlor and Alessi, 2001). The PH domain is a binding site for phosphoinositides and is important for recognition by upstream effectors (Hanada et al., 2004).

Akt has two primary sites, Thr^{308} and Ser^{473}, that are typically phosphorylated after insulin, IGF-1, or VEGF stimulation [Figure 7] (Watson and Pessin, 2006). Specifically, PDK-1 has been shown to phosphorylate Thr^{308} within the insulin signaling cascade (Montagnani et al., 2002; Sen et al., 2003). The mechanism behind Ser^{473} phosphorylation is less well defined. Akt may be directly activated through the serine/threonine phosphorylation sites on IRS-1 or through other kinases (Bjornholm

and Zierath, 2005). Interestingly, Akt may also phosphorylate IRS-1 and heighten the effects of insulin stimulation through a positive feedback response via phosphorylation of Ser^{629} (Gual et al., 2005; Luo et al., 2007).

Akt dysfunction has been linked to hyperinsulinemia, hyperglycemia, and diabetes, as well as cancer and other disease conditions (Sen et al., 2003). Akt knockouts show impaired glucose uptake and diabetes (Welsh et al., 2005). In a different study, several members from the same family carried a missense mutation in the gene encoding Akt2 (George et al., 2004). These individuals displayed severe hyperinsulinemia and diabetes mellitus (George et al., 2004). Though Akt mutations are an unusual culprit for instigating most cases of diabetes, the study supported the concept that Akt is indispensable for normal insulin activity.

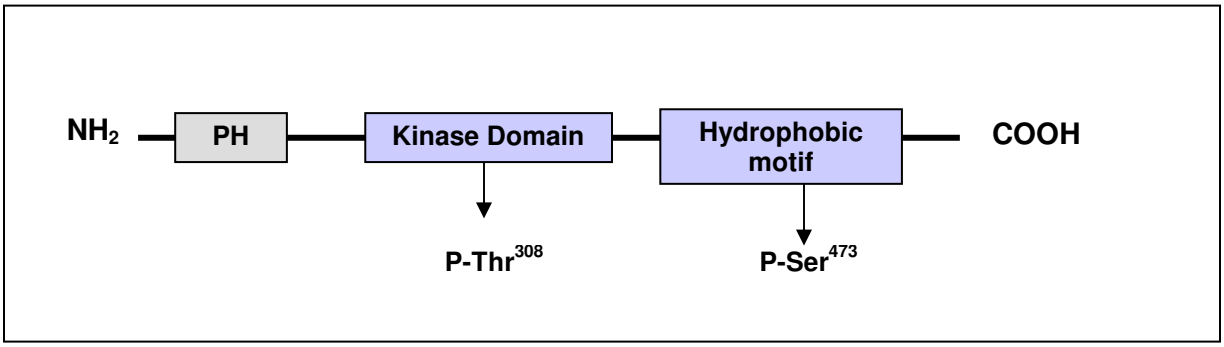

Figure 7. Domain structure of Akt1 with key phosphorylation sites indicated. Phosphorylation of the threonine residue within the kinase domain is essential for full Akt activity. Likewise, all AGC kinases contain a central kinase domain and require phosphorylation of a specific serine/threonine residue within the HM motif for a complete Akt response.

Endothelial Nitric Oxide Synthase and Nitric Oxide

eNOS is responsible for the production of NO in the endothelium. NO is a gaseous molecule that is required for vasodilation, as well as maintaining and protecting the endothelium (Li et al., 2002). Shear stress or outside stimuli (e.g. growth factors or hormones) can activate eNOS, which leads to NO diffusion into vascular smooth muscle tissue and vessel relaxation (Rask-Madsen, 2007).

Insulin stimulates NO release through phosphorylation of eNOS on Ser^{1177} by Akt. This event activates enzymatic activity and secondarily upregulates transcription of eNOS (Federici et al., 2004). Human endothelial cells treated with insulin showed a marked increase in NO production and eNOS protein expression (Li et al., 2002). In addition to phosphorylating and inactivating proapoptotic factors, VEGF-mediated PI3-kinase activation can also elevate eNOS expression levels (Matsumoto and Claesson-Welsh, 2001; Li et al., 2002).

VEGF induced activation of eNOS (via PI3-kinase/Akt or PLC-γ/PKC) leads to some of the most important known physiological responses supplied by endothelial cells. NO functions in most endothelial cell activities including angiogenesis, cell proliferation, motility, and increased permeability. Blanes et al., (2006) reported that phosphorylation of Tyr^{801} on KDR as a requirement for Akt stimulation of eNOS. Others have also confirmed the necessity of KDR activation for eNOS activity and Akt for phosphorylation at Ser^{1177} (Hanada et al., 2004; Feliers et al., 2005).

Abnormalities in eNOS function or expression can result in a lack of NO, which can lead to the appearance of severe endothelial dysfunction and other vascular disorders. These conditions were clearly evident in eNOS knockout mice. These mice exhibited an increased propensity for atherosclerosis, impaired vasodilation, and hypertension (Rask-Madsen, 2007; Li et al., 2002). All of these conditions are associated with the diabetic state and risk of CVD.

In summary, VEGF and insulin signaling are complex events that may be integrated at many different points, depending on cell type and environment. The demonstrated importance of Akt and PLC-γ in cellular responses to insulin and VEGF has led us to examine possible signaling interactions using phosphorylation of these effectors as potential modes of crosstalk.

MATERIALS AND METHODS

I. Creation of GST Fusion Proteins

Recombinant proteins were prepared containing glutathione S-transferase (GST) fused to phosphoprotein binding motifs from IRS-1, PI3-Kinase, SHC, and PLC-γ, in order to test the ability of intermediates principally associated with either the insulin or VEGF signaling pathway to directly interact [Figure 8]. "Phosphotyrosine Binding" (PTB) and Src homology 2 (SH2) domains in signaling proteins are directly responsible for recognizing and binding to specific phosphorylation sites on receptors or other signaling intermediates (van der Geer et al., 1999). For example, phosphorylated IRS-1 provides a binding site for the SH2 domain of PI3-kinase; however, this particular SH2 domain is also capable of direct interaction with other receptor tyrosine kinases (Senthil et al., 2002). Therefore, the approach for analyzing protein interactions was to precipitate activated proteins using recombinant binding domains.

PCR Cloning of Binding Domains

Sequences encoding the PTB domains from human IRS-1 and SHC and the SH2 domain from PI3-kinase were amplified by polymerase chain reaction (PCR) using cDNA from human umbilical vein endothelial cells (HUVECs) (Huckle and Roche, unpublished). As an alternative source of templates for PCR cloning of domains of interest, Mammalian Gene Collection (MGC) clones of PI3-kinase (MGC:22760), IRS-1 (MGC:61462), and SHC (MGC:20839) were plated on Luria-Bertani (LB) plates containing 25 µg/ml chloramphenicol. From these plates, colonies were selected and used to inoculate 1 ml LB/chloramphenicol liquid cultures. After incubation overnight at 37 ºC with shaking at 200 rpm, 200 µl aliquots of the culture suspensions were removed and centrifuged (14,000 x g, 5 minutes). Supernatants were aspirated and pellets resuspended in 100 µl 1x 10 mM Tris-HCl, 1 mM EDTA, pH 8.0 (TE). Samples were heated to 95 ºC in a heat block for 5 min, and 1 µl per sample was used as template in 20 µl PCR reactions. Forward primers (BH-526, -528, and -530) for PCR reactions included a *Bgl*II or *Bam*HI restriction enzyme site. Reverse primers (BH-527, -529, and -531) included an *Eco*RI site and stop codon (Appendix A).

PCR products and DNA size markers (*Hind*III-cut λ phage DNA plus *Hae*III-cut ϕχ180 phage DNA) were fractionated on 1% (w/v) agarose gels in 1x Tris-borate-EDTA (TBE) running buffer at 100 V. Gels were stained for 15 min in a 5 µg/ml solution of ethidium bromide (EtBr) in ddH_2O and destained in ddH_2O for 30 min [Figure 9A]. Bands containing PCR products of predicted size were excised from the gels and purified by reversible binding to silica beads using QiaexII reagents (Qiagen Inc.) and elution into 20 µl ddH_2O. To generate DNA ends compatible with ligation to the fusion protein vector, PCR products were digested with restriction endonucleases (*Bgl*II or *Bam*HI plus *Eco*RI; New England BioLabs) in a total volume of 50 µl, followed by QiaexII purification and elution with 20 µl TE. To generate the fusion vector backbone, a preexisting construct, pGEX-TK (#21Q; Huckle and Earp, unpublished), was digested with *Eco*RI and *Bam*HI, and the 4938 bp fragment [Figure 9B] was purified following electrophoretic separation in a 1% agarose gel. Ligation reactions (~3:1 insert to vector molar ratio, 1 unit DNA ligase [Life Technologies Inc.]) were prepared and incubated overnight at room temperature. Negative control reactions excluded purified DNA from the binding domains (vector only reactions with no insert).

Samples from these ligation reactions were transformed into *E. coli* cells (Fusion-Blue competent cells [Clontech Laboratories, Inc.]). The transformation procedure began with adding ligation reactions (2 µl) to 50 µl thawed competent cells and incubating on ice for 30 minutes. Tubes were then placed in a 42 ºC water bath for 45 seconds and immediately returned to ice for 2 minutes. Transformation reactions were removed from ice and 450 µl SOC medium was added to each. Tubes were incubated at 37 ºC while shaking orbitally (200 rpm, 1 hour). Aliquots (100 µl) of each transformation reaction were plated onto LB plates containing 100 µg/ml ampicillin and incubated at 37 ºC overnight. Transformation reactions and plates were stored at 4 ºC pending screening for desired recombinants.

Transformed colonies were screened by PCR using template derived from 1 ml LB/ampicillin cultures processed as described above and primers spanning the vector-insert junctions. PCR reactions were separated by gel electrophoresis, and bands that matched predicted sizes were excised and purified with QiaexII reagents as described above. PCR-positive clones were sequenced at the Virginia Bioinformatics Institute

Core Laboratory Facility (Virginia Tech, Blacksburg, VA) to confirm the presence of the desired cDNAs as in-frame fusions with GST. Sequence-confirmed clones were streaked on LB/ampicillin plates, and individual clonal colonies were picked with a sterile loop for inoculation of 100 ml LB/ampicillin cultures. These flask cultures were incubated at 37 ºC while shaking (200 rpm, overnight). From these overnight cultures, 0.4 ml samples were removed for archival storage in 25% (v/v) glycerol at -70 ºC; the balance of the culture suspension was centrifuged (6000 x g, 15 min at 4 ºC). Bacterial cell pellets ($\leq$ 0.3 g) were processed for the purification of plasmid DNA using Qiagen Midi Plasmid kit reagents. Final DNA pellets were allowed to air dry for 5 minutes and were dissolved in 150 µl DNase/RNase free water.

The concentrations of purified samples were determined from absorbance readings (260 and 280 nm) from a UV spectrophotometer (Beckman DU 640B). Plasmid compositions were verified by sequencing at the Virginia Bioinformatics Institute Core Laboratory Facility (Virginia Tech, Blacksburg, VA) and stored at 4 ºC for later use. In some cases, after sequences were verified, clones were transformed into alternate strains of competent bacterial cells (RosettaBlue or BL21 (DE3) [Novagen®]) and frozen at -70 ºC.

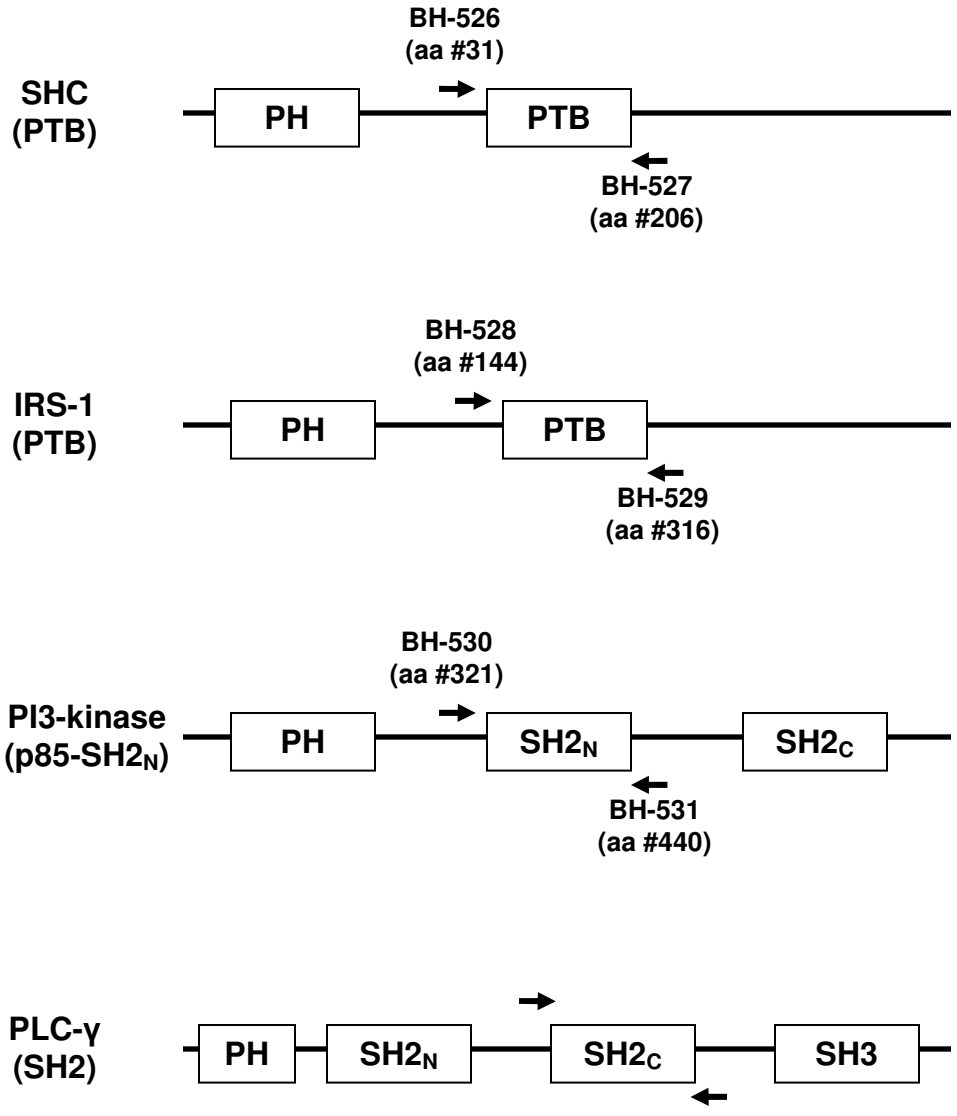

Figure 8. Cloned binding domains used in GST-fusion proteins. Domains from SHC, IRS-1, PI3-kinase, and PLC-γ are shown. Arrows indicate approximate location of primers and aa# refers to the amino acid range of the binding domain. The PLC-γ derived GST-$SH2_C$ fusion protein was created previously (Huckle and Earp, unpublished).

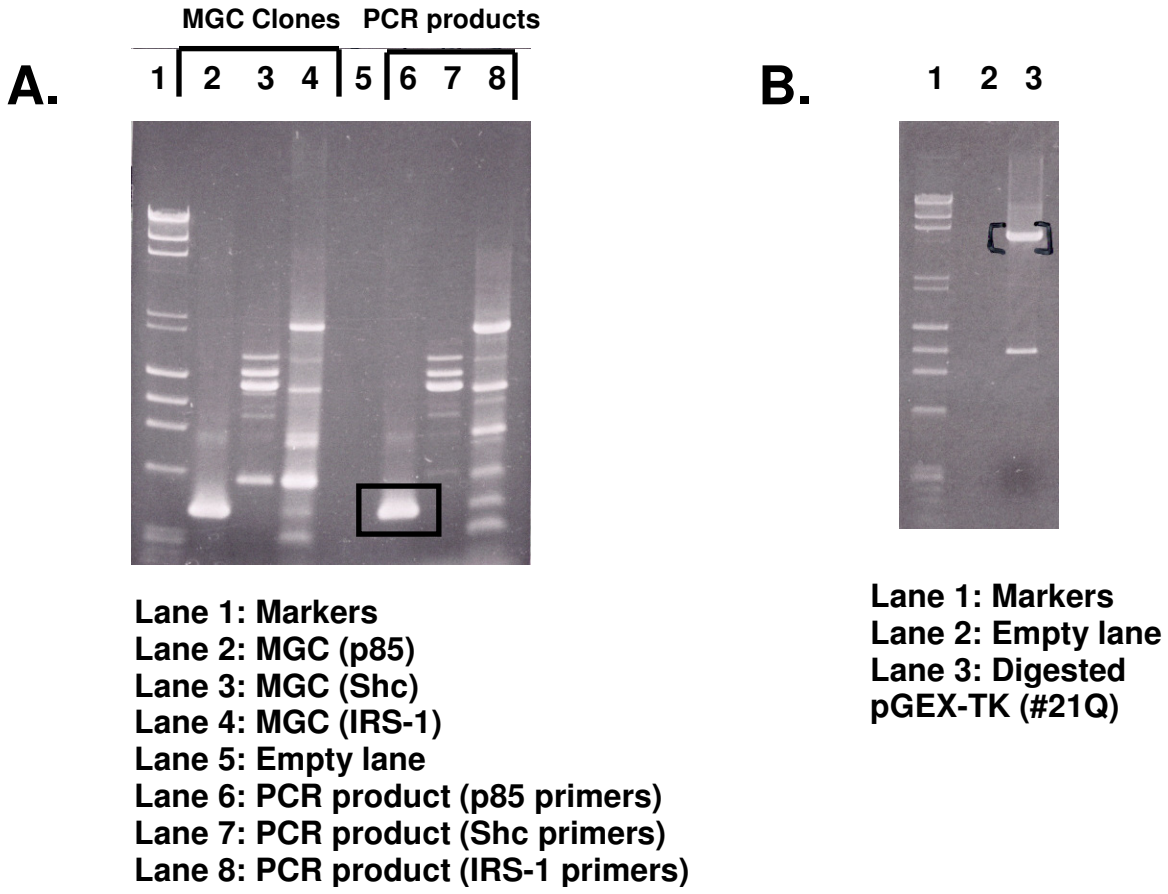

Figure 9. Intermediate products used for the creation of GST-fusion proteins. MGC clones (lanes 2-4) and the PCR products of PTB domains from human IRS-1 and SHC and the SH2 domain from PI3-kinase (lanes 6-8) [A]. The product in lane 6 (black box enclosure) was purified and used in the creation of GST-$SH2_{p85}$ fusion proteins. Also shown are the products from double digest of pGEX-TK (#21Q) with *Bam*HI and *Eco*RI [B]. The larger fragment (black brackets) was excised and used as the fusion protein vector.

Fusion Protein Expression

From -70 ºC frozen glycerol stocks, 10 ml LB/ampicillin cultures were inoculated and grown overnight (200 rpm, 37 ºC). These overnight cultures were diluted into 100 ml LB/ampicillin flask cultures and incubated while shaking (200 rpm, 37 ºC). After 4 hours, 0.5 mM IPTG (isopropyl-β-D-thiogalactopyranoside) was added to induce fusion protein expression, and incubation was continued for 1.5 hrs. Induced cultures were centrifuged (6000 x g, Sorvall GSA rotor, 15 minutes), supernatants were discarded, and pellet kept on ice. Bacterial cells were lysed using Bacterial Protein Extraction Reagent (B-PER, a nonionic detergent with 20 mM Tris-HCl, pH 7.5; Pierce Chemical). Protease inhibitors (100x concentrate: 100 mM AEBSF-HCl, 80 µm Aprotinin, 5 mM Bestatin, 1.5 mM E-64, 2 mM Leupeptin, 1 mM Pepstatin A in DMSO and EDTA; Pierce) were added to 10 ml B-PER and mixed. Pellets were resuspended with the B-PER solution and homogenized (20 strokes) on ice in a Dounce glass homogenizer with pestle B. The homogenates were transferred to 15 ml polypropylene round bottom tubes and centrifuged (10,000 x g, HB-4 rotor, 4 ºC, 15 minutes). Supernatants containing extracted GST-fusion proteins were pipetted into sterile tubes and held on ice until purification with glutathione-agarose beads.

Glutathione Sepharose 4B (GE Healthcare) was used to bind and purify recombinant GST fusion proteins. Beads (in 75% suspension) were resuspended and 1.33 ml (equivalent to 1 ml of packed volume) transferred into a sterile tube and centrifuged (500 x g, 4 ºC, 5 minutes). The supernatant was discarded, and beads washed twice with 10 ml chilled 1x Dulbecco's phosphate buffered saline (DPBS). Washed beads were resuspended in 1 ml of 1x DPBS to yield a 50% suspension.

Previously prepared GST-fusion protein extracts were added directly to the washed Glutathione Sepharose 4B. These protein-bead suspensions were incubated while rotating end-over-end (4 ºC, overnight). The following day, protein-bead suspensions were centrifuged (Eppendorf Centrifuge 5810R, 500 x g, 4 ºC, 10 minutes), supernatants were aspirated, and beads were washed three times in 10 ml of cold 1x DPBS. After the final centrifugation and aspiration, 1 ml of 1x DPBS was added to the beads (50% slurry final). Purified GST-fusion bead samples were stored at 4 ºC.

To verify the protein content on beads, a 10 µl sample of the final bead suspension (containing 5 µl packed beads) was removed and combined with 20 µl 3x Laemmli sample buffer with β-mercaptoethanol (Sigma Chemical). Other samples included uninduced culture aliquots and cell pellet prior to homogenization. All samples were heated to 95 ºC for 5 minutes and either frozen (-20 ºC) or loaded onto precast 10% polyacrylamide Tris-HCl gels (Bio-Rad). Samples were fractionated at 200 V for ~1 hour. Following electrophoresis, gels were washed with ddH_2O (3 times for 5 minutes each), and stained (1 hour with gentle shaking) with Imperial stain (Pierce). Gels were destained overnight in ddH_2O with gentle shaking and visualized on a LI-COR Odyssey® Infrared Imager.

II. Routine Cell Culture

All cell lines were cultured in T75 flasks (Corning) and incubated at 37 ºC in a humidified CO_2 (5%) incubator. Media was composed of Dulbecco's Modified Eagle Medium (4.5 g/L glucose/L-glutamine/sodium pyruvate) plus 10% fetal bovine serum and 50 µg/ml gentamicin sulfate (DMEM/FBS/Gent; all components from Mediatech, Inc.). Cultures of cells stably transfected to overexpress KDR or insulin receptor included the aminoglycoside antibiotic, G418 sulfate (Mediatech) at 500 µg/ml. All procedures involving cell cultures or culture media were performed in a laminar-flow biological safety cabinet using sterile technique.

Cells were permitted to reach 75-95% confluence before subculture, approximately every 5-7 days. Media was aspirated from the flask, and cells were washed with 10 ml of 1x DPBS without calcium or magnesium. After washing, cells were incubated with 2 ml of 0.5 mg/ml trypsin-EDTA for ten minutes in order to dissociate cells from the flask surface. Culture medium (10 ml, DMEM/FBS/Gent) was added and the suspension pipetted repeatedly to break up any cell clumps. A single-cell suspension was desired for accuracy in counting and replating. The suspension was placed in a sterile 15 ml polypropylene conical tube and centrifuged 10 minutes at 150 x g. Liquid was removed and cells resuspended in 10 ml of culture medium. From this suspension cells were counted. A 1:1 mixture of cell suspension and Trypan Blue (0.4%) was placed on a hemocytometer for counting. Cells were reseeded into 10 ml of

culture media at a 1:10 or 1:20 dilution ratio, or 1 ml or 500 µl of the cell suspension respectively. For experiments, cells were plated onto 60 mm poly-D-lysine coated dishes (5 ml culture media containing ~1x10^6 cells/dish) or 24-well plates (1 ml medium containing ~1x10^5 cells/well) (Becton-Dickenson Biocoat).

Culture media in T75 flaks was routinely replaced 3-4 days after passaging and was supplemented with G418 for KDR-overexpressing cells. Other cell types maintained for control experiments and additional work included non-transfected HEK293 cells and human umbilical vein endothelial cells (Clonetics®).

III. Insulin Receptor Expression Construct

The pcDNAIntA-msFlt-1 vector was digested with *Not*I and *Hind*III to provide the vector sequence (6403 bp) [Figure 10A]. The MGC clone of the full length IR coding sequence (GenBank accession number M10051) was digested with *Hind*III and *Psp*OMI [Figure 10B]. The resulting IR sequence (4320 bp) was gel-purified and subcloned into the pcDNAIntA vector backbone, placing the coding sequence under control of the cytomegalovirus (CMV) major immediate-early (I/E) promoter.

Prior to transfection into HEK293 cells, pcDNA-IR plasmids were linearized with *Pvu*I [Figure 10C] and pcDNA-KDR plasmids were linearized with *Sfo*I [Figure 10D]. DNA was linearized in order to increase the efficiency of stable transfections. The *Pvu*I site was selected based on its interference with the ampicillin resistance gene and non-interference with the IR and neomycin resistance sequences. An intact neomycin resistance sequence allowed for initial screening of the IR clones with G418. For co-transfection experiments, pcDNA-KDR plasmids were prelinearized with *Sfo*I, interrupting the neomycin resistance gene. Even though both the IR and KDR plasmids originally carried the same neomycin selection marker, G418 was used for the selection of cells successfully transfected with the IR.

IV. Transfection of 293 Cells

HEK293 cells were used for experimentation due to their ease of maintenance, predictable growth, and ease of transfection (Freshney, 2005). HEK293 cells previously transfected with KDR and isolated as clonal cell line C57 (Huckle, unpublished) were

thawed from liquid nitrogen storage and reintroduced into culture. The plasmid used for expression of KDR also included a neomycin resistance gene. This was important for subsequent selection of KDR expressing cells by G418 (Mediatech, Inc.).

Before stable cells lines were employed, transient transfections were attempted for use in activation experiments. HEK293 cells were plated (~1 x 10^6 cells/60 mm dish) and grown until ~80% confluent. Purified plasmids separately containing sequence encoding insulin receptor and KDR were combined (2 µg each) with 250 µl Opti-MEM (Life Technologies) reduced serum medium (1x with Hepes buffer, 2400 mg/L sodium bicarbonate, and L-glutamine) and Trans-IT-293 transfection reagent (Mirus). These DNA/lipid complexes were slowly added onto cells and the dishes were swirled gently. One mixture without a plasmid DNA sample and controls were also included. Cells were allowed to incubate 48 hours at 37 ºC prior to VEGF or insulin stimulation.

Prior to stable transfection, purified plasmids individually containing the insulin receptor and KDR were linearized with restriction enzymes [Figure 10D]. Completion of cleavage was verified by electrophoresis on a 0.7% agarose gel. Linearized plasmids were purified from solution as above, with elution into 100 µl ddH_20. HEK293 cells (~60% confluent in a 60 mm dish) were transfected with 3 µg of linearized plasmid DNA as above. After 48 hrs in culture, cells were lifted with trypsin-EDTA and replated in their entirety on 10 cm dishes with 10 ml complete medium plus 500 µg/ml G418. Medium was changed every 3-4 days until all cells had vanished from non-transfected control dishes, at which time cells were lifted with trypsin-EDTA for cloning and storage in 7.5% DMSO in liquid nitrogen.

To isolate clonal transfectants, suspensions of G418 resistant cells were counted and diluted to yield a cell density of 2 cells per 100 µl medium+G418. This volume was plated into 96-well plates (one plate per plasmid combination: insulin receptor alone or both the insulin receptor and KDR). The medium was aspirated with a 25 G needle and changed when necessary (about every 6 days). After 20 days, cells from wells that were the most confluent were lifted with trypsin-EDTA and expanded by replating into sterile 24-well plates (1 ml/well). After incubation for 4 days, the 18 most confluent clones were harvested and split into 6-well dishes (2.5 ml total volume plus G418) and 24-well dishes (1 ml total without G418). Cells in the 24-well dishes were then

harvested and screened for receptor expression by Western blotting. The cells in the 6-well dishes were used for propagation and archival storage after screening.

After the cells reached ~90% confluence, the medium was aspirated and cells were washed with 1ml DPBS. Laemmli sample buffer (100 µl; Bio-Rad) was added to each well and the entire dish agitated on a shaker until cells had lifted. Samples were heated to 95 ºC for 5 min and aliquots loaded onto 7.5% SDS-PAGE Tris-HCl gels (Bio-Rad) and run for 45 minutes at 200 V. After transfer to PVDF membrane (Millipore Immobilon^{TM}-FL), the membrane was cut horizontally and probed separately for KDR and insulin receptor β-subunit (230 and 95 kDa, respectively) (Appendix B). Based on the clones with the strongest signals, 14 were chosen and two duplicate gels were run and immunobloted separately for KDR and IR proteins. Based on these results, one clone overexpressing IR alone was selected for further experimentation and cryostorage. From the 6-well dishes above, the IR overexpressing clone, W52, was harvested and reseeded into a T75 flask.

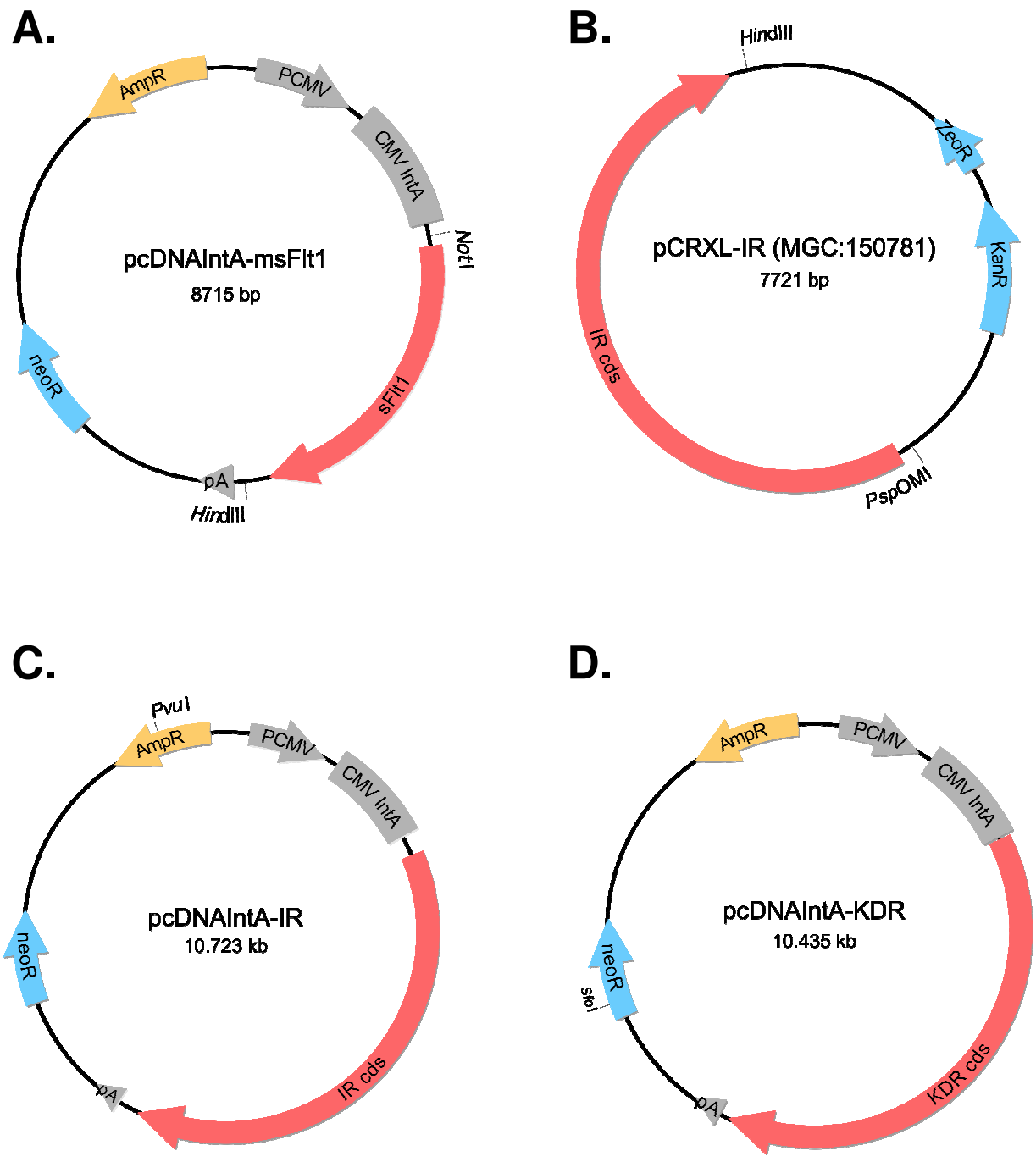

Figure 10. Sequence maps of the pcDNAIntA-msFlt-1 vector, full length IR, and final product. The pcDNAIntA-msFlt-1 construct was digested with *Not*I and *Hind*III that provided a 6403 bp vector backbone [A]. The IR coding sequence was digested with *Hind*III and *Psp*OMI from the pCRXL construct, liberating a 4320 bp insert containing the IR [B]. After ligation, the final product was linearized with *Pvu*I prior to transfection [C]. Likewise, the purified plasmid with KDR was linearized with *Sfo*I [D].

V. Time Course Phosphorylation Experiments

To determine the effects of ligand stimulation over time, cells were treated with VEGF, insulin, IGF-1, or both VEGF and insulin over time increments between 0 and 15 minutes. A mixture of Hank's Buffered Salt Solution (Lonza), bovine serum albumin (MP Biomedicals), and Hepes buffer (Sigma®) were combined (HBSS, 0.1% BSA, 25 mM Hepes, pH 7.3) and warmed to 37 ºC. The desired VEGF treatment concentration was 50 ng/ml in each dish, so VEGF was diluted with pre-warmed HBSS/BSA/Hepes (H/B/H) mixture. Insulin was also diluted (1.92 µl insulin with 3 ml H/B/H) to a per dish desired concentration of 100 nM.

Cell cultures (cells at 90% confluence in 60 mm dishes) were placed on a plate warmer at 37 ºC and medium was aspirated. The cells were washed with 2 ml of warmed H/B/H and incubated under serum starved conditions (in 1.5 ml H/B/H) for 30 minutes. In some experiments, cells were pre-treated for 1 hr with bovine serum albumin-advanced glycation end-product (AGE-BSA; 200 µg/ml). Each dish was then challenged with 150 µl of H/B/H or 11x VEGF, insulin, or both for the appropriate time increment. Treatment media were rapidly aspirated, and the dishes moved directly to ice. Cells were lysed with 1 ml/dish chilled "New Lysis Buffer" (25 mM Hepes, 5 mM EDTA, 50 mM NaF, 1% Triton-X-100, 10% glycerol, 1 mM sodium orthovanadate, and One-Shot Protease Inhibitors [Pierce]). Cells were mechanically dissociated from dishes using plastic scrapers. These lysates were transferred to microfuge tubes and rotated end-over-end at 4 ºC for 1 hour. This incubation allowed for the solubilization of membranes and consequent release of membrane receptors and intracellular proteins. Lysates were centrifuged at 14,000 x g and supernates transferred to sterile microfuge tubes.

Immunoprecipitation

Immunoprecipitations were used for their specificity in isolating and enriching target proteins from whole cell lysates. Clarified cell lysates prepared as described above were rotated end-over-end at 4 ºC overnight with an antibody directed against Akt or PLC-γ (Appendix B). The following day, 20 µl Protein A/G PLUS-agarose beads (Santa Cruz Biotechnology, Inc.) were added to each tube, and samples were agitated

for another 1-3 hours at 4 ºC. These Protein A/G beads were the insoluble antibody binding proteins that capture and precipitate the protein-primary antibody complexes.

Samples were centrifuged at 2500 x g, supernates aspirated with a 25 G needle, and beads were washed twice with 1 ml chilled New Lysis Buffer. Laemmli sample buffer (40 µl, 1x final plus β-mercaptoethanol) was added to each bead pellet to denature proteins for separation based on size. Samples were then heated to 95 ºC in a heat block for 5 minutes and centrifuged briefly prior to SDS-PAGE and immunoblotting.

Incubations with GST-Fusion Beads

Activated receptors and/or downstream targets from whole cell lysates were also precipitated using recombinant GST proteins (described above). These fusion proteins allowed for the analysis of predicted protein-protein interactions. After cells were stimulated with ligand, solubilized, and centrifuged, the clarified lysates were combined with recombinant GST-fusion protein beads (20 µl of bead suspension containing 10 µl of packed beads) and were rotated overnight at 4 ºC. As with immunoprecipitations above, samples were centrifuged at 2500 x g, supernates aspirated with a 25 G needle, and beads washed twice with 1 ml chilled New Lysis Buffer. Laemmli sample buffer (40 µl, 1x final plus β-mercaptoethanol) was added to washed beads before heating to 95 ºC for 5 minutes.

Protein Identification by Immunoblotting and Immunodetection

Western blots were routinely used for confirming the presence (or absence) of protein, as well as estimating the activation/phosphorylation state of proteins and their approximate size. The Criterion (Bio-Rad) Precast Gel System (7.5% Tris-HCl, 18 well comb) was used for the sodium dodecyl sulfate-polyacrylamide gel electrophoresis (SDS-PAGE) separation of protein samples precipitated via immunoprecipitations or fusion proteins.

Gels were placed inside the electrophoresis cell and 1x SDS-PAGE running buffer (25 mM Tris base, 192 mM Glycine, and 1% SDS w/v) was poured into the cell. Samples (30 µl/lane) and ProSieve® color protein molecular weight markers (Covance;

15 µl/lane) were loaded and fractionated at 200 constant V for ~50 minutes, or until the tracking dye front had reached the bottom of the gel.

Electrotransfers were done using the wet (tank) system with the buffer reservoir seated in ice water. Resolved proteins were transferred to polyvinylidene fluoride (PVDF) Immobilon™-FL membrane (0.45 µm pore size) that had been presoaked in 10 ml methanol prior to equilibration in transfer buffer. Transfers were performed in chilled 1x transfer buffer (25 mM Tris base, 192 mM Glycine, and 10% methanol) for 30 minutes at 100 V. Membranes were rinsed with 1x DPBS and incubated (at 4 ºC for 1 hour to overnight) with gentle agitation in 25 ml Blocking Buffer for Near Infrared Fluorescent Western Blotting (Rockland Immunochemicals, Inc.).

After blocking and re-rinsing with DPBS, the blots were incubated (overnight at 4ºC) with 0.1 µg/ml primary antibody (Appendix B) in 10 ml diluted blocking buffer (1:1 with 1x DPBS). Following incubation in the primary antibody, the blots were washed four times for five minutes each with a wash solution (0.05% Tween-20 [BioRad], 1x DPBS, and ddH_2O). This wash step removed unbound antibodies and reduced background. Blots were next incubated with a complementary fluorophore-conjugated secondary antibody (Appendix B [Rockland Immunochemicals, Inc.]) for fluorescent detection of proteins. This method was advantageous due to the long term stability of signals, the detection of multiple proteins on a single blot, and ease of quantification. After incubation for 1-2 hours at room temperature, blots were washed (as above). Immunoblots were then scanned and analyzed using the LI-COR Odyssey® Infrared Imaging System and refrigerated in 1x DPBS.

Membrane Stripping and Reprobing

In some experiments, immunoblots targeted for reprobing were stripped using a low pH method. Blots were incubated in 50 ml stripping buffer (25 mM Glycine, 1% SDS, pH 2) for 5-10 minutes at room temperature with gentle agitation. Each blot was then rinsed with 1x PBS and scanned using the LI-COR Odyssey® Infrared Imaging System to monitor removal of the fluorophore used initially and avoid overexposing blots to the stripping solution. If necessary, blots were incubated in another 50 ml of stripping buffer for 5-10 minutes, rinsed in 1x PBS, and re-scanned. After stripping, membranes

were agitated for 5-10 minutes in wash solution (described above). The blot was re-blocked at 4 ºC for 1 hour to overnight and used for another round of immunodetection.

VI. VEGF Stimulated Hydrolysis of Phosphoinositol Lipids

Current information has proven direct interactions between phosphorylated KDR and PLC-γ activation (Takahashi et al., 2001). Phosphorylated PLC-γ specifically mediates the hydrolysis of phosphatidylinositol 4, 5-bisphosphate to inositol 1,4,5-trisphosphate (IP_3) and diacylglycerol. Therefore, accumulation of inositol phosphates was used as a marker for VEGF signaling through PLC-γ.

KDR-overexpressing cells were plated on 24-well poly-L-lysine coated plates (Becton-Dickenson Biocoat) in 1 ml complete medium (~$1x10^5$ cells/well). When cells were approximately 75% confluent, the standard medium was replaced with 0.5 ml/well of inositol-free DMEM (ICN Biomedicals)/10% FBS/50 µg/ml gentamicin containing [^{3}H]inositol (20 Ci/mmol; PerkinElmer®) at a final concentration of 10 µCi/ml . Cells were incubated for another 24 hours (37 ºC, 5% CO_2) to allow incorporation of [^{3}H]inositol into phosphoinositide lipids. The following day, the labeling medium was replaced with 0.5 ml H/B/H (described above) plus 10 mM LiCl and equilibrated for 30 minutes on a 37 ºC slide warmer. LiCl inhibits the dephosphorylation of inositol phosphates, permitting their accumulation to reflect net phosphoinositide hydrolysis, *i.e.*, PLC activity (Huckle et al., 1989). Exposure to VEGF, insulin, VEGF + insulin, or carbachol (55 µl/well from 11X stock dilutions) was the stimulus for phosphoinositide hydrolysis. Carbachol stimulation was used as a positive control because of its recognized ability to activate a distinct PLC isozyme through binding endogenous muscarinic acetylcholine receptors on HEK293 cells (Tong et al., 1999). Treated cells were incubated for an additional hour at 37 ºC. Ligand stimulation was arrested by aspirating the treatment medium, adding 0.5 ml chilled 0.1 M formic acid, and freezing the plate at -20 ºC.

[^{3}H]inositol phosphates were isolated by anion exchange chromatography and quantified by liquid scintillation counting. While the frozen plates thawed at room temperature, 600 µl aliquots of Dowex 1-X8 anion exchange resin (50% slurry in formate form [BioRad]) were pipetted into minicolumns and allowed to drain into a

common waste vessel. Thawed plate contents were transferred to columns and allowed to flow through. Wells were rinsed with 0.5 ml formic acid (0.1 M), which was also applied to the columns. Columns were washed with 3 x 1 ml volumes of formic acid (0.1 M) to remove free inositol. After washing, columns were removed from the common vessel and positioned over individual 6 ml scintillation vials. [^{3}H]Inositol phosphates were eluted with 3 x 1 ml applications of formic acid (0.1 M) plus ammonium formate (1.2 M) to the columns. After elution, 3 ml of scintillation cocktail (Ultima-Flo™ AF; Packard) were added, and the vials were mixed vigorously. Tritium counts per minute (CPM) were measured by liquid scintillation counting in a Beckman Coulter LS6500 at ~40% counting efficiency. Vials containing 3 ml of formic acid/ammonium formate and 3 ml Ultima-Flo™ AF scintillation cocktail were used as blanks.

RESULTS

Part I. Results addressing Aim 1: Assessing the combined effects of insulin and VEGF on Akt activation

Confirmation of KDR and IR Overexpressing HEK293 Cells

An initial objective of this project was to prepare stably transfected lines of HEK293 cells expressing both KDR and the IR. Toward this end, a series of clonal lines of KDR and IR transfected/G418 resistant cells was isolated, expanded in culture and screened individually for total KDR and total IR [Figure 11A]. The same was also done for a flask of cells that had been transiently transfected for the IR alone. For purposes of immunoblotting, cells transiently transfected for KDR and the IR served as the positive (+/+) control, while a sample of untransfected 293 cells were the negative control. Unfortunately, the KDR +IR co-transfected clones displayed a reciprocal relationship, where one receptor appeared preferentially expressed over the other. Specifically, when KDR expression was high [Figure 11A, lane 1 top half] insulin receptor expression was low [Figure 11A, lane 1 bottom half], and vice-versa [Figure 11A, lane 2]. Though this data discouraged further use of cells overexpressing both IR and KDR, it did confirm overexpression of IR in several clones [Figure 11A, lanes 11-14 (IR only)]. The presence of the IR in the final selected IR-overexpressing line is described and verified below [Figure 11B].

Consequently, all experiments performed in this study utilized HEK293 cells stably transfected with either KDR or the IR. A pcDNAIntA expression vector containing KDR was successfully transfected into HEK293 cells previously in our lab (Huckle, unpublished). However, it was unclear whether or not these clonal transfectants also expressed measurable amounts of the IR. Using immunodetection, whole cell lysates of KDR-expressing cells were separately probed for total KDR (230-kDa) and the IR-β subunit (95-kDa). Each showed a strong signal corresponding to both receptors in their respective cell lines [Figure 11B and 11C]. This was an important verification of the endogenous IR present in the KDR-overexpressing cells [Figure 11A, right panel]. The

existence of both receptors on our clonal cells prompted the expectation of a signaling response to both insulin and VEGF.

Whole cell lysates from the IR overexpressing cells were also separately probed for the IR-β subunit and total KDR. These results showed a very strong signal corresponding to the IR [Figure 11A, left panel] and no signal corresponding to KDR [Figure 11B, left panel]. The other signal present in the IR-expressing cells may correspond with the insulin proreceptor, the uncleaved αβ precursor of the mature $\alpha_2\beta_2$ IR (Knutson, 1991). This clonal line served as an important control for inducing a strong signaling response upon insulin treatment.

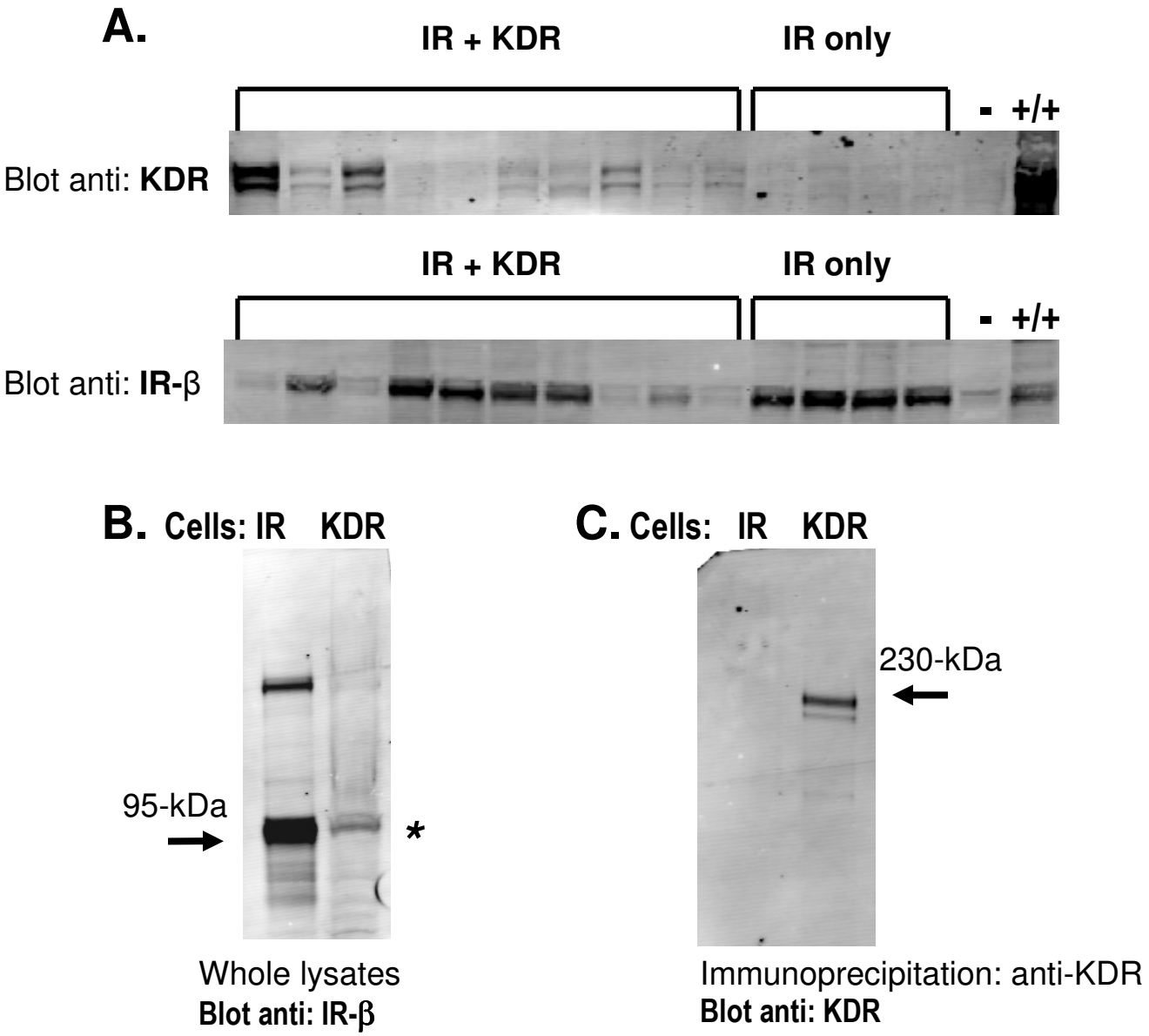

Figure 11. Construction of Cell Lines Overexpressing Receptors for Insulin (IR) or VEGF (KDR). Transfected sample blots probed for total KDR and total IR [A]. Blots of 14 clones transfected for both IR and KDR, or the IR only. Duplicate gels of the same samples were probed individually for total KDR and total IR. As noted in the text, no clones assayed strongly expressed both KDR and insulin receptor. The (+/+) marks the positive control (cells transiently transfected for KDR and IR), while the (–) indicates the negative control: HEK293 cells alone. Note that there was basal IR present in the 293 cells, but no KDR.

Samples of whole cell lysates or immunoprecipitates overexpressing IR or KDR were separated by SDS-PAGE and probed for either total IR [B] or total KDR [C]. The asterisk (*) indicates basal IR expression in the KDR-overexpressing cells [B]. The more rapidly migrating band detected by anti-KDR may represent partially glycosylated KDRs.

Akt Activation in Response to VEGF ± Insulin

Akt was used as an endpoint in phosphorylation experiments because of its documented responsiveness to either insulin or VEGF (Hanada et al., 2004). Akt phosphorylation was induced by treatment with VEGF, insulin, or both over a 15 minute time course. The integrated intensities from the phosphorylation results [Figure 12A] were found using LI-COR Odyssey® Imaging Software and normalized to the integrated intensity of total protein [Figure 12B] from the same samples. The two bands that appeared in each sample after probing for total Akt correspond to a band shifting phenomenon that was consistently observed each time a blot originally probed for phospho-Akt was reprobed for total. Using the photo editing software, GIMP, the phospho and total blots were superimposed and the upper band was found to correspond with the phosphorylated species (data not shown). Previous studies have also reported a shift in Akt mobility corresponding with Akt activation (with phosphorylated Akt running with slightly reduced mobility; Kayali et al., 1998). Therefore, we concluded that the lower band corresponded with the signal for non-P-Ser^{473} Akt.

In order to normalize the amount of phosphorylated protein within each sample for subsequent comparison between samples, ratios were calculated as phosphorylated protein as a fraction of total protein. Following this calculation, the basal (untreated) levels unique to each experiment were subtracted from the activated protein values. Average Akt activation was graphed as a percentage of the maximal Akt activation after treatment with VEGF alone, an observation that occurred at a different time point in each experiment [Figure 12C]. Experiments were performed in triplicate and all values were included in the graphical comparison.

Treatments with the two different ligands, either independently or together, led to unique patterns of activation [Figure 12C]. For instance, stimulation with insulin alone led to an increase in Akt phosphorylation through the 15 minute period. After stimulation with VEGF alone, phosphorylation appeared to increase early post-treatment, but tended to wane towards the end of the time course. Likewise, activation with VEGF and insulin demonstrated time-dependent phosphorylation with the average maximum activation occurring around 3 minutes, before decreasing over the remaining

time. Stimulation with both ligands led to activation of Akt that, on average, fell somewhere between activation with VEGF alone and insulin alone. This trend was unexpected and not easily deduced from the immunoblots alone. Normalizing for total protein and subtracting basal activation levels indicated that perhaps it was the presence of VEGF that inhibited the full insulin response. It is possible that another situation exists: insulin inhibition of the full VEGF response, as seen in the 1 minute time point. However, this conclusion seems less likely given that stimulation with both ligands led to activation averages greater than those seen after VEGF treatment alone, across all time points (1 minute being the exception).

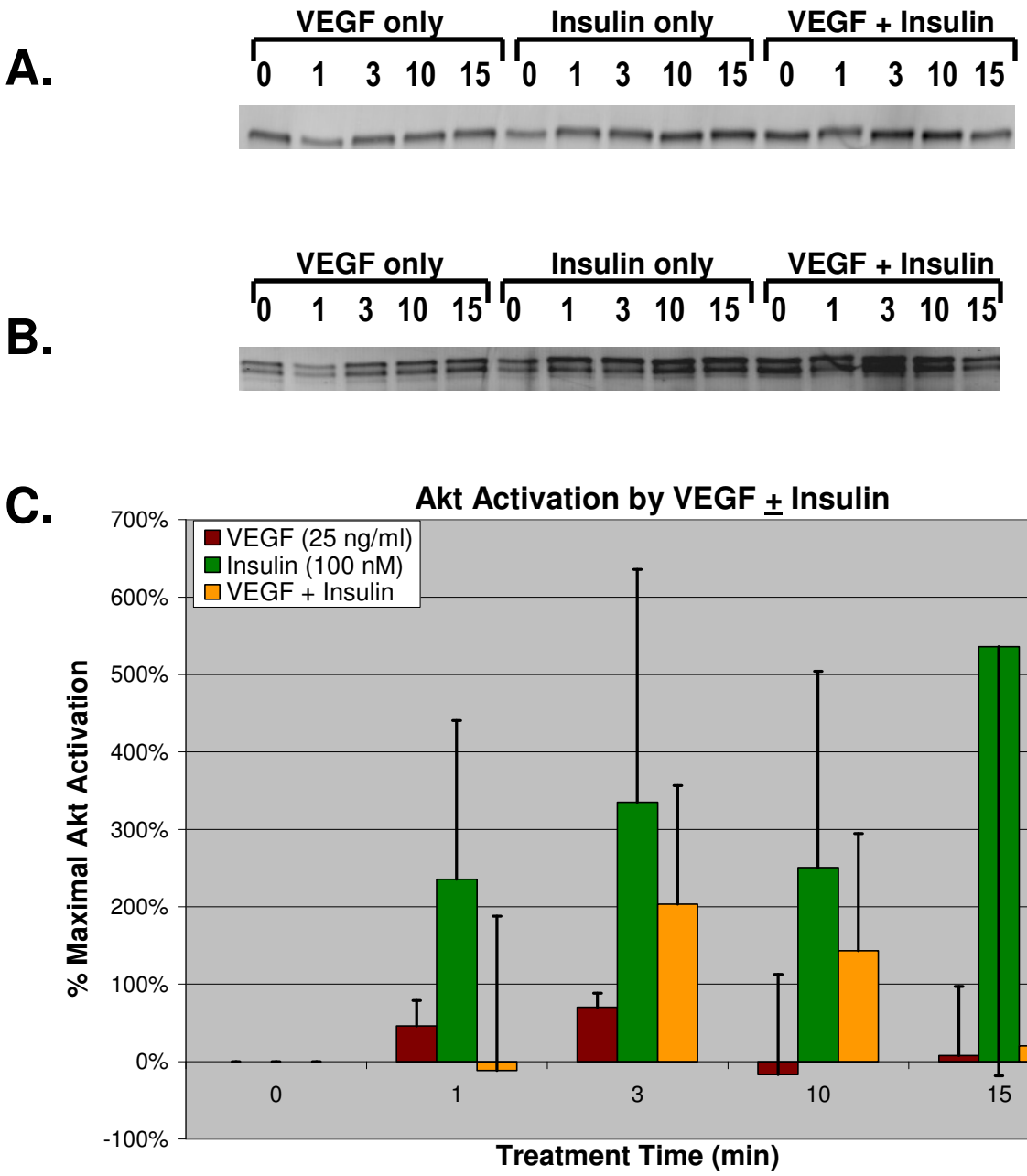

Figure 12. Time course of Akt activation after treating with VEGF, insulin, and both. A representative blot of Akt phosphorylation (Ser^{473}) is shown with treatment times labeled in minutes [A]. The same blot after being stripped and reprobed for total Akt [B]. The combined results from three independent experiments are graphed as percentages of the maximal Akt response after stimulation with VEGF alone (mean ± sem) [C]. Error bars represent the standard error values calculated from the standard deviations found between experiments.

The Effects of Exposure to AGEs on Akt Phosphorylation

Since protein glycation is associated with endothelial dysfunction and upregulated in diabetic conditions (Wautier and Schmidt, 2004), cell pretreatment with AGE-BSA was used to mimic a hyperglycemic/diabetic state. After pretreatment with or without AGE-BSA for one hour, KDR-overexpressing cells were stimulated with either VEGF, or VEGF and insulin. As with the Akt immunoprecipitation/phosphorylation experiments (described above), Akt phosphorylation was induced by this ligand treatment, but over a 10 minute time course [Figure 13A]. The phosphorylation data had confirmed Akt activation occurred before 15 minutes, so the time course was shortened by eliminating the 15 minute time point. Fewer total time points per ligand treatment group also facilitated running all samples on the same polyacrylamide gel.

As above, the integrated intensities from the phosphorylation results [Figure 13A] were determined using LI-COR Odyssey® Imaging Software and compared to the integrated intensity of total Akt protein [Figure 13B] from the same samples. As with the Akt data (above), the phosphorylation signal was normalized by calculating phosphorylated protein as a fraction of total protein. Again, the basal (no ligand) levels for the AGE treated and AGE untreated groups (unique to each experiment) were subtracted from the activation values. Average Akt activation was graphed as a percentage of the maximal Akt activation after treatment with VEGF alone, which occurred at a different time point within each experiment [Figure 13C]. Experiments were performed in triplicate and all values were included in the graphical comparison.

These experiments showed an increase in Akt activation after pretreatment with AGE-BSA, even in the absence of added ligand [Figure 13C]. Compared to the maximal Akt activation from non-AGE pretreated samples (stimulated with VEGF), AGEs appeared to increase Akt activation in a time dependent fashion. This observed Akt activation also appeared unaffected by treatment ligand(s), as AGE pretreatment led to increased Akt phosphorylation, except after the 1 minute stimulation with VEGF and insulin. As with the other Akt phosphorylation experiments, the deviation of the 1 minute sample (treated with VEGF and insulin) from the consensus might be explained by the variation represented by the standard error values.

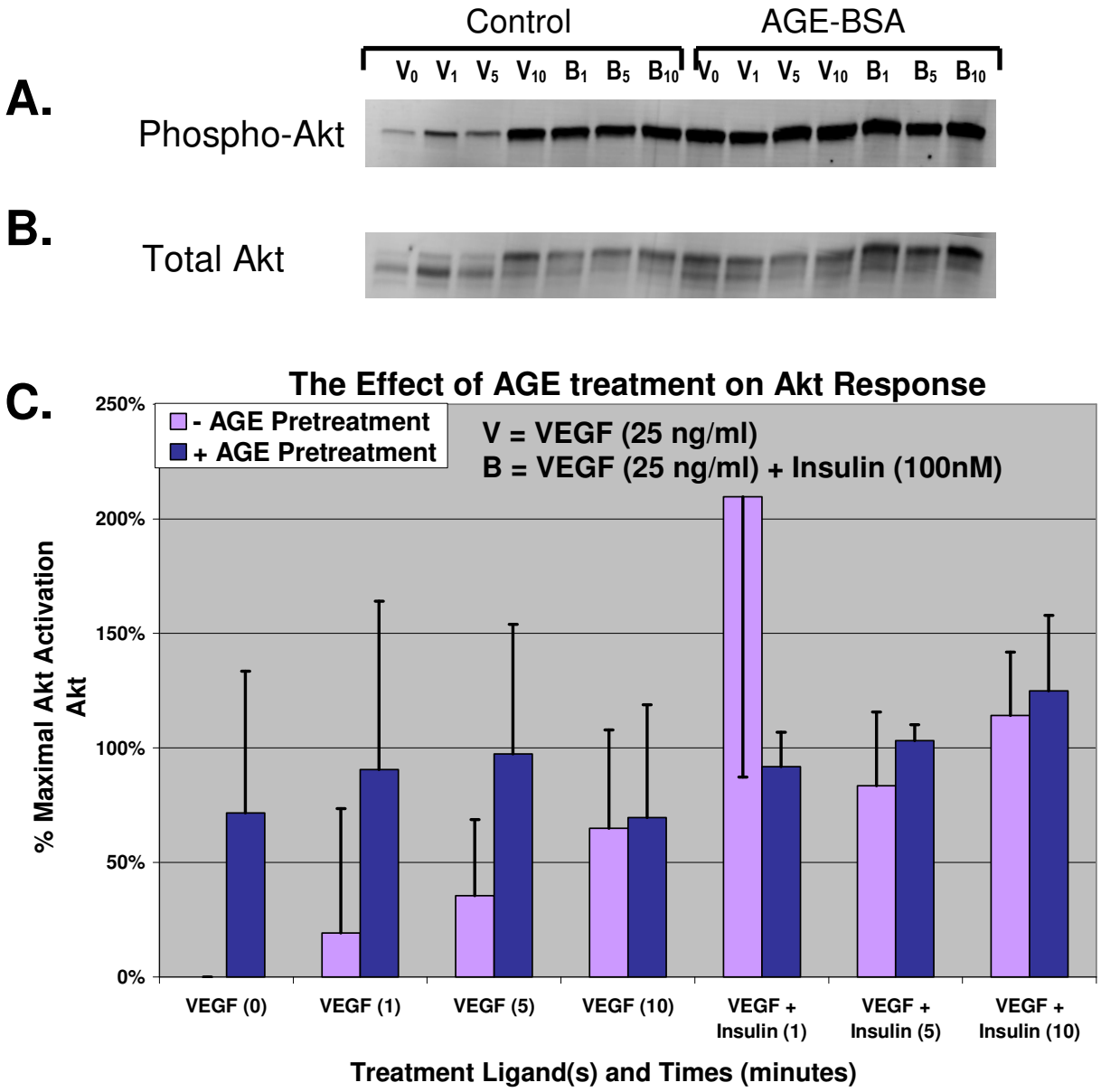

Figure 13. Changes in Akt activation after pretreatment with advanced glycation end products. A representative blot of Akt phosphorylation (Ser^{473}) is shown with treatment times labeled in minutes [A]. Below, the same blot after being stripped and reprobed for total Akt [B]. The combined results (mean $\pm$ sem) from three independent experiments are graphed as percentages of the maximal Akt response after stimulation with VEGF alone [C]. Error bars represent the standard error values calculated from the standard deviations found between experiments.

Part II. Results addressing Aim 2: Assessing the effects of insulin on VEGF-stimulated signaling responses.

PLC-γ Activation in Response to VEGF ± Insulin

PLC-γ phosphorylation was used as an indicator of direct VEGF induced signaling through the PLC-γ/PKC signaling pathway (Chattopadhyay, et al., 1999). Co-immunoprecipitations were performed for PLC-γ and Akt (data shown above) in order to demonstrate Akt and PLC-γ activation in samples exposed to identical treatments over identical stimulation times. Samples were fractionated on a single gel, but blotted separately with phospho-Akt and phospho-PLC-γ specific antibodies. Individual immunoprecipitation experiments for both Akt and PLC-γ were also performed in order to confirm antibody specificity and the presence of a signaling response over our set time course (data not shown).

Similar to the Akt data, blots probed for phosphorylated PLC-γ [Figure 14A] were stripped and reprobed for total PLC-γ [Figure 14B]. The phosphorylated values were then expressed as a fraction of total values, in order to normalize the phosphorylation signal within each sample to total PLC-γ protein. Likewise, for the final comparison between the three experiments, experimentally determined basal (untreated) response values were subtracted from the average activation values (as ratios of phosphorylated protein to total protein). Average PLC-γ activation was graphed as a percentage of the maximal PLC-γ activation after treatment with VEGF, an observation that occurred at a different time point in each experiment [Figure 14C]. Experiments were performed in triplicate and all values were included in the graphical comparison.

Treatment with insulin alone led to no observable phosphorylation signal from PLC-γ, which was unlike the Akt activation results (shown above) after insulin stimulation. However, VEGF did induce a time-dependent response with maximum activation occurring at 3 minutes, followed by a steady decline in phosphorylation. Treatment with both ligands led to a response very similar to that seen with VEGF alone. The presence of insulin appeared to only slightly alter the PLC-γ phosphorylation response to VEGF. In particular, VEGF activation of PLC-γ appeared somewhat reduced in the presence of insulin, particularly at the extreme time points (1 and 15

minutes) of this study. It should be noted that the standard error measurements between experiments showed variations in activation that were greater than or equal to the average activation values from VEGF stimulation alone.

A.

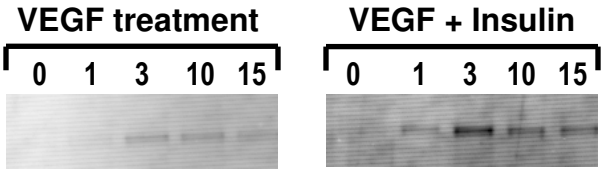

B.

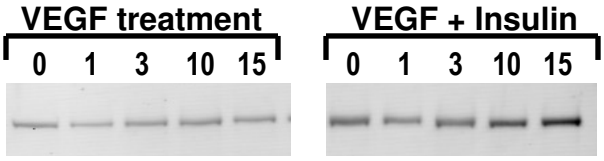

C.

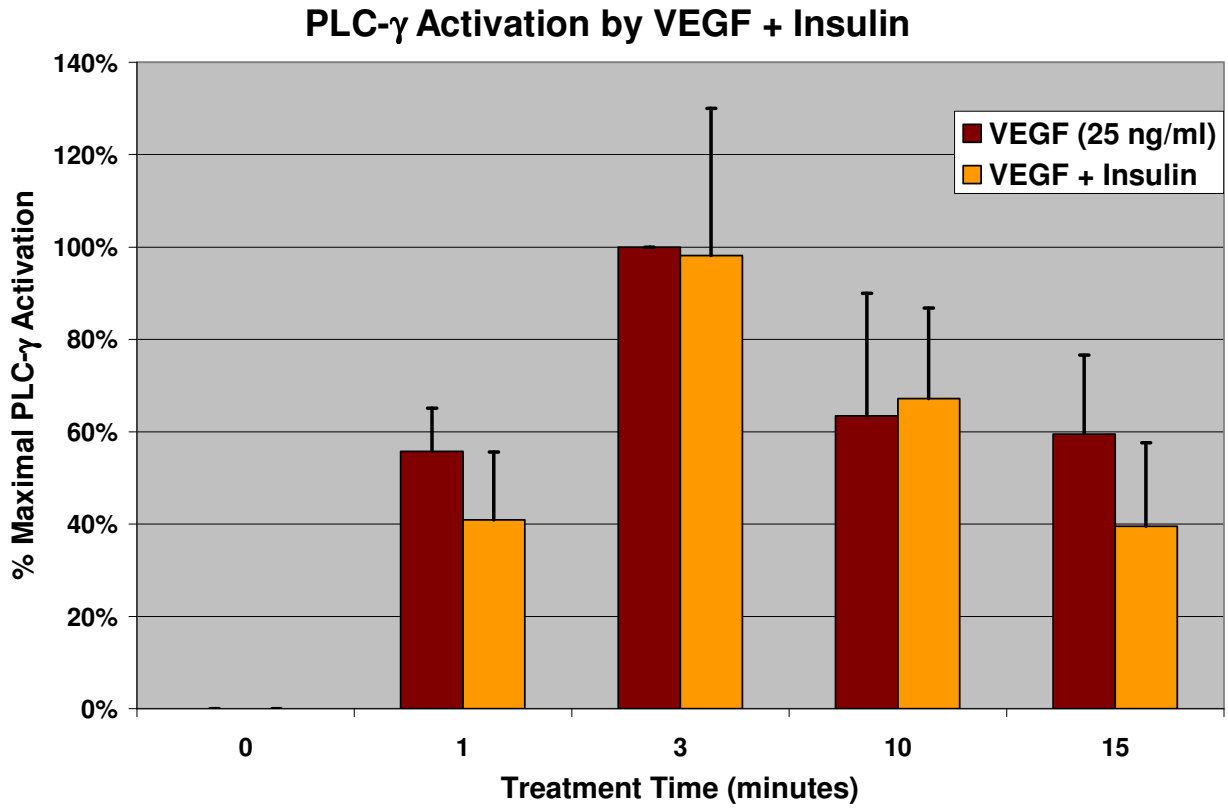

Figure 14. Time course activation of PLC-γ after treating with VEGF, insulin, or both VEGF and insulin. No measurable response to insulin alone was found. A representative blot of PLC-γ tyrosine phosphorylation is shown with treatment times labeled in minutes [A]. The same blot after being stripped and reprobed for total PLC-γ [B]. The combined results (mean ± sem) from three independent experiments are graphed as percentages of the maximal PLC-γ response after stimulation with VEGF alone [C].

Phosphoinositide Hydrolysis in Response to VEGF and Insulin

To specifically look at VEGF signaling through KDR activation of PLC-γ, membrane phosphoinositides were prelabeled with [^{3}H]inositol, and accumulation of soluble [^{3}H]inositol phosphate metabolites was measured after ligand stimulation. In order to gauge the sensitivity of this assay to VEGF stimulation, a dose response experiment was performed using KDR-overexpressing cells [Figure 15]. VEGF concentrations between 2-50 ng/ml were used to induce a VEGF-stimulated response. Cells showed a strong dose-response to VEGF over this range. Insulin alone (100 nM) had no measureable effect on phosphoinositide hydrolysis, and insulin had no obvious impact on the VEGF activated response.

Similarly, a concentration response experiment was performed in IR-overexpressing cells [Figure 16]. As with the VEGF dose response experiment, cells were treated for one hour with different concentrations of insulin (10-200 nM) and [^{3}H]inositol phosphate accumulation was measured. Untreated cells and cells treated with VEGF served as negative controls, while treatment with carbachol (20 μM) was the positive control. Consistent with results seen with the KDR-overexpressing cells, cells overexpressing the IR did not produce a measurable inositol phosphate response. The strong response to carbachol confirmed the viability of these cells and the success of the labeling procedure. These results confirm that insulin signaling through PLC-γ is minimal and that any crosstalk between VEGF and insulin most likely occurs at up- or downstream effectors in their pathways.

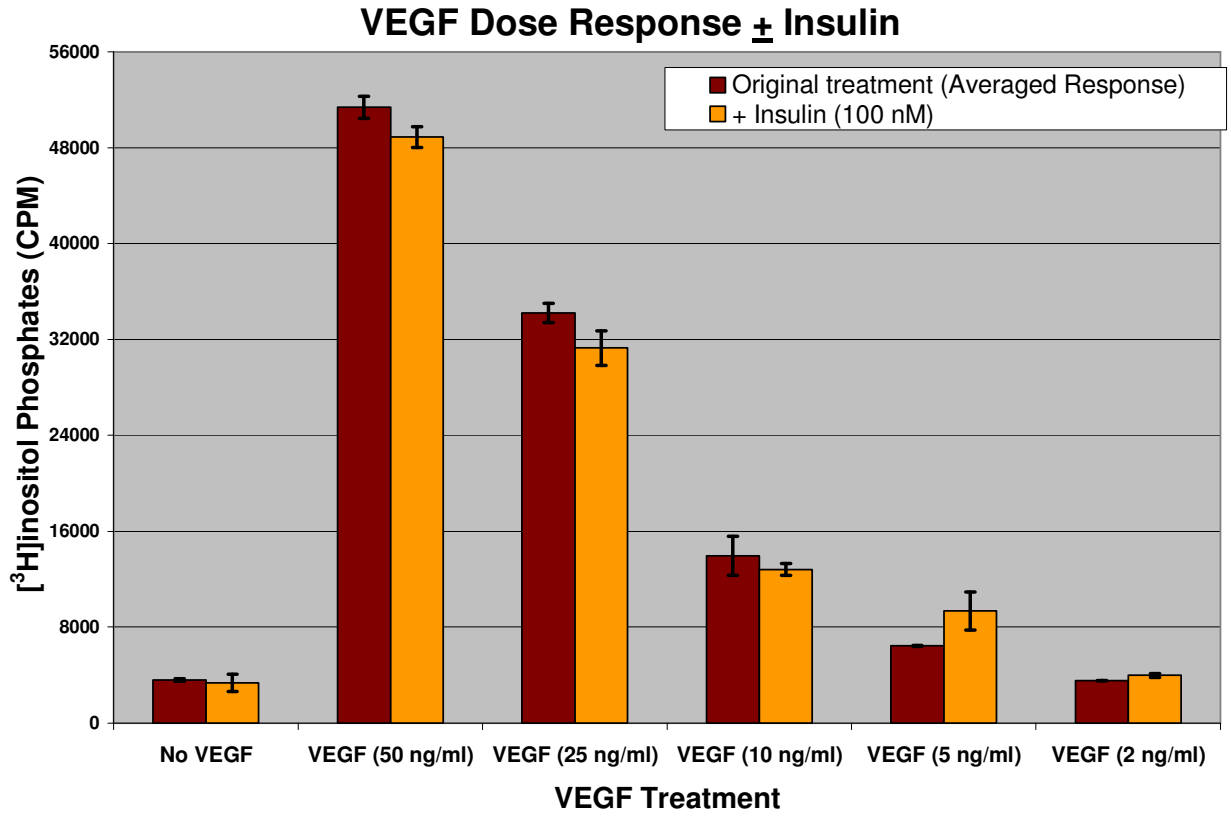

Figure 15. VEGF dose response curve as a function of hydrolysis of [3H] inositol labeled phosphoinositides. Inositol phosphate activity and accumulation was quantified as described in the Methods section. KDR-overexpressing cells were treated for one hour with varying concentrations of VEGF ± 100 nM insulin. The averages of two replicate treatment are graphed above; error bars represent the raw maximum and minimum sample values.

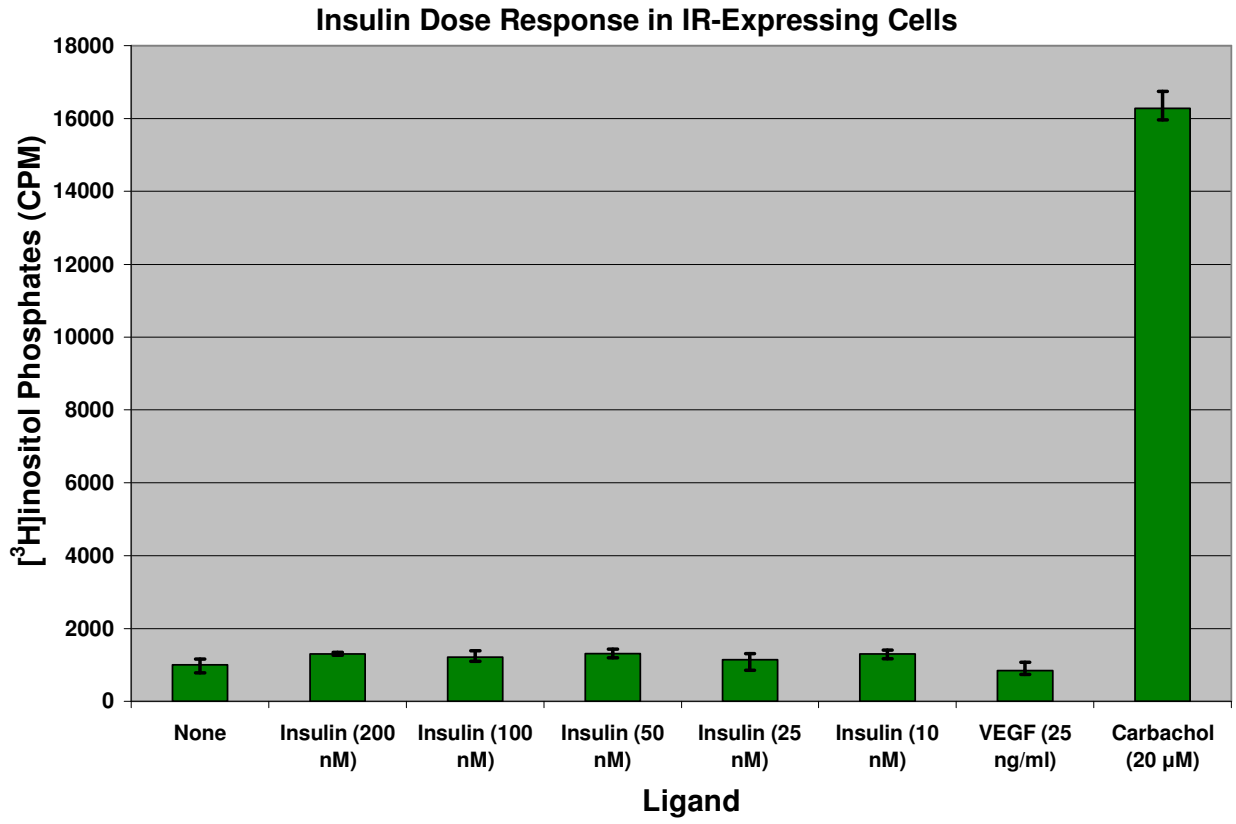

Figure 16. Insulin dose response curve as a function of hydrolysis of [^{3}H]inositol labeled phosphoinositides. IR-overexpressing cells were treated for one hour with insulin concentrations of 10-200 nM. Stimulation with carbachol (20 µM) was used as positive control. Untreated samples and cells treated with VEGF were negative controls. The means $\pm$ sd of data from three replicate treatment wells are graphed above.

The Effect of Insulin on VEGF Activation of Phosphoinositide Hydrolysis

Three identical experiments were performed to assess the effect, if any, of insulin on VEGF-stimulated phosphoinositide hydrolysis [Figure 17]. High and low (25 and 5 ng/ml, respectively) concentrations of VEGF with or without the addition of insulin (100 nM) were used to treat KDR-overexpressing cells for one hour. Untreated samples and those treated with insulin alone served as negative controls, while carbachol (20 μM) treatment was a positive control. Comparable to previous experiments, treatment with insulin alone led to a minimal response from these cells.

At the lower VEGF concentration, insulin appeared to slightly inhibit the average VEGF response. In contrast, at the higher VEGF concentration, insulin appeared to increase the average percent maximal inositol phosphate activity. However, after noting the variation in CPM readings between experiments and considering the standard error values, it appeared that insulin had no consistent effect on VEGF-stimulated phosphoinositide hydrolysis in KDR-overexpressing cells.

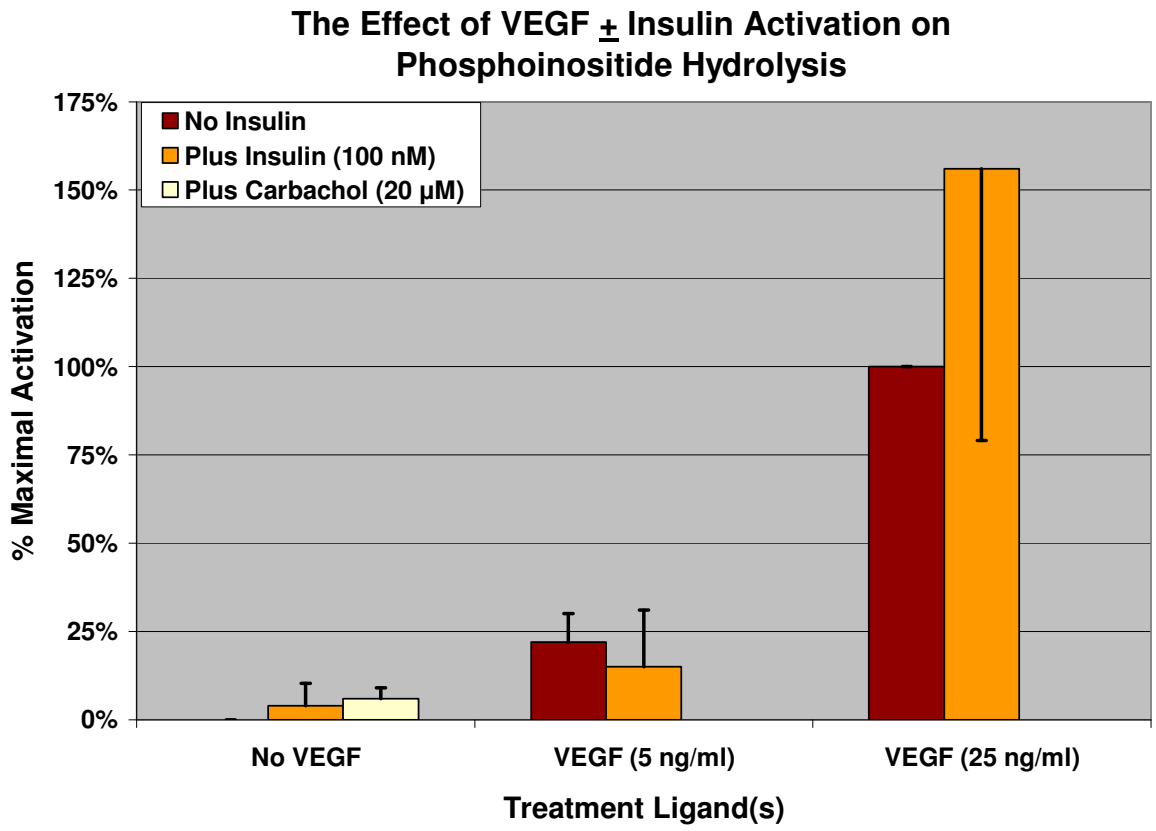

Figure 17. Effect of insulin on VEGF stimulated inositol phosphate accumulation. The columns in the graph above represent average percent maximal activation (mean ± sem) in three separate experiments. The basal (untreated) inositol phosphate responses were subtracted from the average responses, before being standardized as a percentage of VEGF activation at 25 ng/ml.

GST Fusion Proteins Used for the Detection of Signaling Interactions

Recombinant reagents for selective isolation of activated IR and KDR were generated in order to determine whether signaling intermediates principally associated with one pathway or the other would interact. The coding sequence from the SH2 domain of PI3-kinase was used for the successful creation of the "insulin signaling related" fusion protein, labeled GST-$SH2_{p85}$. The "VEGF signaling related" fusion protein was generated from the SH2 domain of PLC-γ. Results from a 10% Tris-HCl gel confirmed: 1) the presence of the protein domains of interest, and 2) that the attached protein domains were in fact fused to the GST and were therefore associated with the glutathione beads [Figure 18A].

IR-overexpressing cells and KDR-overexpressing cells were treated with insulin and VEGF, respectively. IR-cell samples were precipitated with immobilized GST-$SH2_{p85}$ and KDR-cell samples precipitated with GST-$SH2_{PLC-\gamma}$ before being probed with an anti-phosphotyrosine antibody [Figure 18B]. Surprisingly, this blot did not precipitate any phosphorylated proteins associated with VEGF activation of KDR [Figure 18B, right half]. An interaction between the GST-$SH2_{PLC-\gamma}$ fusion protein and KDR was expected, since phosphorylated KDR binds to the SH2 domain of PLC-γ. This blot also showed a strong ligand dependent interaction between the GST-$SH2_{p85}$ beads and what was suspected to be phosphorylated insulin receptor [Figure 18B, left half]. To confirm this, IR-expressing cells were treated with insulin and probed using an anti-phosphotyrosine antibody [Figure 18C, left blot]. Another sample of IR-overexpressing cells was treated with a mixture of hydrogen peroxide and sodium vanadate (a global inhibitor of tyrosine phosphatases) as a positive control. Stripping and reprobing this blot confirmed that the signal from the original phosphotyrosine blot was the IR [Figure 18C, right blot].

Repeating these experiments led to similar results with each set of glutathione fusion beads. However, additional experiments using both the GST-$SH2_{PLC-\gamma}$ and GST-$SH2_{p85}$ beads failed to provide any signal from VEGF treated KDR-cells. The GST-$SH2_{p85}$ beads consistently associated with a protein suggested to be the IR-β subunit, but other interactions were not reproducibly detected.

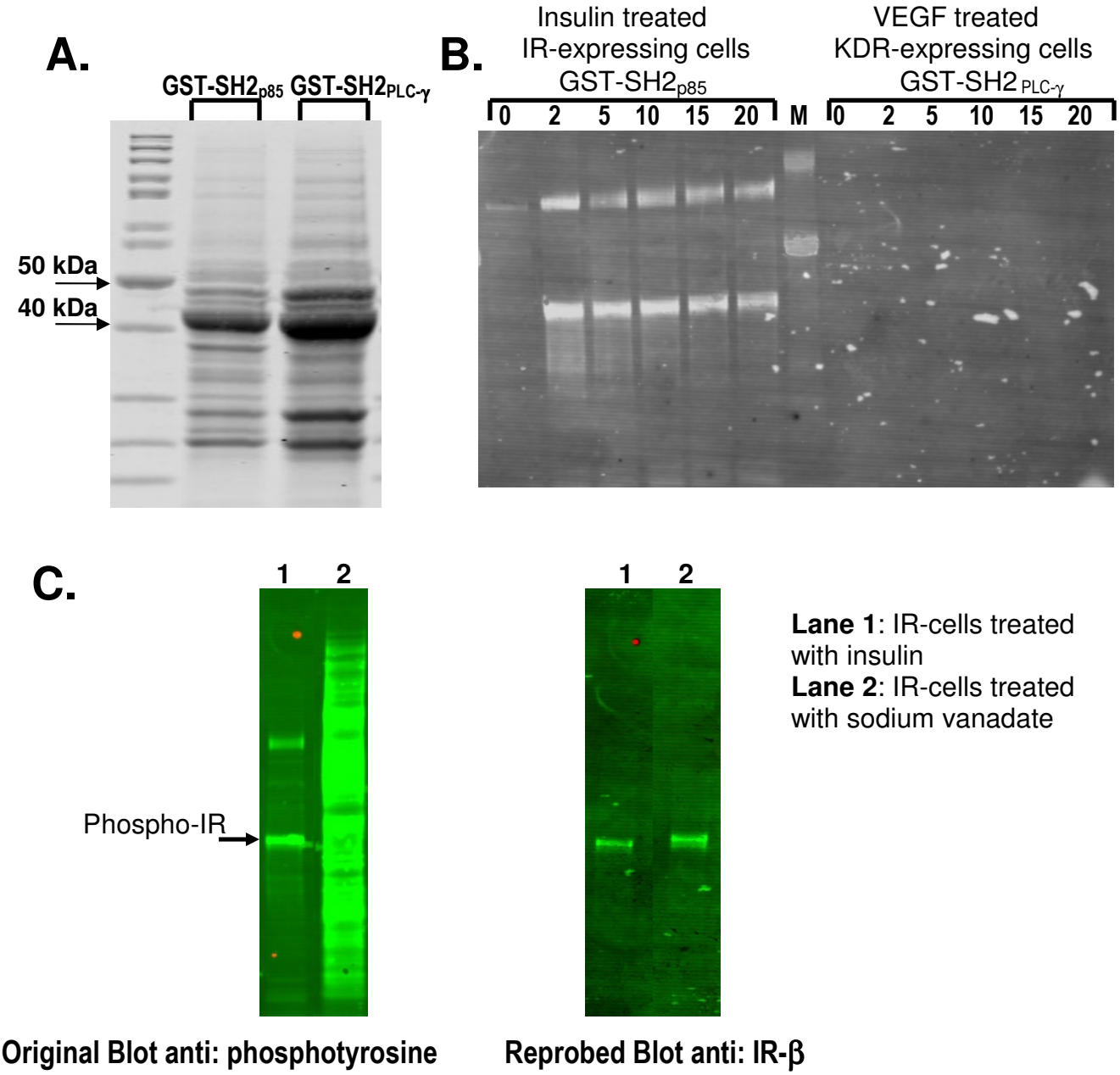

Figure 18. Protein precipitation using GST-SH2 fusion proteins. Gel confirming that the protein domains of interest were bound to GST and therefore associated with the glutathione beads [A]. Expected protein sizes for GST-SH2p85 and GST-SH2 were 40 and 41 kDa, respectively. Time course activation (in minutes) of IR-expressing cells treated with insulin and precipitated using the GST-$SH2_{p85}$ [B, left half]. Insulin treatment led to a ligand dependent response that decreased over time. Similar time course activation of KDR-expressing cells treated with VEGF and precipitated using GST-SH2 fusion beads [B, right half]. No signal was present after VEGF treatment and incubation with GST-SH2. IR-overexpressing cells treated with insulin (lane 1) or hydrogen peroxide + sodium vanadate (lane 2) before GST-$SH2_{p85}$precipitation [C, left blot]. The GST-$SH2_{p85}$ beads precipitated tyrosine-phosphorylated proteins the size of the IR. The blot was stripped and reprobed for total IR-β for confirmation [C, right blot].

DISCUSSION

Importance and Relevance of VEGF signaling

VEGF signaling is important to understand in detail because of its relevance to vital cellular and physiological processes. Interaction between substrates within VEGF pathways reveals alternative routes to the same outcome. This is a fairly novel concept, considering that activation of signaling elements downstream of KDR have been thought to be independently activated (Wu et al., 1999). The pathological relevance of endothelial dysfunction in diseases, such as diabetes, emphasizes the importance of VEGF signaling mechanisms in disease conditions. Since VEGF and insulin are both necessary for normal growth and maintenance of the endothelium, and given what we know about diabetes-associated vascular dysfunction, we asked the question: how does insulin affect VEGF signaling in the endothelium?

To answer this question, we decided to examine: 1) the effect of VEGF and insulin on shared downstream signaling activation in a model cell culture system, and 2) the ability of signaling proteins principally associated with the VEGF pathway to be altered by insulin. Given their direct relevance to the applications of this project, early cell treatment experiments utilized human umbilical vein endothelial cells. These cells were an unsuitable choice for these experiments, as signals for phosphorylated KDR and other proteins were not reproducibly detected after repeated trials. Handling and stability were also issues with the HUVECs, so an alternative line was selected for subsequent experiments. Since our lab has obtained reliable results from HEK293 cells transfected with KDR (Huckle unpublished; Rittler dissertation), using these cells was a viable alternative. HEK293 cells are often used because of their ease of transfection and handling (Tong et al., 1999). The KDR-overexpressing cells provided a model cell system for eliciting a measurable VEGF-induced response. This selection also provided an opportunity to stably transfect 293 cells with the IR. The IR-overexpressing cell line was a convenient control for analyzing changes in the insulin signaling pathway.

Akt Activation

It has been thoroughly documented that both VEGF and insulin induce Akt phosphorylation within their own signaling cascades. The physiological responses associated with insulin signaling Akt include translocation of the glucose transporter, while Akt phosphorylation is an important step in VEGF-stimulated eNOS activation. Both insulin and VEGF are associated with inducing the anti-apoptotic functions of Akt (Hermann et al., 2000; Gerber et al., 1998). Signaling through Akt has also been implicated in several disease conditions, such as cancer and impaired glucose metabolism (Sen et al., 2003).

Realizing the significance of possible crosstalk between insulin and VEGF signaling, Akt was chosen as a point of activation in phosphorylation studies. Interestingly, we noticed stronger average activation of Akt by insulin than VEGF in KDR-overexpressing cells. This was surprising, as it has been well documented that VEGF alone is capable of inducing a sufficient pro-survival response (Gerber et al., 1998). However, the presence of both ligands induced an effect that was less than additive, but greater than average VEGF activation alone. This finding suggests that the insulin and VEGF pathways may compete for an intermediate whose abundance is limiting, or that VEGF engages a negative regulatory step in the insulin-Akt cascade.

Immunoprecipitation with Akt provided clean, consistent results over several experimental trials, as well as a viable alternative to precipitation with GST fusion proteins. Previous studies have also used Akt phosphorylation as evidence of VEGF-induced activation of the PI3-kinase/Akt pathway (Feliers et al., 2005). Drawbacks from these studies included the specificity and availability of antibodies. Quantified results from the Akt and PLC-γ phosphorylation experiments underscored the importance of normalizing the amount of phosphorylated protein to total. Often, apparent phosphorylation patterns were a consequence of the amount of cells/protein present in each dish. Examining phosphorylated protein compared with total was an effective technique for normalizing results.

Similar Akt activation studies were performed in cells pretreated with AGE-BSA. The purpose of these experiments was to detect changes in Akt activation that may occur in a hyperglycemic/diabetic state. The connection between diabetes and the

rapid formation/accumulation of AGEs, which leads to endothelial dysfunction, is a well documented observation (Wautier and Schmidt, 2004). AGEs have been specifically implicated in the pathogenesis of diabetic retinopathy (Yamagishi et al., 2006). Experiments testing the effects of AGEs on the endothelium have shown increases in VEGF mRNA and VEGF mediated effects (Yamagishi et al., 1997; Yamagishi et al., 2002). This data corresponds with the excessive production of VEGF by diabetics and provides a mechanism for the high occurrence of microangiopathies in diabetics (Yamagishi et al., 2002). This group also concluded that treatment with AGE-BSA led to increased apoptotic cell death (Yamagishi et al., 2002).

Surprisingly, Akt activation (as indicated by increased P-Ser^{473}) was observed after AGE pretreatment in our studies. Changes in the concentration of VEGF might not have produced this Akt response, since the AGE+VEGF responses were approximately additive. Cell apoptosis is counteracted by Akt phosphorylation of pro-apoptotic factors; therefore, the increase in Akt phosphorylation may be occurring, via an unknown mechanism, in response to activation of an apoptotic pathway by AGE pretreatment. We did not measure markers of apoptosis in these studies. One unexpected observation was the irrelevance of the treatment ligand(s) on Akt response after AGE treatment. Specifically, AGE treated cells showed an elevated Akt response in the presence or absence of insulin. One trend not apparent in the Akt phosphorylation experiments was the slight increase in Akt activation in the presence of insulin. This may be a significant observation when considering the use of anti-VEGF or anti-AGE therapeutics.

PLC-γ Activation

PLC-γ is also a biologically meaningful signaling molecule that was targeted in our studies for its primary association with VEGF signaling through KDR. VEGF-induced phosphorylation of KDR leads to a direct interaction between phospho-KDR and PLC-γ that is independent of other intracellular effectors, such as PI3-kinase and PKC (Wu et al., 2000; Meyer et al., 2003). From our data, the lack of an insulin-induced response by PLC-γ is consistent with numerous previous reports and likely reflects the degree of selectivity of interaction between receptors (KDR and IR) and effectors (PLC-

γ and IRS-1/p85 et al.). This information also suggests an explanation as to why maximum PLC-γ activation occurs so soon after VEGF treatment.
Although PLC-γ activation is not typically associated with insulin signaling, other investigators have reported an increase in PLC-γ activity in adipocytes after treatment with insulin and proposed that PLC-γ may participate in the metabolic and mitogenic signaling of insulin (Kayali et al., 1998). The disagreement between these earlier findings and ours highlights the shortage of experimental evidence specifically examining the effect of insulin on PLC-γ in a wide variety of cell types. Our results suggest either a lack of interaction between insulin and PLC-γ, or perhaps a competitive binding event that elements in the VEGF response pathway ultimately wins. Alternatively, differences in cell type/receptor overexpression and the prevailing signaling cascade may alter the responsiveness of PLC-γ to insulin treatment.

The combined results of our [^{3}H]inositol labeling experiments lead us to several conclusions. From this data, we confirmed a dose-dependent response of VEGF activation of PLC-γ stimulated phosphoinositide hydrolysis. As in PLC-γ phosphorylation experiments, there was no evidence that insulin alone activated phosphoinositide hydrolysis. There was, however, a tantalizing suggestion that insulin may interfere with VEGF-stimulated inositol phosphate accumulation: in two of the three replicate experiments, 100 nM insulin reduced the response to 5 ng/ml VEGF by >50%. The high levels of variation across all three replicates prevented us from reaching a stronger conclusion on this point. This variation may be due in part to differences in the number of cells present in each sample or experimental error. Variation may be reduced in future studies through increasing the number of identically treated samples, or simply repeating these experiments. As it stands, these experiments reinforced the idea that insulin has only a marginal effect on VEGF signaling at or upstream of PLC-γ.

Recombinant Binding Domain Studies

Another initial goal of the project was to create GST-fusion proteins incorporating specific binding domains for testing possible cross-reactivity between insulin and VEGF signaling molecules. Previous results from our lab (Rittler dissertation) and numerous others indicate that GST-SH2$_{PLC\text{-}\gamma}$ fusion proteins would precipitate phosphorylated

KDR. This information led us to expect precipitated phospho-KDR, as well as other signaling proteins, which we hoped would reveal additional signaling interactions. Although the GST-$SH2_{PLC-\gamma}$ fusion protein was successfully produced for our experiments, we were unable to reproducibly co-precipitate phospho-KDR. This outcome raised doubts regarding the long term stability of the fusion proteins

In contrast to the GST-$SH2_{PLC-\gamma}$ beads, the GST-$SH2_{p85}$ beads regularly precipitated proteins corresponding (in size and after immunodetection) to the IR after IR-cells were treated with insulin. These experiments confirmed the association of our GST-fusion beads with phosphorylated IR and the rationale for creating GST-fusion proteins to show intracellular protein interactions. The IR-GST-$SH2_{p85}$ association was not unexpected, as phosphorylated IR is known to interact through IRS-1 with the SH2 domain (of the p85 regulatory subunit) in PI3-kinase (Cohen, 1999). In our studies, the presence of other tyrosine-phosphorylated proteins in precipitates was variable, as was the strength of the IR signal and the apparent stability of the fusion proteins.

In general, the GST fusion proteins did not interact with other signaling molecules as expected (or at all). Even after repeated preparations and gel confirmations of our GST fusion proteins, their behavior, especially that of GST-$SH2_{PLC-\gamma}$, was erratic. Other possible explanations for the difficulties we encountered with the fusion proteins might include: integrity of the binding domain cDNA, difficulty extracting protein from frozen bacterial stocks, disassociation/other unexpected reactions between the GST proteins and intracellular proteins, and dominance of innate signaling events over binding with artificially created proteins.

Future Work

There are many possible avenues for future work that would supplement the results of this project. For instance, it would be interesting to see if similar results were observed after changing the experimental design to include treatment over a longer time course or over a broader range of ligand concentrations. Though signal responses from Akt and PLC-γ were detectable within a matter of minutes, it might make more physiological sense to expose cells to ligands over a longer period. Performing different time course activation studies on cells prelabeled with [^{3}H]inositol might be a good way

to confirm results seen after our other radio labeling studies that included treatment with ligand(s) for 1 hour. [^{3}H]inositol labeling, coupled with AGE pretreatment may be a fruitful way to learn if diabetic conditions lead to the upregulation of other intracellular activities, specifically PLC-γ hydrolysis of phosphoinositides.

In addition to changing the activation period of the phosphorylation experiments, looking at the collective effect of insulin and VEGF on other shared downstream effectors (e.g. PI3-kinase, PKC, eNOS, MAP-kinase) would be useful. Conclusions about the effect of insulin on VEGF signaling would be far more reliable if they were substantiated by similar results from other signaling proteins. Functional products of these effectors, such as NO released from eNOS, or an increase in intracellular Ca^{2+} might also serve as alternative response to activation, rather than looking at phosphorylation alone.

There are also less conventional methods of examining Akt activation. For example, "in-cell" Western assays scanned with the Odyssey® Infrared Imaging System could verify the Akt phosphorylation detected after immunoprecipitation and immunoblotting. Akt phosphorylation can also be detected and quantified using specific ELISA (FACE™ Akt ELISA Kits, Active Motif North America) experiments that include fixation of cells with specific protein modifications. Primary antibodies are then used to probe for phosphorylated or total Akt. These experiments eliminate the need for prepared whole cell lysates and separation of proteins by SDS-PAGE.

Another suggestion for increasing the relevance of this project to *in vivo* conditions would be to develop protocols for use endothelial cells that generate reliable responses to VEGF and insulin stimulation. Our results from work with HUVECs did not turn out as expected, so we were obliged to use KDR-expressing HEK293 cells. Other groups have also had success using porcine aortic endothelial cells transfected for KDR (Waltenberger et al., 1994).

Bibbins et al. (1993) verified that SH2 binding reactions could be imitated with phosphopeptides and isolated SH2 domains. They used Affi-Gel-coupled phosphopeptides and GST-$SH2_{Src}$ fusion proteins to study binding affinity. Using these principles, it would be interesting to screen for interactions between our GST-fusion proteins and immobilized tyrosine containing phosphopeptides. Results from these

studies might lead to improvements of the GST-SH2 precipitation experiments we attempted in this project.

Final Conclusions

We had suspected additive effects of insulin on VEGF based on their known behavior in endothelial cells and their mutual involvement in several disease states. Considering all of the experiments performed in this project, it was concluded that our hypothesis, which predicted an additive effect of insulin on VEGF signaling, was not supported. Insulin and VEGF did not appear to have an additive effect on shared signaling proteins under normal conditions. In fact, the opposite trend, or a decrease in downstream activation of VEGF signaling was observed more often than not, particularly with Akt. This insulin-induced down regulation of VEGF activity suggests a somewhat deleterious or competitive effect between the two ligands. This response was also altered under modeled hyperglycemic conditions (AGE pretreatment). The observed increase in Akt activation in the presence of AGEs provided evidence for an imbalance in insulin and VEGF signaling within the diabetic state.

We can also conclude that VEGF activation of PLC-γ is an overriding signaling event, minimally affected by the presence of insulin. We showed that accumulation of [3H]inositol phosphates was directly correlated with VEGF concentration and a reliable method for examining outside effects (e.g. co-treatment with insulin) on the early events of VEGF signaling. Though novel interactions were not detected between binding domains principally associated with one pathway or the other, GST-fusion proteins still confirmed the phospho-IR/PI3-kinase binding event and the principle behind precipitation with glutathione beads.

More experimental evidence is needed to confirm the trends observed in these experiments. The variation in quantitative measurements often overwhelmed changes observed in phosphorylation or [^{3}H]inositol phosphate accumulation. Repetition of the described experiments might clarify patterns of activation and additional data would be useful for statistical analysis.

The overriding result from this project was insulin co-treatment with VEGF responses that were less than additive. Signaling responses demonstrated in this work

confirmed data previously established and provided evidence of unexplored mechanisms linking the VEGF and insulin pathways. Any additional information concerning the integration of VEGF and insulin signaling would certainly benefit ongoing diabetes research. Hopefully, future work in this area will contribute to the development of novel therapeutics, enhanced detection methods, and a greater overall understanding of the correlation between diabetes and cardiovascular disease.

LITERATURE CITED

(2005). Centers for Disease Control and Prevention. National diabetes fact sheet: general information and national estimates on diabetes in the United States, 2005., H.a.H. Services, ed., pp. 9.

Abe, H., Yamada, N., Kamata, K., Kuwaki, T., Shimada, M., Osuga, J., Shionoiri, F., Yahagi, N., Kadowaki, T., Tamemoto, H., et al. (1998). Hypertension, hypertriglyceridemia, and impaired endothelium-dependent vascular relaxation in mice lacking insulin receptor substrate-1. J Clin Invest 101, 1784-1788.

Accili, D., Drago, J., Lee, E.J., Johnson, M.D., Cool, M.H., Salvatore, P., Asico, L.D., Jose, P.A., Taylor, S.I., and Westphal, H. (1996). Early neonatal death in mice homozygous for a null allele of the insulin receptor gene. Nat Genet 12, 106-109.

Ahmad, S., Hewett, P.W., Wang, P., Al-Ani, B., Cudmore, M., Fujisawa, T., Haigh, J.J., le Noble, F., Wang, L., Mukhopadhyay, D., et al. (2006). Direct evidence for endothelial vascular endothelial growth factor receptor-1 function in nitric oxide-mediated angiogenesis. Circ Res 99, 715-722.

Ahmed, A., Dunk, C., Ahmad, S., and Khaliq, A. (2000). Regulation of placental vascular endothelial growth factor (VEGF) and placenta growth factor (PIGF) and soluble Flt-1 by oxygen--a review. Placenta 21 Suppl A, S16-24.

Araki, E., Lipes, M.A., Patti, M.E., Bruning, J.C., Haag, B., 3rd, Johnson, R.S., and Kahn, C.R. (1994). Alternative pathway of insulin signalling in mice with targeted disruption of the IRS-1 gene. Nature 372, 186-190.

Bansilal, S., Farkouh, M.E., and Fuster, V. (2007). Role of insulin resistance and hyperglycemia in the development of atherosclerosis. Am J Cardiol 99, 6B-14B.

Bevan, P. (2001). Insulin signalling. J Cell Sci 114, 1429-1430.

Bibbins, K.B., Boeuf, H., and Varmus, H.E. (1993). Binding of the Src SH2 domain to phosphopeptides is determined by residues in both the SH2 domain and the phosphopeptides. Mol Cell Biol 13, 7278-7287.

Bierhaus, A., Hofmann, M.A., Ziegler, R., and Nawroth, P.P. (1998). AGEs and their interaction with AGE-receptors in vascular disease and diabetes mellitus. I. The AGE concept. Cardiovasc Res 37, 586-600.

Bjornholm, M., and Zierath, J.R. (2005). Insulin signal transduction in human skeletal muscle: identifying the defects in Type II diabetes. Biochem Soc Trans 33, 354-357.

Blanes, M.G., Oubaha, M., Rautureau, Y., and Gratton, J.P. (2007). Phosphorylation of tyrosine 801 of vascular endothelial growth factor receptor-2 is necessary for Akt-dependent endothelial nitric-oxide synthase activation and nitric oxide release from endothelial cells. J Biol Chem 282, 10660-10669.

Bliss, M. (1982). The Discovery of Insulin (Toronto, McClelland & Stewart Inc.).

Cai, W., He, J.C., Zhu, L., Chen, X., Striker, G.E., and Vlassara, H. (2008). AGE-receptor-1 counteracts cellular oxidant stress induced by AGEs via negative regulation of p66shc-dependent FKHRL1 phosphorylation. Am J Physiol Cell Physiol 294, C145-152.

Campbell, N.A., and Reece, J.B. (2002). Biology, 6th edn (San Francisco, Benjamin Cummings).

Cardone, M.H., Roy, N., Stennicke, H.R., Salvesen, G.S., Franke, T.F., Stanbridge, E., Frisch, S., and Reed, J.C. (1998). Regulation of cell death protease caspase-9 by phosphorylation. Science 282, 1318-1321.

Chakravarthy, U., Hayes, R.G., Stitt, A.W., McAuley, E., and Archer, D.B. (1998). Constitutive nitric oxide synthase expression in retinal vascular endothelial cells is suppressed by high glucose and advanced glycation end products. Diabetes 47, 945-952.

Chang, L., Chiang, S.H., and Saltiel, A.R. (2004). Insulin signaling and the regulation of glucose transport. Mol Med 10, 65-71.

Chattopadhyay, A., Vecchi, M., Ji, Q., Mernaugh, R., and Carpenter, G. (1999). The role of individual SH2 domains in mediating association of phospholipase C-gamma1 with the activated EGF receptor. J Biol Chem 274, 26091-26097.

Cheng, S.Y., Nagane, M., Huang, H.S., and Cavenee, W.K. (1997). Intracerebral tumor-associated hemorrhage caused by overexpression of the vascular endothelial growth factor isoforms VEGF121 and VEGF165 but not VEGF189. Proc Natl Acad Sci U S A 94, 12081-12087.

Chuang, L.M., Hausdorff, S.F., Myers, M.G., Jr., White, M.F., Birnbaum, M.J., and Kahn, C.R. (1994). Interactive roles of Ras, insulin receptor substrate-1, and proteins with Src homology-2 domains in insulin signaling in Xenopus oocytes. J Biol Chem 269, 27645-27649.

Claesson-Welsh, L. (2003). Signal transduction by vascular endothelial growth factor receptors. Biochem Soc Trans 31, 20-24.

Cohen, P. (1999). The Croonian Lecture 1998. Identification of a protein kinase cascade of major importance in insulin signal transduction. Philos Trans R Soc Lond B Biol Sci 354, 485-495.

Collombat, P., Hecksher-Sorensen, J., Serup, P., and Mansouri, A. (2006). Specifying pancreatic endocrine cell fates. Mech Dev 123, 501-512.

De Meyts, P. (2004). Insulin and its receptor: structure, function and evolution. Bioessays 26, 1351-1362.

Duvillie, B., Cordonnier, N., Deltour, L., Dandoy-Dron, F., Itier, J.M., Monthioux, E., Jami, J., Joshi, R.L., and Bucchini, D. (1997). Phenotypic alterations in insulin-deficient mutant mice. Proc Natl Acad Sci U S A 94, 5137-5140.

Dvorak, H.F. (2002). Vascular permeability factor/vascular endothelial growth factor: a critical cytokine in tumor angiogenesis and a potential target for diagnosis and therapy. J Clin Oncol 20, 4368-4380.

Dvorak, H.F., Brown, L.F., Detmar, M., and Dvorak, A.M. (1995). Vascular permeability factor/vascular endothelial growth factor, microvascular hyperpermeability, and angiogenesis. Am J Pathol 146, 1029-1039.

Farese, R.V., Sajan, M.P., and Standaert, M.L. (2005). Atypical protein kinase C in insulin action and insulin resistance. Biochem Soc Trans 33, 350-353.

Farese, R.V., Sajan, M.P., and Standaert, M.L. (2005). Insulin-sensitive protein kinases (atypical protein kinase C and protein kinase B/Akt): actions and defects in obesity and type II diabetes. Exp Biol Med (Maywood) 230, 593-605.

Federici, M., Pandolfi, A., De Filippis, E.A., Pellegrini, G., Menghini, R., Lauro, D., Cardellini, M., Romano, M., Sesti, G., Lauro, R., et al. (2004). G972R IRS-1 variant impairs insulin regulation of endothelial nitric oxide synthase in cultured human endothelial cells. Circulation 109, 399-405.

Feliers, D., Chen, X., Akis, N., Choudhury, G.G., Madaio, M., and Kasinath, B.S. (2005). VEGF regulation of endothelial nitric oxide synthase in glomerular endothelial cells. Kidney Int 68, 1648-1659.

Ferrara, N. (2001). Role of vascular endothelial growth factor in regulation of physiological angiogenesis. Am J Physiol Cell Physiol 280, C1358-1366.

Ferrara, N., Gerber, H.P., and LeCouter, J. (2003). The biology of VEGF and its receptors. Nat Med 9, 669-676.

Franke, T.F. (2008). Intracellular signaling by Akt: bound to be specific. Sci Signal 1, pe29.

George, S., Rochford, J.J., Wolfrum, C., Gray, S.L., Schinner, S., Wilson, J.C., Soos, M.A., Murgatroyd, P.R., Williams, R.M., Acerini, C.L., et al. (2004). A family with severe insulin resistance and diabetes due to a mutation in AKT2. Science 304, 1325-1328.

Gerber, H.P., McMurtrey, A., Kowalski, J., Yan, M., Keyt, B.A., Dixit, V., and Ferrara, N. (1998). Vascular endothelial growth factor regulates endothelial cell survival through the phosphatidylinositol 3'-kinase/Akt signal transduction pathway. Requirement for Flk-1/KDR activation. J Biol Chem 273, 30336-30343.

Gerber, H.P., McMurtrey, A., Kowalski, J., Yan, M., Keyt, B.A., Dixit, V., and Ferrara, N. (1998). Vascular endothelial growth factor regulates endothelial cell survival through the phosphatidylinositol 3'-kinase/Akt signal transduction pathway. Requirement for Flk-1/KDR activation. J Biol Chem 273, 30336-30343.

Groop, P.H., Forsblom, C., and Thomas, M.C. (2005). Mechanisms of disease: Pathway-selective insulin resistance and microvascular complications of diabetes. Nat Clin Pract Endocrinol Metab 1, 100-110.

Gual, P., Le Marchand-Brustel, Y., and Tanti, J.F. (2005). Positive and negative regulation of insulin signaling through IRS-1 phosphorylation. Biochimie 87, 99-109.

Gugliucci, A. (2000). Glycation as the glucose link to diabetic complications. J Am Osteopath Assoc 100, 621-634.

Guyton A.C., and Hall, J.E. (2006). Textbook of Medical Physiology, 11 edn (Philadelphia, Elsevier Inc.).

Hadi, H.A., Carr, C.S., and Al Suwaidi, J. (2005). Endothelial dysfunction: cardiovascular risk factors, therapy, and outcome. Vasc Health Risk Manag 1, 183-198.

Hanada, M., Feng, J., and Hemmings, B.A. (2004). Structure, regulation and function of PKB/AKT--a major therapeutic target. Biochim Biophys Acta 1697, 3-16.

He, H., Venema, V.J., Gu, X., Venema, R.C., Marrero, M.B., and Caldwell, R.B. (1999). Vascular endothelial growth factor signals endothelial cell production of nitric oxide and prostacyclin through flk-1/KDR activation of c-Src. J Biol Chem 274, 25130-25135.

Heller, S., Kozlovski, P., and Kurtzhals, P. (2007). Insulin's 85th anniversary—An enduring medical miracle. Diabetes Res Clin Pract 78, 149-158.

Hermann, C., Assmus, B., Urbich, C., Zeiher, A.M., and Dimmeler, S. (2000). Insulin-mediated stimulation of protein kinase Akt: A potent survival signaling cascade for endothelial cells. Arterioscler Thromb Vasc Biol 20, 402-409.

Hiratsuka, S., Maru, Y., Okada, A., Seiki, M., Noda, T., and Shibuya, M. (2001). Involvement of Flt-1 tyrosine kinase (vascular endothelial growth factor receptor-1) in pathological angiogenesis. Cancer Res 61, 1207-1213.

Huckle, W.R., Hawes, B.E., and Conn, P.M. (1989). Protein kinase C-mediated gonadotropin-releasing hormone receptor sequestration is associated with uncoupling of phosphoinositide hydrolysis. J Biol Chem 264, 8619-8626.

Hurwitz, H., Fehrenbacher, L., Novotny, W., Cartwright, T., Hainsworth, J., Heim, W., Berlin, J., Baron, A.,

Griffing, S., Holmgren, E., et al. (2004). Bevacizumab plus irinotecan, fluorouracil, and leucovorin for metastatic colorectal cancer. N Engl J Med 350, 2335-2342.

Insel, P.M., and Roth, W.T. (2006). Core Concepts in Health, 10 edn (The McGraw-Hill Companies, Inc.).

Ishiki, M., and Klip, A. (2005). Minireview: recent developments in the regulation of glucose transporter-4 traffic: new signals, locations, and partners. Endocrinology 146, 5071-5078.

Ishisaki, A., Tsunobuchi, H., Nakajima, K., and Imamura, T. (2004). Possible involvement of protein kinase C activation in differentiation of human umbilical vein endothelium-derived cell into smooth muscle-like cell. Biol Cell 96, 499-508.

Jiang, Z.Y., He, Z., King, B.L., Kuroki, T., Opland, D.M., Suzuma, K., Suzuma, I., Ueki, K., Kulkarni, R.N., Kahn, C.R., et al. (2003). Characterization of multiple signaling pathways of insulin in the regulation of vascular endothelial growth factor expression in vascular cells and angiogenesis. J Biol Chem 278, 31964-31971.

Kaburagi, Y., Yamamoto-Honda, R., Tobe, K., Ueki, K., Yachi, M., Akanuma, Y., Stephens, R.M., Kaplan, D., Yazaki, Y., and Kadowaki, T. (1995). The role of the NPXY motif in the insulin receptor in tyrosine phosphorylation of insulin receptor substrate-1 and Shc. Endocrinology 136, 3437-3443.

Kanzaki, M. (2006). Insulin receptor signals regulating GLUT4 translocation and actin dynamics. Endocr J 53, 267-293.

Kayali, A.G., Eichhorn, J., Haruta, T., Morris, A.J., Nelson, J.G., Vollenweider, P., Olefsky, J.M., and Webster, N.J. (1998). Association of the insulin receptor with phospholipase C-gamma (PLCgamma) in 3T3-L1 adipocytes suggests a role for PLCgamma in metabolic signaling by insulin. J Biol Chem 273, 13808-13818.

Kendall, R.L., Rutledge, R.Z., Mao, X., Tebben, A.J., Hungate, R.W., and Thomas, K.A. (1999). Vascular endothelial growth factor receptor KDR tyrosine kinase activity is increased by autophosphorylation of two activation loop tyrosine residues. J Biol Chem 274, 6453-6460.

Kendall, R.L., and Thomas, K.A. (1993). Inhibition of vascular endothelial cell growth factor activity by an endogenously encoded soluble receptor. Proc Natl Acad Sci U S A 90, 10705-10709.

King, G.L., and Loeken, M.R. (2004). Hyperglycemia-induced oxidative stress in diabetic complications. Histochem Cell Biol 122, 333-338.

Kliche, S., and Waltenberger, J. (2001). VEGF receptor signaling and endothelial function. IUBMB Life 52, 61-66.

Knutson, V.P. (1991). Cellular trafficking and processing of the insulin receptor. FASEB J 5, 2130-2138.

Koschinsky, T., He, C.J., Mitsuhashi, T., Bucala, R., Liu, C., Buenting, C., Heitmann, K., and Vlassara, H. (1997). Orally absorbed reactive glycation products (glycotoxins): an environmental risk factor in diabetic nephropathy. Proc Natl Acad Sci U S A 94, 6474-6479.

Krasilnikov, M.A. (2000). Phosphatidylinositol-3 kinase dependent pathways: the role in control of cell growth, survival, and malignant transformation. Biochemistry (Mosc) 65, 59-67.

Kroll, J., and Waltenberger, J. (1999). A novel function of VEGF receptor-2 (KDR): rapid release of nitric oxide in response to VEGF-A stimulation in endothelial cells. Biochem Biophys Res Commun 265, 636-639.

Kruger, D.F., Martin, C.L., and Sadler, C.E. (2006). New insights into glucose regulation. Diabetes Educ 32, 221-228.

Laakso, M. (1999). Hyperglycemia and cardiovascular disease in type 2 diabetes. Diabetes 48, 937-942.

Lantz, M., Vondrichova, T., Parikh, H., Frenander, C., Ridderstrale, M., Asman, P., Aberg, M., Groop, L., and Hallengren, B. (2005). Overexpression of immediate early genes in active Graves' ophthalmopathy. J Clin Endocrinol Metab 90, 4784-4791.

Lawlor, M.A., and Alessi, D.R. (2001). PKB/Akt: a key mediator of cell proliferation, survival and insulin responses? J Cell Sci 114, 2903-2910.

Leung, D.W., Cachianes, G., Kuang, W.J., Goeddel, D.V., and Ferrara, N. (1989). Vascular endothelial growth factor is a secreted angiogenic mitogen. Science 246, 1306-1309.

Li, H., Wallerath, T., and Forstermann, U. (2002). Physiological mechanisms regulating the expression of endothelial-type NO synthase. Nitric Oxide 7, 132-147.

Luo, M., Langlais, P., Yi, Z., Lefort, N., De Filippis, E.A., Hwang, H., Christ-Roberts, C.Y., and Mandarino, L.J. (2007). Phosphorylation of human insulin receptor substrate-1 at Serine 629 plays a positive role in insulin signaling. Endocrinology 148, 4895-4905.

Matsumoto, T., and Claesson-Welsh, L. (2001). VEGF receptor signal transduction. Sci STKE 2001, RE21.

Meyer, R.D., Latz, C., and Rahimi, N. (2003). Recruitment and activation of phospholipase Cgamma1 by vascular endothelial growth factor receptor-2 are required for tubulogenesis and differentiation of endothelial cells. J Biol Chem 278, 16347-16355.

Montagnani, M., Ravichandran, L.V., Chen, H., Esposito, D.L., and Quon, M.J. (2002). Insulin receptor substrate-1 and phosphoinositide-dependent kinase-1 are required for insulin-stimulated production of nitric oxide in endothelial cells. Mol Endocrinol 16, 1931-1942.

Morisco, C., Lembo, G., and Trimarco, B. (2006). Insulin resistance and cardiovascular risk: New insights from molecular and cellular biology. Trends Cardiovasc Med 16, 183-188.

Myers, M.G., Jr., Sun, X.J., Cheatham, B., Jachna, B.R., Glasheen, E.M., Backer, J.M., and White, M.F. (1993). IRS-1 is a common element in insulin and insulin-like growth factor-I signaling to the phosphatidylinositol 3'-kinase. Endocrinology 132, 1421-1430.

Neid, M., Datta, K., Stephan, S., Khanna, I., Pal, S., Shaw, L., White, M., and Mukhopadhyay, D. (2004). Role of insulin receptor substrates and protein kinase C-zeta in vascular permeability factor/vascular endothelial growth factor expression in pancreatic cancer cells. J Biol Chem 279, 3941-3948.

Neid, M., Datta, K., Stephan, S., Khanna, I., Pal, S., Shaw, L., White, M., and Mukhopadhyay, D. (2004). Role of insulin receptor substrates and protein kinase C-zeta in vascular permeability factor/vascular endothelial growth factor expression in pancreatic cancer cells. J Biol Chem 279, 3941-3948.

Ornskov, D., Nexo, E., and Sorensen, B.S. (2006). Insulin-induced proliferation of bladder cancer cells is mediated through activation of the epidermal growth factor system. FEBS J 273, 5479-5489.

Peppa, M., and Vlassara, H. (2005). Advanced glycation end products and diabetic complications: a general overview. Hormones (Athens) 4, 28-37.

Peters, K.G., De Vries, C., and Williams, L.T. (1993). Vascular endothelial growth factor receptor expression during embryogenesis and tissue repair suggests a role in endothelial differentiation and blood vessel growth. Proc Natl Acad Sci U S A 90, 8915-8919.

Rask-Madsen, C., and King, G.L. (2007). Mechanisms of Disease: endothelial dysfunction in insulin resistance and diabetes. Nat Clin Pract Endocrinol Metab 3, 46-56.

Roach, P.J. (2002). Glycogen and its metabolism. Curr Mol Med 2, 101-120.

Robinson, C.J., and Stringer, S.E. (2001). The splice variants of vascular endothelial growth factor (VEGF) and their receptors. J Cell Sci 114, 853-865.

Rosen, E.D., and Spiegelman, B.M. (2006). Adipocytes as regulators of energy balance and glucose homeostasis. Nature 444, 847-853.

Rother, K.I., and Accili, D. (2000). Role of insulin receptors and IGF receptors in growth and development. Pediatr Nephrol 14, 558-561.

Saltiel, A.R., and Kahn, C.R. (2001). Insulin signalling and the regulation of glucose and lipid metabolism. Nature 414, 799-806.

Sawano, A., Iwai, S., Sakurai, Y., Ito, M., Shitara, K., Nakahata, T., and Shibuya, M. (2001). Flt-1, vascular endothelial growth factor receptor 1, is a novel cell surface marker for the lineage of monocyte-macrophages in humans. Blood 97, 785-791.

Sen, P., Mukherjee, S., Ray, D., and Raha, S. (2003). Involvement of the Akt/PKB signaling pathway with disease processes. Mol Cell Biochem 253, 241-246.

Senthil, D., Ghosh Choudhury, G., Bhandari, B.K., and Kasinath, B.S. (2002). The type 2 vascular endothelial growth factor receptor recruits insulin receptor substrate-1 in its signalling pathway. Biochem J 368, 49-56.

Shalaby, F., Rossant, J., Yamaguchi, T.P., Gertsenstein, M., Wu, X.F., Breitman, M.L., and Schuh, A.C. (1995). Failure of blood-island formation and vasculogenesis in Flk-1-deficient mice. Nature 376, 62-66.

Sheetz, M.J., and King, G.L. (2002). Molecular understanding of hyperglycemia's adverse effects for diabetic complications. JAMA 288, 2579-2588.

Shibuya, M. (2003). Vascular endothelial growth factor receptor-2: its unique signaling and specific ligand, VEGF-E. Cancer Sci 94, 751-756.

Shibuya, M. (2006). Differential roles of vascular endothelial growth factor receptor-1 and receptor-2 in angiogenesis. J Biochem Mol Biol 39, 469-478.

Shibuya, M. (2006). Vascular endothelial growth factor (VEGF)-Receptor2: its biological functions, major signaling pathway, and specific ligand VEGF-E. Endothelium 13, 63-69.

Sonnenburg, E.D., Gao, T., and Newton, A.C. (2001). The phosphoinositide-dependent kinase, PDK-1, phosphorylates conventional protein kinase C isozymes by a mechanism that is independent of phosphoinositide 3-kinase. J Biol Chem 276, 45289-45297.

Spranger, J., and Pfeiffer, A.F. (2001). New concepts in pathogenesis and treatment of diabetic retinopathy. Exp Clin Endocrinol Diabetes 109 Suppl 2, S438-450.

Sun, X.J., Rothenberg, P., Kahn, C.R., Backer, J.M., Araki, E., Wilden, P.A., Cahill, D.A., Goldstein, B.J., and White, M.F. (1991). Structure of the insulin receptor substrate IRS-1 defines a unique signal transduction protein. Nature 352, 73-77.

Takahashi, T., Yamaguchi, S., Chida, K., and Shibuya, M. (2001). A single autophosphorylation site on KDR/Flk-1 is essential for VEGF-A-dependent activation of PLC-gamma and DNA synthesis in vascular endothelial cells. EMBO J 20, 2768-2778.

Tamemoto, H., Kadowaki, T., Tobe, K., Yagi, T., Sakura, H., Hayakawa, T., Terauchi, Y., Ueki, K., Kaburagi, Y., Satoh, S., et al. (1994). Insulin resistance and growth retardation in mice lacking insulin receptor substrate-1. Nature 372, 182-186.

Tennyson, G.E. (2002). Understanding type 2 diabetes mellitus and associated cardiovascular disease: linked by insulin resistance. Am J Manag Care 8, S450-459.

Thirone, A.C., Huang, C., and Klip, A. (2006). Tissue-specific roles of IRS proteins in insulin signaling and glucose transport. Trends Endocrinol Metab 17, 72-78.

Tong, J., Du, G.G., Chen, S.R., and MacLennan, D.H. (1999). HEK-293 cells possess a carbachol- and thapsigargin-sensitive intracellular Ca2+ store that is responsive to stop-flow medium changes and insensitive to caffeine and ryanodine. Biochem J 343 Pt 1, 39-44.

Ullrich, A., Bell, J.R., Chen, E.Y., Herrera, R., Petruzzelli, L.M., Dull, T.J., Gray, A., Coussens, L., Liao, Y.C., Tsubokawa, M., et al. (1985). Human insulin receptor and its relationship to the tyrosine kinase family of oncogenes. Nature 313, 756-761.

van der Geer, P., Wiley, S., and Pawson, T. (1999). Re-engineering the target specificity of the insulin receptor by modification of a PTB domain binding site. Oncogene 18, 3071-3075.

Wada, R., and Yagihashi, S. (2005). Role of advanced glycation end products and their receptors in development of diabetic neuropathy. Ann N Y Acad Sci 1043, 598-604.

Waltenberger, J., Claesson-Welsh, L., Siegbahn, A., Shibuya, M., and Heldin, C.H. (1994). Different signal transduction properties of KDR and Flt1, two receptors for vascular endothelial growth factor. J Biol Chem 269, 26988-26995.

Watson, R.T., and Pessin, J.E. (2006). Bridging the GAP between insulin signaling and GLUT4 translocation. Trends Biochem Sci 31, 215-222.

Wautier, J.L., and Schmidt, A.M. (2004). Protein glycation: a firm link to endothelial cell dysfunction. Circ Res 95, 233-238.

Welsh, G.I., Hers, I., Berwick, D.C., Dell, G., Wherlock, M., Birkin, R., Leney, S., and Tavare, J.M. (2005). Role of protein kinase B in insulin-regulated glucose uptake. Biochem Soc Trans 33, 346-349.

Williams, M.R., Arthur, J.S., Balendran, A., van der Kaay, J., Poli, V., Cohen, P., and Alessi, D.R. (2000). The role of 3-phosphoinositide-dependent protein kinase 1 in activating AGC kinases defined in embryonic stem cells. Curr Biol 10, 439-448.

Wolf, G., Trub, T., Ottinger, E., Groninga, L., Lynch, A., White, M.F., Miyazaki, M., Lee, J., and Shoelson, S.E. (1995). PTB domains of IRS-1 and Shc have distinct but overlapping binding specificities. J Biol Chem 270, 27407-27410.

Wong, E.Y., Morgan, L., Smales, C., Lang, P., Gubby, S.E., and Staddon, J.M. (2000). Vascular endothelial growth factor stimulates dephosphorylation of the catenins p120 and p100 in endothelial cells. Biochem J 346 Pt 1, 209-216.

Wu, L.W., Mayo, L.D., Dunbar, J.D., Kessler, K.M., Baerwald, M.R., Jaffe, E.A., Wang, D., Warren, R.S., and Donner, D.B. (2000). Utilization of distinct signaling pathways by receptors for vascular endothelial cell growth factor and other mitogens in the induction of endothelial cell proliferation. J Biol Chem 275, 5096-5103.

Xu, B., Chibber, R., Ruggiero, D., Kohner, E., Ritter, J., and Ferro, A. (2003). Impairment of vascular endothelial nitric oxide synthase activity by advanced glycation end products. FASEB J 17, 1289-1291.

Xu, J., Xie, Z., Reece, R., Pimental, D., and Zou, M.H. (2006). Uncoupling of endothelial nitric oxidase synthase by hypochlorous acid: role of NAD(P)H oxidase-derived superoxide and peroxynitrite. Arterioscler Thromb Vasc Biol 26, 2688-2695.

Yamagishi, S., Inagaki, Y., Okamoto, T., Amano, S., Koga, K., Takeuchi, M., and Makita, Z. (2002). Advanced glycation end product-induced apoptosis and overexpression of vascular endothelial growth factor and monocyte chemoattractant protein-1 in human-cultured mesangial cells. J Biol Chem 277, 20309-20315.

Yamagishi, S., Nakamura, K., and Imaizumi, T. (2005). Advanced glycation end products (AGEs) and diabetic vascular complications. Curr Diabetes Rev 1, 93-106.

Yamagishi, S., Nakamura, K., and Matsui, T. (2006). Advanced glycation end products (AGEs) and their receptor (RAGE) system in diabetic retinopathy. Curr Drug Discov Technol 3, 83-88.

Yamagishi, S., Nakamura, K., Matsui, T., Takenaka, K., Jinnouchi, Y., and Imaizumi, T. (2006). Cardiovascular disease in diabetes. Mini Rev Med Chem 6, 313-318.

Yamagishi, S., Yonekura, H., Yamamoto, Y., Katsuno, K., Sato, F., Mita, I., Ooka, H., Satozawa, N., Kawakami, T., Nomura, M., et al. (1997). Advanced glycation end products-driven angiogenesis in vitro. Induction of the growth and tube formation of human microvascular endothelial cells through autocrine vascular endothelial growth factor. J Biol Chem 272, 8723-8730.

Yonekura, H., Yamamoto, Y., Sakurai, S., Petrova, R.G., Abedin, M.J., Li, H., Yasui, K., Takeuchi, M., Makita, Z., Takasawa, S., et al. (2003). Novel splice variants of the receptor for advanced glycation end-products expressed in human vascular endothelial cells and pericytes, and their putative roles in diabetes-induced vascular injury. Biochem J 370, 1097-1109.

Zeng, G., Nystrom, F.H., Ravichandran, L.V., Cong, L.N., Kirby, M., Mostowski, H., and Quon, M.J. (2000). Roles for insulin receptor, PI3-kinase, and Akt in insulin-signaling pathways related to production of nitric oxide in human vascular endothelial cells. Circulation 101, 1539-1545.

Zimmet, P., Alberti, K.G., and Shaw, J. (2001). Global and societal implications of the diabetes epidemic. Nature 414, 782-787.

APPENDICES

Appendix A. Sequences of primers used in PCR and sequencing reactions

Primer	Domain	Incorporated Restriction Site
BH-526	SHC-PTB 5'	*Bgl*II
BH-527	SHC-PTB 3'	*Eco*RI and stop codon
BH-528	IRS-1 PTB 5'	*Bam*HI
BH-529	IRS-1 PTB 3'	*Eco*RI and stop codon
BH-530	p85-SH2 5'	*Bam*HI
BH-531	p85-SH2 3'	*Eco*RI and stop codon

BH-20, TGGCAAGCCACGTTTGG
BH-21, GTCAGAGGTTTTCACCG
BH-526, TGGACCCGCCACGGGAGATCTGTCAATAAGCCCACGC
BH-527, GACCAGTTTGGGTGGAATTCAGAGGTATTGTTTGAAGCGCAA
BH-528, GGCAGCTGCAGCGGATCCTCCGGCCTTGGTGAGGCTGGGG
BH-529, GGAGCCTGGCTTCCGAATTCACATGCTGGCCGGGGAGGTGGC
BH-530, AAACCTACTACTGTAGCCGGATCCGGTATGAATAACAATA
BH-531, TCCCTACAGCTTGAATTCAATCTTCTTTGACAACTTGATCCTG
BH-553, GCGATGGCGGTTTCATCT
BH-554, GTGACACTGCGGAAGGAACTC
BH-555, GTCCCTCCGGGTACACGAT
BH-556, CTTCTAGGAGGTGGCACACCTT
BH-580, CCACTATCGACTGGTCCCGTATC
BH-581, GATACGGGACCAGTCGATAGTGG
BH-582, TGACGCATGAAATCTTTGAGAACAACG
BH-583, CGTTGTTCTCAAAGATTTCATGCGTCA

Restriction endonuclease sites are underlined

Appendix B. Antibodies used in immunoprecipitations and immunoblotting

	Antibody Target	Immunogen	Vendor	Catalog No.	Species
Primary Antibodies	Phospho-tyrosine	phospho-peptide	Cell Signaling	9411	Mouse
	Phospho-tyrosine, Clone 4G10	phosphotyramine-KLH	Millipore	05-321	Mouse
	KDR	m1158-1344	Santa Cruz	sc-6251	Mouse
	KDR	m1158-1345	Santa Cruz	sc-504	Rabbit
	KDR-PY^{1175}	phospho-peptide	Cell Signaling	2478	Rabbit
	KDR-PY^{996}	phospho-peptide	Cell Signaling	2474	Rabbit
	Akt-1	C-termimus	Santa Cruz	sc-1618R	Rabbit
	Akt-P-Ser^{473}	phospho-peptide	Cell Signaling	4051S	Rabbit
	Insulin Receptor-β	C-termimus	Santa Cruz	sc-711	Rabbit
	IGF-1 Receptor-β	C-termimus	Santa Cruz	sc-713	Rabbit
	PLC-γ1	C-termimus	Santa Cruz	sc-7290	Mouse
	PLC-γ1	C-termimus	Santa Cruz	sc-81	Mouse
	PLC-γ-PY^{783}	phospho-peptide	Cell Signaling	2821S	Rabbit
	IRS-1	C-termimus	Cell Signaling	2382S	Rabbit
	IRS-1-PY^{632}	phospho-peptide	Santa Cruz	sc-17196	Goat
IRDye® 800 Conjugated Antibodies	Anti-mouse	Mouse IgG	Rockland	610-732-124	Donkey
	Anti-rabbit	Rabbit IgG	Rockland	611-732-127	Donkey
	Anti-goat	Goat IgG	Rockland	605-732-125	Donkey
IRDye® 700 Conjugated Antibodies	Anti-mouse	Mouse IgG	Rockland	610-730-124	Donkey
	Anti-rabbit	Rabbit IgG	Rockland	611-730-127	Donkey
	Anti-goat	Goat IgG	Rockland	605-730-125	Donkey